DEPARTMENT OF THE INTERIOR

U.S. GEOLOGICAL SURVEY

Guidebook for Field Trip to the Mount Bachelor-South Sister-Bend Area, Central Oregon High Cascades

Edited by

William E Scott[1], Cynthia A. Gardner[1], and Andrei M. Sarna-Wojcicki[2]

Open-File Report 89-645

1. David A. Johnston Cascades Volcano Observatory
U.S. Geological Survey
5400 MacArthur Boulevard
Vancouver, WA 98661

2. U.S. Geological Survey
345 Middlefield Road
Menlo Park, CA 94025

1989

CONTENTS

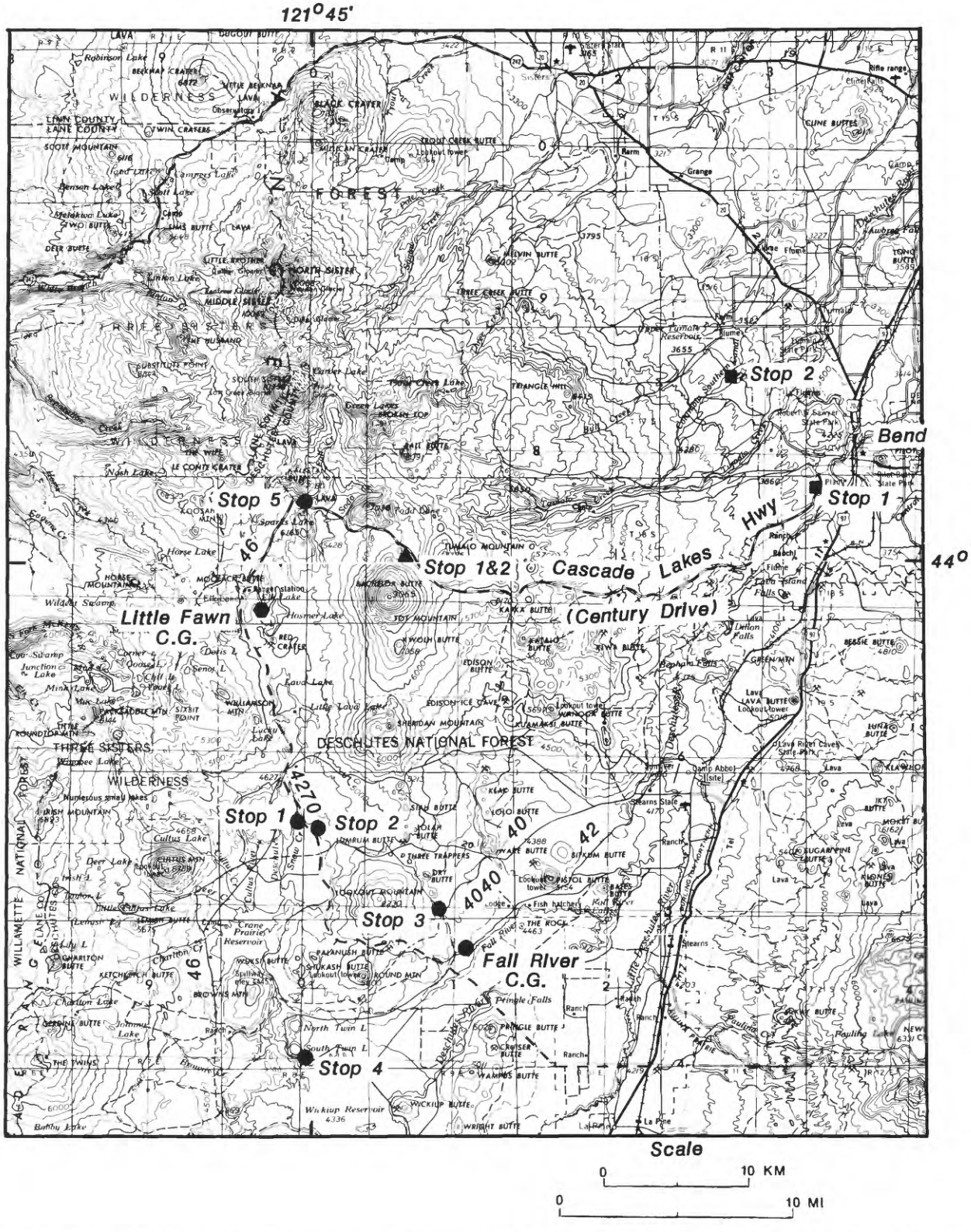

Figure 1. Map of field-trip area. Basemap uses former name of Mount Bachelor, "Bachelor Butte". Selected Forest Service roads are identified by 4-digit numerals. Triangles, stops for day 1; circles, stops for day 2; squares, stops for day 3.

INTRODUCTION

by
William E. Scott

This field excursion to the central Oregon High Cascades highlights aspects of the Quaternary volcanic and glacial history in the vicinity of Mount Bachelor (formerly Bachelor Butte), South Sister, and Bend (fig. 1). The guidebook includes a roadlog that contains brief descriptions of the stops interspersed with papers that discuss some of the key features and interpretations of the stops. Each day's stops are numbered beginning with 1 and are referred to by day and stop number (for example Day 2–Stop 4). Figures and tables are numbered consecutively from the introduction through the last contribution; references from all sections are combined at the end of the guidebook. Each day's log begins at Little Fawn Campground, a group campground run by the U.S. Forest Service on the south end of Elk Lake.

Regional Geologic Setting

The High Cascades of Oregon is a north-trending belt of upper Miocene to Quaternary volcanic rocks that were erupted on the east margin of the upper Eocene to Miocene Western Cascades volcanic province (fig. 2; Taylor, 1981; Priest and others, 1983). Upper Pliocene and Quaternary rocks of the High Cascades form a broad platform of chiefly basalt and basaltic andesite volcanoes that fill a structurally subsided zone in the older rocks of the High Cascades (Taylor, 1981; Hughes and Taylor, 1986; Smith and others, 1987). Each of four major Quaternary volcanic centers along this platform (Mount Hood, Mount Jefferson, Three Sisters-Broken Top, and Crater Lake caldera (Mount Mazama)), have erupted lava flows and pyroclastic material that range in composition from basalt to dacite; except for Mount Hood, they have also erupted rhyolite. Newberry volcano, which lies east of the High Cascades, is also a compositionally diverse Quaternary volcanic center (MacLeod and others, 1981).

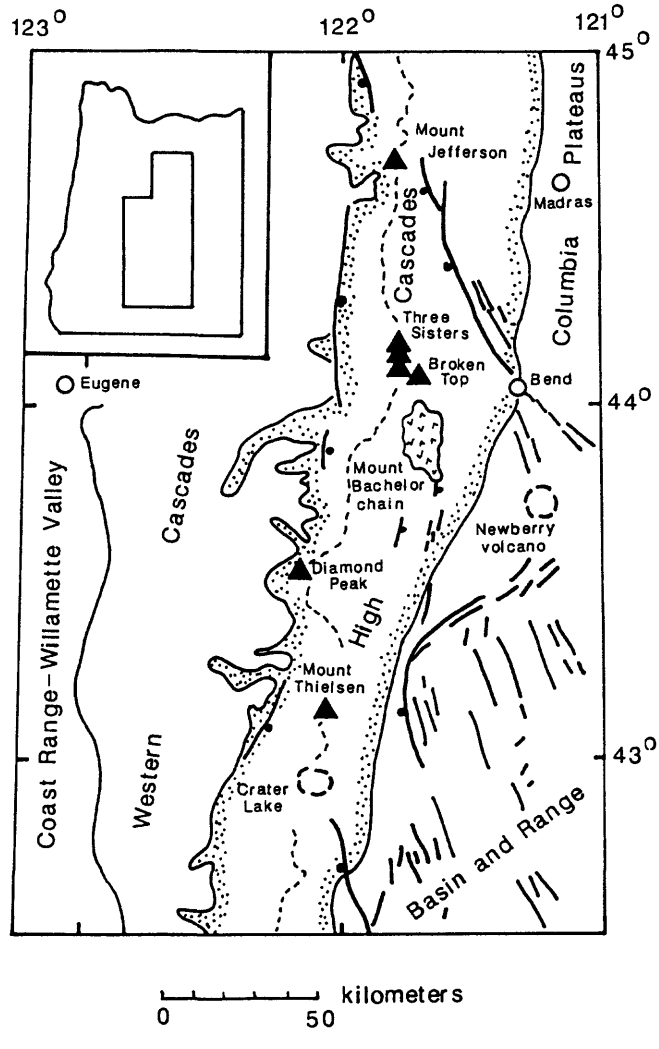

Figure 2. Geologic setting of the Three Sisters-Mount Bachelor area within the upper Miocene to Holocene High Cascades (stippled border). The Western Cascades are composed of upper Eocene to middle Miocene volcanic and volcaniclastic rocks. The parts of the Columbia Plateaus and Basin-and-Range physiographic provinces shown on the map are composed dominantly of Tertiary volcanic and sedimentary rocks; Quaternary volcanic rocks cover most of the area near Newberry volcano. Heavy line, fault; where shown, bar and ball on downthrown sides; dashed line, crest of Cascade Range. Broken circle, caldera; triangle, major volcano. Figure compiled from Hammond (1979), Priest and others (1983), and Sherrod (1986).

Three Sisters-Broken Top area

The Three Sisters-Broken Top area is a long-lived center of basaltic to rhyolitic volcanism (Taylor, 1981; Hill and Taylor, this volume). The clustering of large composite cones sets the area apart from others in the High Cascades, although the Mount Mazama area, prior to the formation of Crater Lake caldera, was also a cluster of composite cones (Bacon, 1983).

The ages of most volcanoes in the Three Sisters area are not precisely known. North Sister, a basaltic andesite pyroclastic and lava cone that rests on a shield volcano, is the oldest of the Three Sisters (Taylor, 1981) and postdates (Taylor, 1987) the 0.3-Ma (Sarna-Wojcicki and others, this volume) Shevlin Park Tuff of Taylor (1981). Middle Sister is intermediate in age between North and South Sister and, like South Sister, is compositionally diverse. Broken Top volcano is also younger than the Shevlin Park Tuff (Hill and Taylor, this volume) and is older than South Sister, but its age relation to Middle and North Sister is not known. The relative degree of erosion of Broken Top suggests an age probably equal to or greater than that of North Sister. Broken Top is a complex composite cone of dominantly basaltic andesite that intermittently erupted andesite, dacite, and rhyolite as lava flows, pyroclastic flows, and pyroclastic falls (Crowe and Nolf, 1977; Taylor, 1978). Cayuse Crater and two nearby vents on the southwest flank of Broken Top (figs. 5, 17) erupted during earliest Holocene or latest Pleistocene time, but these events were probably unrelated to the long-inactive Broken Top system.

South Sister is the youngest composite volcano of the Three Sisters-Broken Top center and has erupted lavas ranging from basaltic andesite through rhyolite (Taylor, 1981; Wozniak, 1982; Clark, 1983). Although not dated directly, most, if not all, of South Sister is probably of late Pleistocene age. This subjective judgement is based on the relatively little eroded profile of the volcano and the reasonably good preservation of lava-flow levees and other features, especially on the south and west flanks. The cone of basaltic andesite that forms the summit of South Sister is probably of latest Pleistocene age (Wozniak and Taylor, 1981; Scott, 1987); its crater is still closed and is filled with 60 m (Driedger and Kennard, 1986) of ice and snow. Le Conte Crater (fig. 17), a basaltic andesite scoria cone on the south flank, is between about 15,000 and 6,850 yr old. The youngest eruptions recognized on the volcano occurred at a series of vents on the south and northeast flanks that erupted rhyolite tephra and lava flows and domes between about 2,200 and 2,000 yr B.P. (fig. 17; Taylor, 1978; Taylor and others, 1987; Wozniak, 1982; Clark, 1983; Scott, 1987).

Mount Bachelor volcanic chain

The Mount Bachelor volcanic chain provides one example of the type and scale of eruptive activity that has produced most of the High Cascades platform, which consists chiefly of scoria cones and lava flows, shield volcanoes, and a few steep-sided cones of basalt and basaltic andesite. The chain is 25 km long; its lava flows cover 250 km^2 and constitute a total volume of 30-50 km^3 (Scott and Gardner, in press).

Many vents in the field-trip area, including those of the Mount Bachelor volcanic chain and the Holocene rhyolite lava flows and domes on South Sister, define NNW-NNE-trending alignments (fig. 3; E.M. Taylor and N.S. MacLeod, written commun., 1981, in Bacon, 1985; Hughes and Taylor, 1986; Scott, 1987). Normal-slip faults in the region, including one at the south end of the Bachelor chain, also have this orientation (figs. 2, 3, 5; Venkatakrishnan and others, 1980; Kienle and others, 1981). These alignments are oriented parallel to the north-south direction of maximum horizontal compressive stress that affects the region (Zoback and Zoback, 1980).

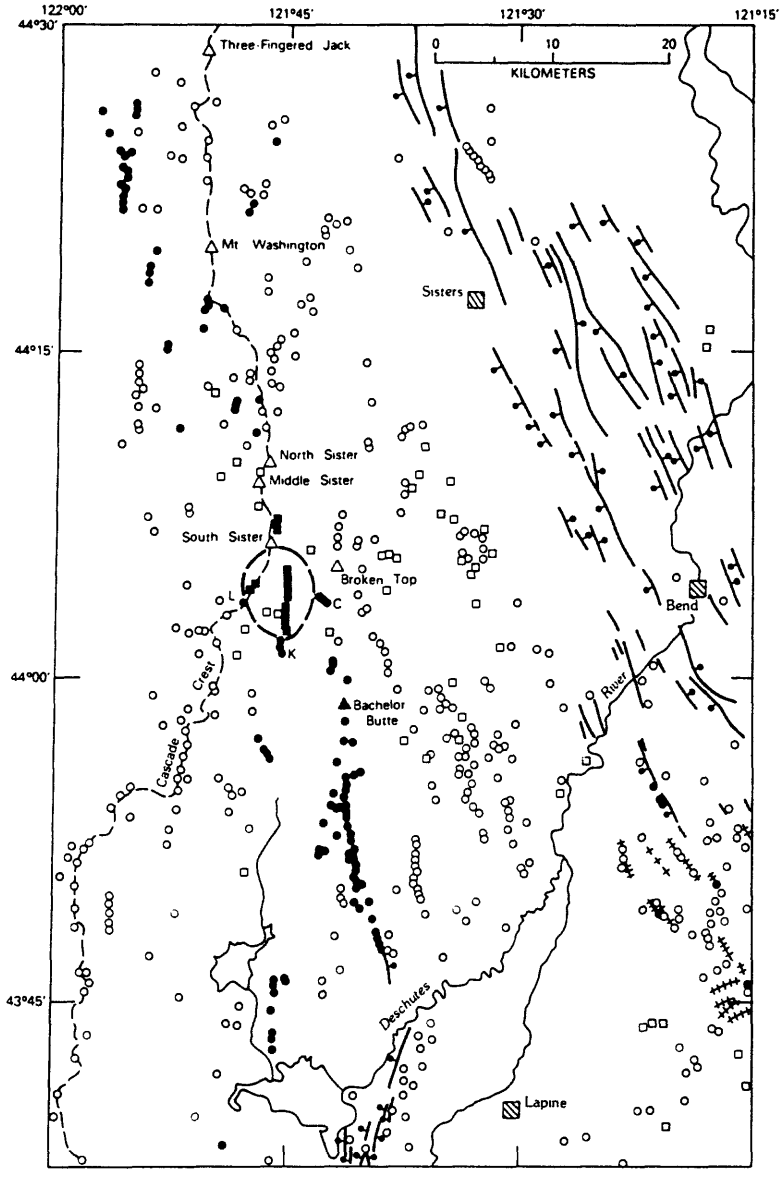

Figure 3. Compilation of vents of Quaternary age and faults in the Three Sisters area (Scott, 1987). Triangles are stratovolcanoes; circles are vents of mafic (basalt and basaltic andesite), mostly monogenetic volcanoes; squares are vents of silicic (dacite and rhyolite) lava domes and flows. Numerous silicic vents on the flanks of South and Middle Sister are not shown. Solid symbols represent vents of latest Quaternary (< 15,000 yr) age; open symbols are vents of pre-latest Quaternary age. L, Le Conte Crater; K, Katsuk and Talapus Buttes; C, Cayuse Crater. Heavy lines are faults; bar and ball on downthrown side. Crossed lines are fissures. The dashed circle represents the maximum extent of an hypothesized magma chamber south of South Sister (Scott, 1987).

ROAD LOG FOR DAY 1--MOUNT BACHELOR

by

William E. Scott

This day-long trip (fig. 1) consists of a drive on the Cascade Lakes Highway to Mount Bachelor (formerly Bachelor Butte), one stop at the base of the ski area, a chairlift ride to the summit for an overview, a chairlift ride down to mid-mountain, and a hiking tour of features that relate to the eruptive history of Mount Bachelor and to late Pleistocene and Holocene glaciation. The geologic map (fig. 5) shows most of the major geologic features that are mentioned in the road log.

Mileage	Description of features along route
0	At junction of entrance road to Little Fawn Campground on Elk Lake and USFS Road 4600-470; turn right; at 0.4 mi. bear right onto paved road.
1.1	On left, Red Crater, northernmost and largest of 2.5-km-long chain of postglacial scoria cones; road ahead is on the lava flow of Red Crater that dams Elk Lake.
1.7	Intersect Cascade Lakes Highway (Road 46) near margin of Red Crater lava flow; turn right (north). Road follows west margin of lava flow.
2.4	Roadcut on right exposes a thin layer of 2-ka pumice lapilli from the Rock Mesa vent on South Sister, Mazama ash, as much as 50 cm of scoria of Red Crater, and till of Suttle Lake age. Lack of significant weathering of the till below the scoria indicates that the eruption of Red Crater occurred not long after deglaciation.
3.5	Turnout on right; view east across Elk Lake to the three major volcanoes of the Mount Bachelor chain (Mount Bachelor, Kwolh Butte, and Sheridan Mountain) and Red Crater.
4.7	Intersection with road to Sunset View. Roadcuts expose till of Suttle Lake age. This is a good location at which to observe the degree of soil development in till of Suttle Lake age. The depth of the soil is exaggerated here by a mantle of Mazama ash that is mixed into the top of the till; weathering rinds on stones from the B horizon are <0.2 mm thick, which is typical for till of Suttle Lake age.
6.8	West margin of postglacial basaltic andesite lava flow from Le Conte Crater, a scoria cone just south of South Sister. The lava flow is older than Mazama ash, and may be similar in age to parts of the Mount Bachelor chain. Note the thickening and coarsening blanket of Rock Mesa and Devils Hill tephra. Views of Broken Top ahead.
8.5	On right through trees are Talapus and Katsuk Buttes, scoria cones that rise above a steep-sided plateau, the upper part of which is composed of thin basalt lava flows. As discussed later, this plateau owes its peculiar shape to having been erupted against glacier ice. View ahead to Devils Hill, a glaciated rhyolite dome. The south end of the Holocene Devils Hill chain of vents lies on the east flank of Devils Hill. The rugged, blocky surface of the Holocene rhyolite lava domes and flows contrasts markedly with the glacially smoothed and rounded form of Devils Hill.
9.3	On right, Devils Lake, which is dammed by the lava flow from Le Conte Crater. Road cuts on left are in hyaloclastite formed by the initial eruptions that built Talapus and Katsuk Buttes and the surrounding basalt plateau. See Day 2–Stop 5 for discussion of these ice-contact features.
9.6	On right, hyaloclastite at base of Talapus Butte. On left, southernmost rhyolite lava flow of 2-ka Devils Hill chain of vents. Chain extends 10 km from here to northeast flank of South Sister (figs. 5, 17). Rhyolite flow overlies tephra of the Devils Hill eruptive episode, tephra of the Rock Mesa eruptive episode, Mazama ash, and hyaloclastite of Talapus and Katsuk Butte. In roadcuts immediately to east, till of Suttle Lake age overlies the hyaloclastite.
10.8	View of Mount Bachelor to east. Note prominent vent on north flank skyline (lodge lies just south of vent) that is the source for an apron of lava flows (covered with ski trails) that were erupted following formation of the upper part of Mount Bachelor. View to left of Broken Top volcano and postglacial (>9,500, <12,000 yr B.P.) Cayuse Crater (red scoria cone; figs. 5, 17) that is visible just above trees at edge of meadow.
11.2	Road cuts through the end of the basalt lava flow from Cayuse Crater. Immediately past the Cayuse flow is Soda Creek. On October 7, 1966, a flood and debris flow originating from the moraine-dammed lake of the glacier on the east flank of Broken Top descended

the channel and piled debris on the road (Nolf, 1969). Fine-grained flood sediment covered about 35-45 percent of Sparks Lake meadow south of the road. Lava flow south of the highway and east of Soda Creek is one of several lava flows that form the youngest unit of the Mount Bachelor volcanic chain and that dam Sparks Lake. They erupted from Egan cone (informal name), a scoria cone on the north flank of Mount Bachelor (fig. 5). Their stratigraphic relation to the Cayuse flow is unknown, as the flows are not in contact; however several lines of evidence suggest that the Egan flows are younger (see Stop 1). Road ahead rises onto flank of Todd Lake volcano (Taylor, 1978), a glaciated dacite volcano that predates Broken Top volcano.

13.2 On right, margin of basaltic andesite lava flows from Egan cone. On left, unweathered or only slightly weathered till of Suttle Lake age is overlain by basaltic scoria from the northernmost vents of the Mount Bachelor volcanic chain that lie south of highway. Mazama ash and tephra of the Rock Mesa and Devils Hill eruptive episodes overlie the scoria.

14.5 On left, glaciated outcrops of basaltic andesite lava flow from a cone of the Tumalo Mountain chain that is locally overlain by scoria of Bachelor chain, Mazama ash, and tephra of the Rock Mesa and Devils Hill eruptive episodes. Tumalo Mountain is the shield volcano ahead on the left. On the right is a glaciated scoria cone. Ahead is Dutchman Flat, a basin that is closed on the south by lava flows of the Bachelor shield volcano. The upper part of the basin fill is composed mostly of fluvial gray sand, minor silt, and fine gravel; much of the sediment is reworked tephra.

15.2 Turn right at entrance road to West Village of Mount Bachelor Ski Area; at next intersection bear right. Egan cone, composed of red scoria, is visible ahead.

16.0 **STOP 1--MAZAMA ASH**

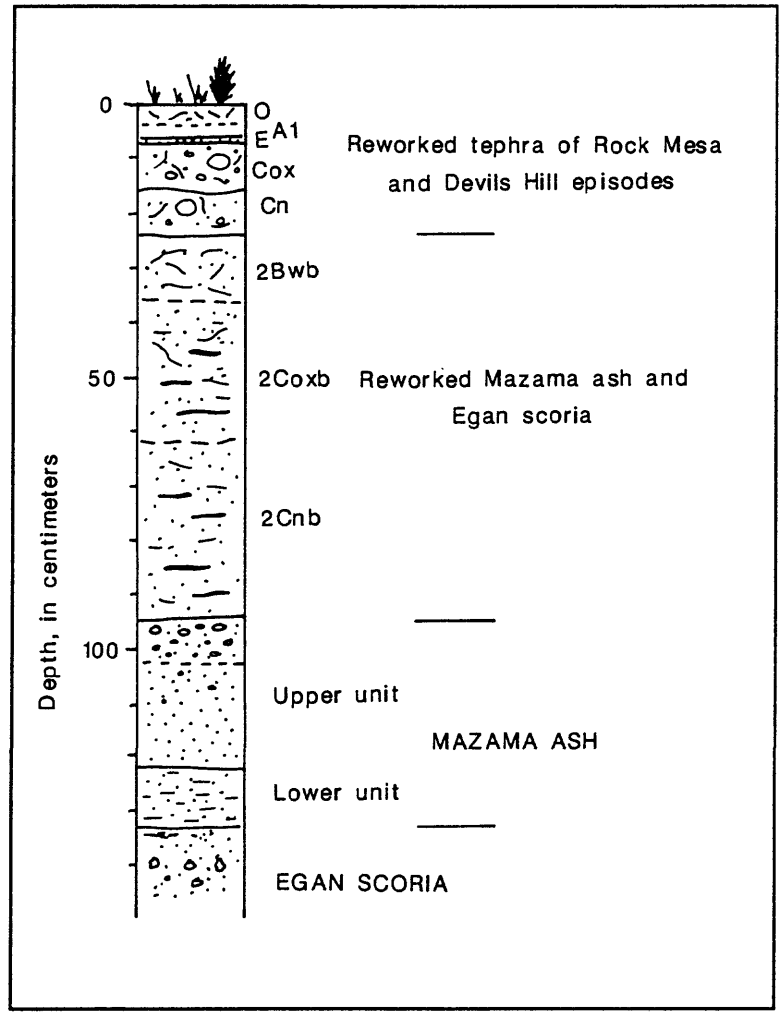

Figure 4. Stratigraphic section of Mazama ash exposed at Stop 1-Day 1 in excavation at West Village parking lot. Letter and number symbols to right of column are horizon designations of surface and buried soils.

A shallow excavation in the southwest part of the West Village parking lot contains a good exposure of Mazama ash, which serves as a valuable stratigraphic marker in the central High Cascades. The age of Mazama ash is 6,845 ± 50 ^{14}C yr B.P. (Bacon, 1983; about 7,700 calendar yr ago). The ash (fig. 4) lies on unweathered or slightly weathered scoria from nearby Egan cone, the youngest vent of the Mount Bachelor volcanic chain. This lack of substantial weathering suggests that the tephra eruptions of Egan

cone are only slightly older than Mazama ash. Mostly reworked Rock Mesa and Devils Hill tephra lies above Mazama ash.

The original thickness of Mazama ash at this site is about 38 cm. The in-place fall deposit is buried by about 70 cm of reworked Mazama ash and scoriaceous ash of Egan cone. The position of this site at the base of a slope probably ensured rapid burial of the fall deposit by reworked material.

Mazama ash exposed here is composed of two distinct units. The lower unit is fine- to medium-grained, light-gray to white ash, and contains abundant ferromagnesian minerals and lithic fragments. It is also conspicuously laminated. The upper unit is thicker, coarser-grained, and distinctly more yellow than the lower unit. The upper unit ranges from medium to coarse ash at its base to coarse ash and fine lapilli in its upper part. This sequence is typical of Mazama ash in azimuths north-northeast of Crater Lake.

Mazama ash serves as an important stratigraphic marker in central Oregon; its thickness and character make it readily identifiable in the field. Determining the relation of a deposit or surface to Mazama ash is a fundamental task, and, although obvious at this stop, the relation is not always so clear. The deposit of thick reworked ash seen here indicates that the ash has been thinned or removed entirely from other places. The problem of reworking is especially significant at high altitudes where slope processes occur at high rates, as we shall see on the upper slopes of Mount Bachelor.

Return to Cascade Lakes Highway.

16.8 Cascade Lakes Highway, turn right. Good view of Broken Top and the Three Sisters to northwest.

17.4 Turn right into entrance road to Sunrise Lodge; follow road 0.3 mi. to parking lot.

STOP 2--MOUNT BACHELOR

Ride Sunrise Chairlift to mid-mountain. Lift towers are numbered with metal tabs on the cross bar.

Tower	Description of features along route
Base	Sunrise Lodge and the base of the lift are on an outwash fan that heads at the only significant stream channel on Mount Bachelor (fig. 9). The channel originates in the cirque on the northeast flank; the drainage proceeds around the northeast and east margin of Bachelor lava flows as Dutchman Creek. Dutchman Creek is typically dry except during spring and early summer snowmelt periods. During lift and lodge construction, excavations in this area exposed, from top down, 1 m of gravel and sand with no or slight soil development, 4-5 cm of Rock Mesa and Devils Hill tephra, 4 m of gravel and sand; about 40 cm of Mazama ash; and several meters of gravel and sand. At a depth of 7 m, the base of the outwash was not exposed, but is assumed to be on Bachelor lava flows.
5	Approaching head of outwash fan (just past tower 6). Prior to construction and grading, this area contained a sequence of bouldery debris-flow and(or) flood levees. The excavation for tower 5 exposed 1.3 m of levee deposit of late neoglacial age that overlies a weakly oxidized soil developed in Rock Mesa and Devils Hill tephras and underlying gravel and sand of probable early neoglacial age. Charcoal fragments on the contact between the buried soil and levee deposit yielded an age of 1,240 ± 70 yr B.P. (W-5023). The buried soil consisted of a 2- to 3-cm-thick A1 horizon; 5-cm-thick patchy E horizon; and 15-cm-thick, weakly oxidized C horizon.
7,8,9	Basaltic andesite lava flows of Mount Bachelor summit cone.
10	Distal slope of end moraine of Canyon Creek age that overlies lava flows of summit cone. Remainder of lift line is in drift of Canyon Creek age. Scoria of Egan cone, Mazama ash, and Rock Mesa and Devils Hill tephras locally lie on the till.
top	The top of the lift is on a thick drift of reworked Mazama ash. Take Summit Chairlift to top of Mount Bachelor.

Summit Chairlift

Up to tower 11, the Summit Lift crosses the distal slope of a right-lateral moraine that postdates Mazama ash and is of early neoglacial age. Clasts of Rock Mesa and Devils Hill tephra are scattered on the crest and upper slopes of the moraine, but typically do not form a layer. Excavations for the lift towers and power cables formerly exposed till, colluvium derived from till, and Rock Mesa and Devils Hill tephras in beds, lenses, and as scattered clasts in colluvium. Little of the tephra is in place; most has been reworked by wind and slope processes. Above tower 11, the lift crosses a lava-flow surface eroded by glaciers of Canyon Creek age (and somewhat smoothed by bulldozers); glacial grooves and striae are common on outcrops of dense rock. Till and drifts of Mazama ash are present locally. The terminal building at the summit is nestled between several vents.

Summit

The summit of Mount Bachelor has numerous vents, most of which discharged basaltic andesite lava flows. The summit vents and plugs exposed in the headwall of the cirque are arrayed in a northwest-southeast-trending cluster that forms an elongate summit ridge. The vents are marked mostly by low, blocky domes, but also by several shallow collapse craters. Pyroclastic material is scarce, forming only a few remnants of cones of dense scoria that are older than most of the dome vents. The scarcity of pyroclastic material at the summit and on the flanks of the cone indicate that at least the latter summit eruptions were dominantly effusive.

Views from the summit include Newberry volcano to the southeast and the Mount Bachelor volcanic chain to the south. Farther to the south and southwest, numerous shield volcanoes form the bulk of the High Cascades. Some of these shields predate the Brunhes Polarity Chron. Diamond Peak, Mount Thielsen, and Mount Scott (on the east side of Crater Lake) are prominent distant peaks. To the southwest and west, the upper Deschutes River valley contains several lakes dammed by lava flows. The four northern ones (Sparks, Elk, Hosmer, and, except for brief periods, Lava) have no surface outlets; water drains out through the permeable post-glacial lava flows and emerges as springs along the down-valley margins of the flows. Little Lava Lake (and during high water, Lava Lake) usually forms the head of the Deschutes River. The Three Sisters, Broken Top, and the silicic highland of Taylor (1981; renamed the Tumalo volcanic center by Hill (1988) and Hill and Taylor, this volume) east of Broken Top dominate the northern view, with Three-Fingered Jack, Mount Jefferson, Mount Hood, and Mount Adams in the distance.

Mid-mountain

From the base of the Summit Lift, hike west to view the moraine sequence of late glacial and neoglacial age and late lava flows of Mount Bachelor that overlie moraines of Canyon Creek age (fig. 9).

TEMPORAL RELATIONS BETWEEN ERUPTIONS OF THE MOUNT BACHELOR VOLCANIC CHAIN AND FLUCUATIONS OF LATE QUATERNARY GLACIERS

by
William E. Scott

INTRODUCTION

Eruptions of the 25-km-long Mount Bachelor volcanic chain (MBVC) and some other nearby vents (fig. 5) coincided with or closely followed the retreat of late Pleistocene glaciers (Scott and Gardner, in press). These eruptions were dominantly effusive and covered a 250-km^2 area with lava flows. Owing to limited radiocarbon dating of the volcanic deposits, information about the timing of the eruptions relies heavily on the stratigraphic relation of various volcanic units to glacial deposits. Additional details of the volcanic history have been obtained through stratigraphic relations among the volcanic units, which are defined on the basis of their lithology and source, and especially through the use of secular-variation, paleomagnetic dating techniques (Gardner, this volume). The age constraints derived from these studies suggest that the bulk of the chain was formed during a period of less than 10,000 yr, perhaps substantially less.

This short paper discusses the glacial-stratigraphic framework of the central Oregon Cascades, the eruptions of the MBVC and how they fit into the glacial framework, and the neoglacial deposits on the mountain. The stratigraphic nomenclature used in this report and key radiocarbon ages are given in Table 1.

REGIONAL GLACIAL STRATIGRAPHY

Suttle Lake advance

A mountain ice sheet covered the Oregon High Cascades during the last major glacial advance (Russell, 1905; Crandell, 1965), which is locally called the Suttle Lake advance (Scott, 1977). Although not radiometrically dated, the Suttle Lake advance is broadly equivalent in age to the Evans Creek stade of the Fraser glaciation of Washington (Crandell, 1965; Crandell and Miller, 1974) on the basis of similarities in soil development, weathering-rind thickness, and morphology (Scott, 1977). Although not dated directly in the United States, the Evans Creek stade probably culminated about 18-22 ka based on radiocarbon ages from British Columbia (Porter and others, 1983).

The maximum extents of glaciers of Suttle Lake age are marked in most valleys by conspicuous belts of end moraines (fig. 5). Valleys are typically free of well-developed moraines between these belts and a younger moraine belt that occupies many valley heads. This distribution of moraines implies that, following their maximum stands, glaciers gradually retreated, with minor stillstands and readvances, leaving a considerable volume of drift in the outer moraine belt. Rates of retreat must have been greater during the time that termini crossed the mid-sections of valleys, because these areas contain no conspicuous moraines and relatively thin drift. Rates of retreat again slowed (and glaciers may even have readvanced some distance) as ice tongues became restricted to valley heads and built conspicuous moraine belts.

Valley-head moraines and the Canyon Creek advance

The belts of moraines in valley heads cover a broad altitude range, and are deposits of glaciers that represent a range of equilibrium-line altitudes (ELA; fig. 6). The moraines extend up to several kilometers beyond moraines of neoglacial age and record the final activity of late Pleistocene glaciers. Unfortunately, these deposits are not well dated. The only radiometric-age control from central Oregon indicates that moraines on Broken Top, which represent an ELA similar to that of the moraines on Mount Bachelor, predate the scoria of Cayuse Crater, which is older than 9,500 yr B.P. (table 1).

The type Canyon Creek drift (Scott, 1977) is composed of a broad belt of valley-head moraines that lies on the northeast side of Three-Fingered Jack in the Metolius River valley (50 km north of Mount Bachelor). Canyon Creek drift is correlated with Hyak drift (Porter, 1976; Porter and others, 1983) of the Washington Cascades on the basis of similarity of reconstructed glacier equilibrium-line altitudes (ELA) relative to those of present-day glaciers and those of glaciers of Fraser age. The age of the Hyak is between 12.5 and 11 ka (Porter and others, 1983).

Many valley-head-moraine systems in the Three Sisters-Mount Bachelor area have ELAs that are up to several hundred meters higher relative to present-day, neoglacial, and Suttle Lake ELAs than those of Canyon Creek age on Three-Fingered Jack (fig. 6). By assuming that ELAs rose steadily with minor halts and reversals as the last glaciation ended, the moraines on Mount Bachelor could be somewhat younger than the Hyak and type-Canyon Creek moraines. Alternately, some of these differences in late-glacial ELAs may

Table 1. Stratigraphic framework of selected volcanic and glacial deposits in the Three Sisters-Mount Bachelor area. Parenthetical terms are for correlative events in Washington.

Glacial events			Eruptive products	Age
	+	Late neoglacial		Culminated during
	+	advance		mid?-19th century
	+			
	+		Younger lava flows of Belknap Crater	1400-1600 B.P.
	+		Collier Cone tephra and lava flows	1600 ± 100 B.P.
Neoglaciation	+		Four-in-One Cone tephra and lava flows	1980 ± 160 B.P.
	+		Devils Hill tephra and lava flows and domes	ca. 2000 B.P.
	+		Rock Mesa tephra and lava flows and domes	2150 ± 150 B.P.
	+			
	+	Early neoglacial		
	+	advance		
			Mazama ash	6845 ± 50 B.P.
			Egan cone tephra and lava flow	6845-12,500 B.P.
			Cayuse Crater tephra and lava flow	9500-12,500 B.P.
			Late lava flows (and tephra) of Mount Bachelor summit cone	6845-12,500 B.P.
	+	Canyon Creek		
	+	advance		11,000-12,500 B.P
	+	(Hyak advance)		
	+		Mount Bachelor summit cone and shield	12,000-18,000 B.P.
	+		Shield of Kwolh Butte	12,000-18,000 B.P.
	+		Siah chain of vents tephra and lava flows	12,000-18,000 B.P.
Cabot Creek	+		Sheridan Mountain tephra and lava flows	12,000-18,000 B.P.
(Fraser)	+		Red Crater tephra and lava flows	12,000-18,000 B.P.
glaciation	+		Le Conte Crater tephra and lava flows[a]	6845-18,000 B.P.
	+		Katsuk-Talapus hyaloclastite, tephra and lava	
	+		flows	15,000-18,000 B.P.
	+		Wuksi-Twin Lakes chain of vents[a]	6845-18,000 B.P.
	+		Summit cone of South Sister[b]	>11,000 B.P.
	+	Suttle Lake		Culminated
	+	advance		18,000-22,000 B.P.
		(Evans Creek stade)		
				South Sister tephras
			Formation of Tumalo Mountain shield and chain of scoria cones	
			Much(?) of South Sister	
Jack Creek	+			75,000 or
(Hayden Cr)	+			140,000 B.P.
glaciation	+			

[a] Stratigraphic relations to Red Crater, Sheridan, Siah, Kwohl, Mount Bachelor, and Cayuse units uncertain.
[b] Stratigraphic relation to Suttle Lake advance uncertain.

Figure 5. Generalized geologic map of the Mount Bachelor volcanic chain.

Correlation

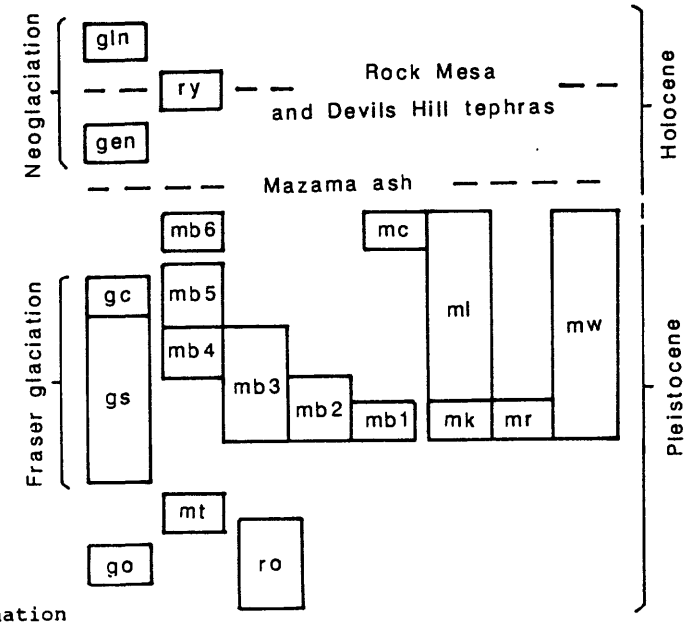

Explanation

Glacial deposits

Neoglaciation
gln late neoglacial drift
gen early neoglacial drift

Cabot Creek glaciation of Scott (1977)
gc Canyon Creek drift
gs Suttle Lake drift

go older drift

Volcanic rocks and deposits

ry rhyolite lava flows and tephra of Rock Mesa and Devils Hill eruptive episodes

ro rhyolite lava flows of pre-Suttle Lake age

Mount Bachelor volcanic chain
mb6 lava flows and tephra of Egan cone
mb5 lava flows and tephra of Mount Bachelor summit cone
mb4 lava flows and tephra of Bachelor shield volcano
mb3 lava flows and tephra of Kwolh shield volcano
mb2 lava flows and tephra of Siah chain of vents
mb1 lava flows and tephra of Sheridan shield volcano

mc lava flow and tephra of Cayuse Crater
ml lava flow and tephra of Le Conte Crater
mw lava flow and tephra of Wuksi, Shukash, and Palanush Buttes
mk lava flows, tephra, and hyaloclastite of Katsuk and Talapus Buttes
mr lava flows and tephra of Red Crater chain of vents

mt lava flows and tephra of Tumalo Mountain
mo undifferentiated mafic lava flows and tephra of pre-Suttle Lake age

Symbols
• vent
----- moraine crest
····· approximate glacial limit on Tumalo Mountain

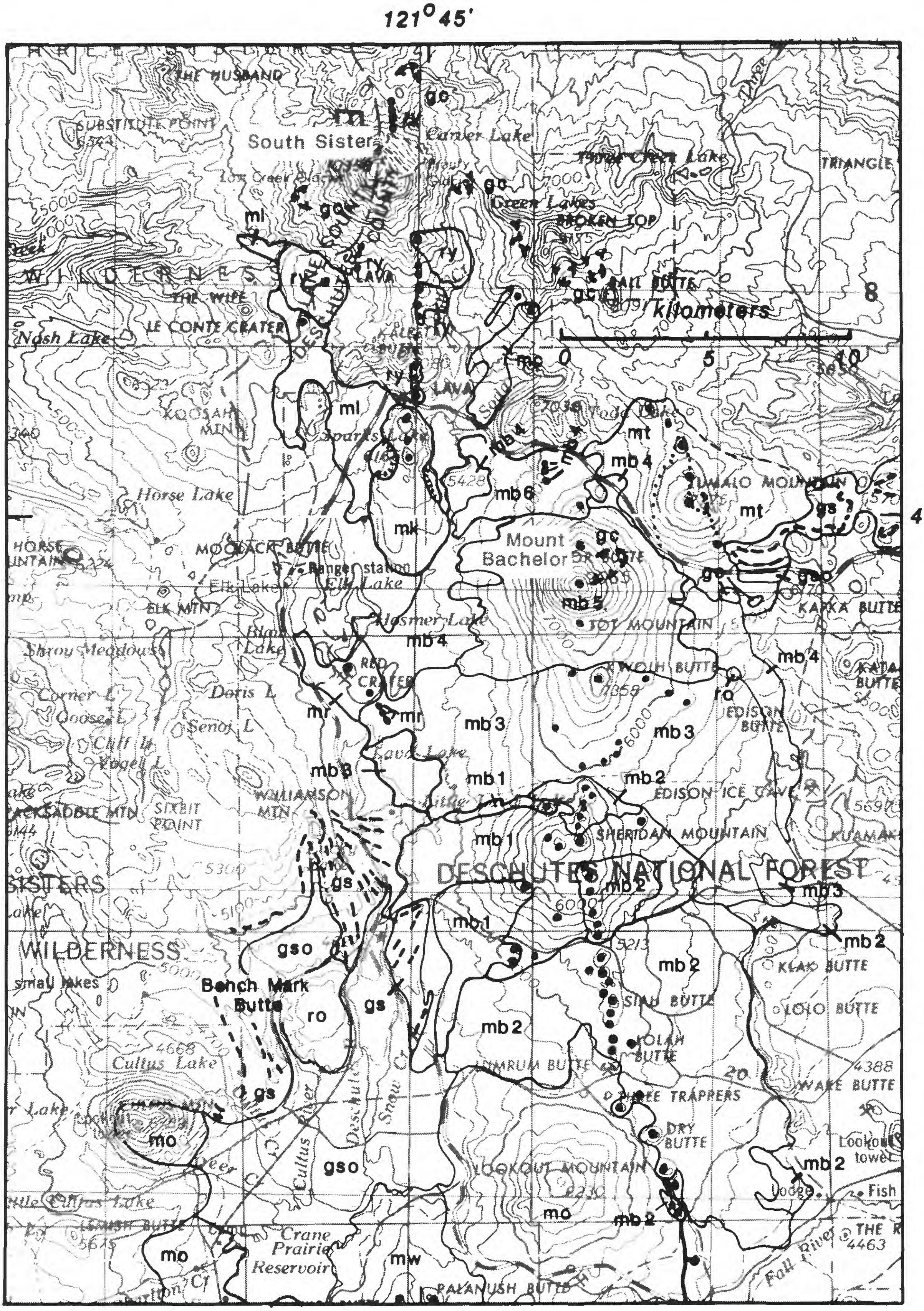
121°45'
44°
kilometers
0
5
10
South Sister
Mount Bachelor
DESCHUTES NATIONAL FOREST
WILDERNESS
Bench Mark Butte
Nash Lake
LE CONTE CRATER
Horse Lake
Elk Lake
Hosmer Lake
Doris L
Cultus Lake
Crane Prairie Reservoir
SHERIDAN MOUNTAIN
LOOKOUT MOUNTAIN
KWOLH BUTTE
EDISON ICE CAVE
TUMALO MOUNTAIN
KAFKA BUTTE
KLAK BUTTE
LOLO BUTTE
WAKE BUTTE
DRY BUTTE
THREE TRAPPERS
PALANUSH BUTTE
Fall River
gc
ml
ry
mt
mb 4
mb 6
mk
mb 5
mb 3
mb 1
mb 2
mb 8
mr
ro
gs
gso
mo
mw

relate to variations of ELA gradients in the region, and the valley-head moraines may all be broadly correlative in age.

One view of late-glacial history is of a time interval of several thousand years during which ELAs were generally rising, glaciers were retreating into valley heads, and glacier termini were becoming more debris laden as their distance from cirque headwall decreased. Conspicuous moraines were built during successive short pauses or readvances. The configuration of valleys was also important in determining the character of the moraine record. For example, on lower-altitude peaks such as Three-Fingered Jack and Mount Washington, the valley-head moraines of Canyon Creek age were deposited by short glaciers largely confined to cirques. In contrast, glaciers with similar ELAs in high-altitude areas like the Three Sisters-Broken Top area would have covered broad upland areas and probably not left much of a depositional record. Not until ELAs had risen to the level that the glaciers were confined to cirques could conspicuous moraines have been deposited. By that time, glaciers on lower peaks like Mount Washington and Three-Fingered Jack might have been very small or absent, unless, as mentioned above, regional variations in ELA gradients are reponsible for some of the observed differences.

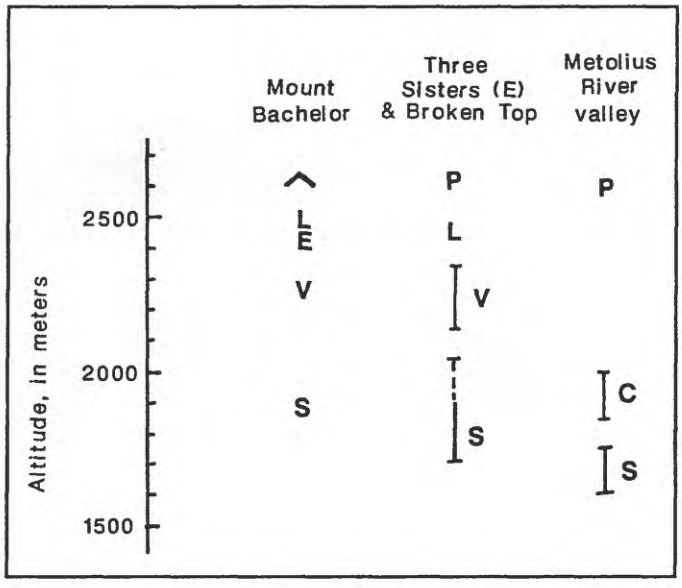

Figure 6. Equilibrium-line altitudes (ELAs) of present-day and reconstructed glaciers in central Oregon. Values for Mount Bachelor and Three Sisters-Broken Top area east (E) of Cascade crest are from Dethier (1980) and this study; values for the Metolius River valley are from Scott (1977). P, present-day glaciers, ^ indicates minimum value; L, glaciers of late neoglacial age; E, glaciers of early neoglacial age; V, valley-head moraines; C, valley-head glaciers of the type Canyon Creek advance; S, glaciers of Suttle Lake age. Bars represent ranges of values that result from ELAs defining surfaces that have substantial gradients.

Some of the moraines in the Three Sisters-Broken Top area that are older than Mazama ash, but lie close to neoglacial moraines may date from the early Holocene (Dethier, 1980) as has been suggested for moraines in the North Cascades of Washington (Beget, 1984; Waitt and others, 1982). However, no compelling evidence has been found to support such an interpretation for the late-glacial moraines discussed here. The relation of the >9500-yr-old Cayuse Crater tephra to moraines on Broken Top shows that they and correlative moraines on Mount Bachelor are pre-Holocene in age. In addition, the 25-50-m difference in ELAs between the early Holocene and maximum neoglacial glaciers in the North Cascades is less than the >100-m difference between glaciers of neoglacial and late-glacial age on Broken Top and Mount Bachelor.

Neoglaciation

In the field-trip area, I recognize evidence of two minor glacier advances that post-date the deposition of Mazama ash and informally call them early and late neoglacial. Evidence for an early-neoglacial advance is typically found immediately beyond late-neoglacial ice limits. However, many glaciers reached their post-Mazama maxima during late-neoglacial time and obliterated any moraine record of early-neoglacial advances. Moraines of early-neoglacial age are less steeply sloping and more round-crested than those of late-neoglacial age; they commonly support stands of whitebark pines. Soils are typically poorly developed owing to active erosional processes; however, where best preserved their profiles consist of a 5-cm-thick A1 horizon, and a 15- to 25-cm-thick weak color B or oxidized C horizon. The ca.-2-ka Rock Mesa and Devils Hill tephras are found on early neoglacial drifts and ca.-7-ka Mazama ash is found on surfaces immediately beyond them.

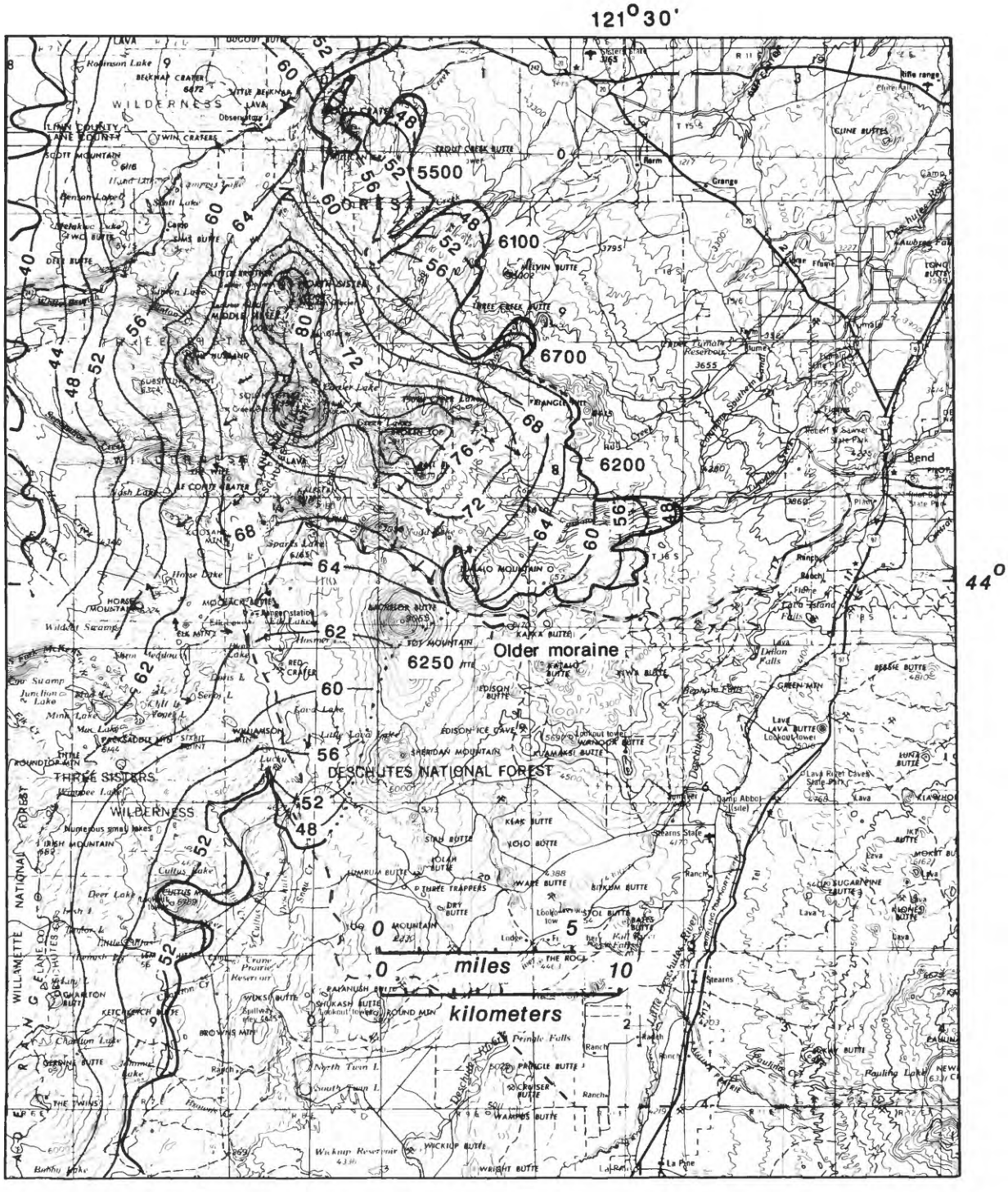

Figure 7. Reconstructed ice cap of Suttle Lake age in the Three Sisters-Broken Top area. Arrows indicate ice-flow direction as determined from geologic evidence. Contours on the glacier surface are in feet; contour interval is 400 ft., except in the upper Deschutes valley where a supplementary 6200-ft contour is shown. ELA (in feet) for several lobes is given by underlined numerals. Older moraine east of Mount Bachelor predates the Suttle Lake advance, but is older than Tumalo Mountain.

Deposits of the late-neoglacial advance post-date the ca.-2-ka Rock Mesa and Devils Hill tephras, form steep, unstable, sharp-crested, and virtually unvegetated moraines. Based on limited dendrochonologic evidence and historical observations, the stand at the outer late neoglacial moraines probably culminated during the 19th century (Russell, 1905; Dethier, 1980; Scott, 1977; Burke and Birkeland, 1983). Since then, glaciers have thinned and retreated drastically. The glacier that occupied the cirque on Mount Bachelor has essentially disappeared and only a small perennial snowbank remains, clinging to the west wall of the cirque. Snow drifted into the cirque by westerly winds probably provides significant additional accumulation to nourish the snowbank.

RECONSTRUCTED GLACIERS OF SUTTLE LAKE AGE

During the Suttle Lake advance, a continuous mountain ice cap covered the crest of the Cascade Range in southern and central Oregon, and outlet glaciers flowed down valleys draining both the east and west sides of the range. The highland area around Broken Top provided a broader accumulation area than in other parts of the range, making the ice cap there larger and more complex (fig. 7). In the field-trip area, ice flowed east from the crest of the Cascade Range and south from the Three Sisters-Broken Top area into the upper part of the Deschutes valley to form a large south-flowing glacier that terminated immediately north of Bench Mark Butte (referred to here as the upper Deschutes glacier; figs. 5, 7). The eastward extension of the ice cap that occupied the highland east of Broken Top terminated north of the Cascade Lakes Highway and formed a major outlet glacier in the canyon of Tumalo Creek.

A longitudinal profile of the reconstructed upper Deschutes glacier (fig. 8) illustrates several general characteristics of the ice cap. Basal shear stresses of the glacier calculated using the method of Pierce (1979) range from 0.5-1.4 bars (50-140 kPa), which is within the range observed for modern and other reconstructed glaciers (Patterson, 1981; Pierce, 1979). In addition, the lower values occur in areas of compressing (decelerating) flow and the higher values occur in areas of extending (accelerating) flow as is typical. The maximum thickness of the glacier, about 1400 ft (425 m; altitudes of the reconstructed glacier are given in feet to agree with base map), lay near Elk Lake, where the surface slope was small. On the steep upper slopes of South Sister, maximum ice thickness was probably no more than 200 ft (60 m), which is not much greater than the thickness of present-day glaciers (Driedger and Kennard, 1986).

Equilibrium-line altitudes on the ice cap in the Three Sisters-Broken Top area varied greatly (fig. 7), probably largely as a result of differences in precipitation rate. ELAs in the northeastern part of the area near Three Creek Butte were much higher than those farther west. ELAs on the west slope of the High Cascades were more than 1000 ft (300 m) lower than those on the east side. These patterns probably result from moisture sources lying to the west and southwest and precipitation rates decreasing strongly across the range in a northeasterly direction, which is similar to present conditions.

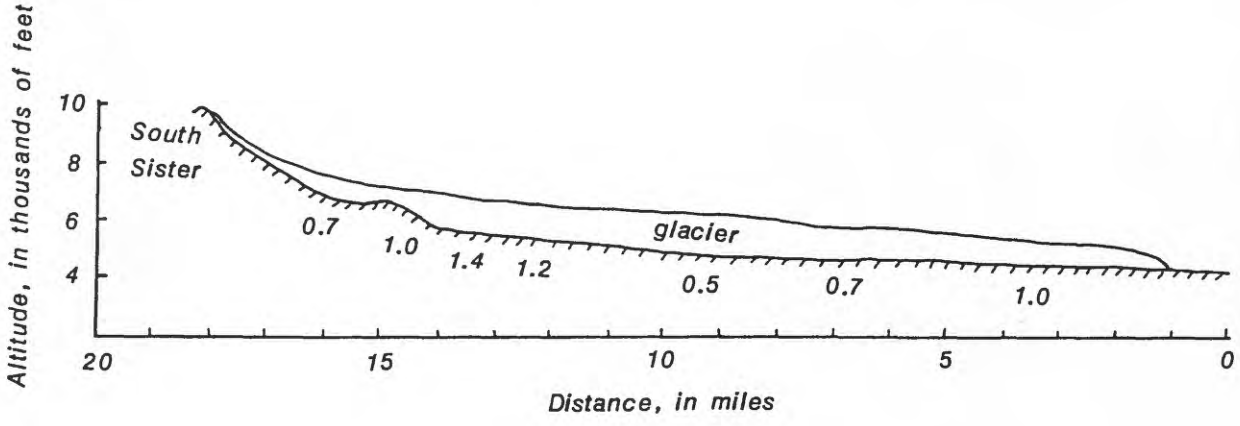

Figure 8. Longitudinal profile of the reconstructed glacier in the upper Deschutes valley. Values along the glacier are basal shear stresses in bars calculated using the method of Pierce (1979).

TEMPORAL RELATIONS OF ERUPTIVE AND GLACIAL EVENTS

Early eruptive history

End moraines of the upper Deschutes glacier of Suttle Lake age form a 7-km-wide belt between Lava Lake and Bench Mark Butte (fig. 5). Lava flows of the Sheridan shield (unit mb1), which include some of the earliest recognized lava flows of the Mount Bachelor volcanic chain, bury much of the east margin of the moraine belt. Therefore, activity along the chain began after about 22-18 ka, the assumed age of the culmination of late Wisconsin alpine glaciation in the Pacific Northwest (Porter and others, 1983). However, it is possible that eruptions began earlier and their products are buried by younger lava flows.

The following three lines of evidence suggest that some of the earliest eruptions of the Mount Bachelor volcanic chain and eruptions at other vents in the area date from a time after glaciers had retreated from their maximum stands, but while glacial conditions still prevailed in the area.

(1) Lava flows of the Sheridan shield and Siah chain (units mb1 and mb2) on the east side of the outwash-covered basin north of Crane Prairie Reservoir, as well as nearby till of the Suttle Lake advance, have thin (<40 cm) mantles of loess (windblown silt and fine sand). The loess must have been deflated before the end of outwash deposition and before the outwash surfaces became stabilized by vegetation.

(2) As discussed in the road guide (Day 2–Stop 5), eruptions that formed Katsuk and Talapus Buttes probably began in a lake melted into the retreating glacier that occupied the area around present Sparks Lake.

(3) Scoria erupted from Red Crater (unit mr) directly overlies gray, unweathered till of Suttle Lake age in roadcuts along the Cascade Lakes Highway (roadlog for Day 1, mi. 2.4). The lack of a recognizable weathering profile in the till in a location that appears to be geomorphically stable, indicates that the eruptions must have occurred shortly after that site had been deglaciated.

Later eruptive history

Stratigraphic evidence on Mount Bachelor indicates that the eruptive activity along the chain was waning by the end of late-glacial time (fig. 9). The moraines of Canyon Creek age on Mount Bachelor postdate the construction of most of the summit cone, which is among the youngest features of the Mount Bachelor volcanic chain. The left-lateral moraine is overlain by lava flows erupted from vents on the lower north flank of Mount Bachelor (fig. 5); these flows account for only a small fraction of the cone's volume. Some lava flows on the west, south, and east flanks may also postdate the Canyon Creek advance, but these are separated geographically and cannot be related stratigraphically to the moraines.

As discussed in the previous section on glacial history, the moraines of Canyon Creek age on Mount Bachelor may be somewhat younger than those of the type Canyon Creek drift, which is thought to be 12.5-11 ka on the basis of correlations with the Hyak drift of the Washington Cascades. Evidence obtained locally suggests that the moraines of Canyon Creek age on Mount Bachelor are no younger than 9.5 ka, because a correlative moraine on Broken Top is overlain by the >9.5-ka tephra of Cayuse Crater. Thus, the construction of most of the Mount Bachelor summit cone must have been completed before 9.5 ka and perhaps as early as 12.5 ka.

Stratigraphic evidence indicates that all eruptive activity ended by about 7 ka, because the products of the Mount Bachelor volcanic chain are overlain by Mazama ash, which was erupted from the Crater Lake area 6850 yr B.P. (Bacon, 1983). The original thickness of the ash was about 50 cm at the south end of the chain and about 30-40 cm at the north end (Day 1–Stop 1). The degree of soil development in scoria of the summit cone and shield volcano of Mount Bachelor (units mb5 and mb4) prior to deposition of Mazama ash suggests that these deposits predate the ash by at least several thousand years. Typically, the soil buried by Mazama ash consists of a cambic B horizon that is 10-20 cm thick and displays weak oxidation extending an additional 10-30 cm into the scoria. In contrast, minimal weathering occurs in the scoria of Egan cone (unit mb6) where it is buried by Mazama ash. This suggests that unit mb6, the youngest eruptive products of the Mount Bachelor volcanic chain, may be close in age to Mazama ash.

Figure 9. (following page) Geologic map of the upper flanks of Mount Bachelor. Unit symbols are the same as in Figure 5 except that the lava flows of the Mount Bachelor summit cone (unit mb5) are locally subdivided into lava flows that predate (unit mb5a) and post-date (unit mb5b) the moraines of Canyon Creek age (gc). mo, lava flows of Tumalo Mountain

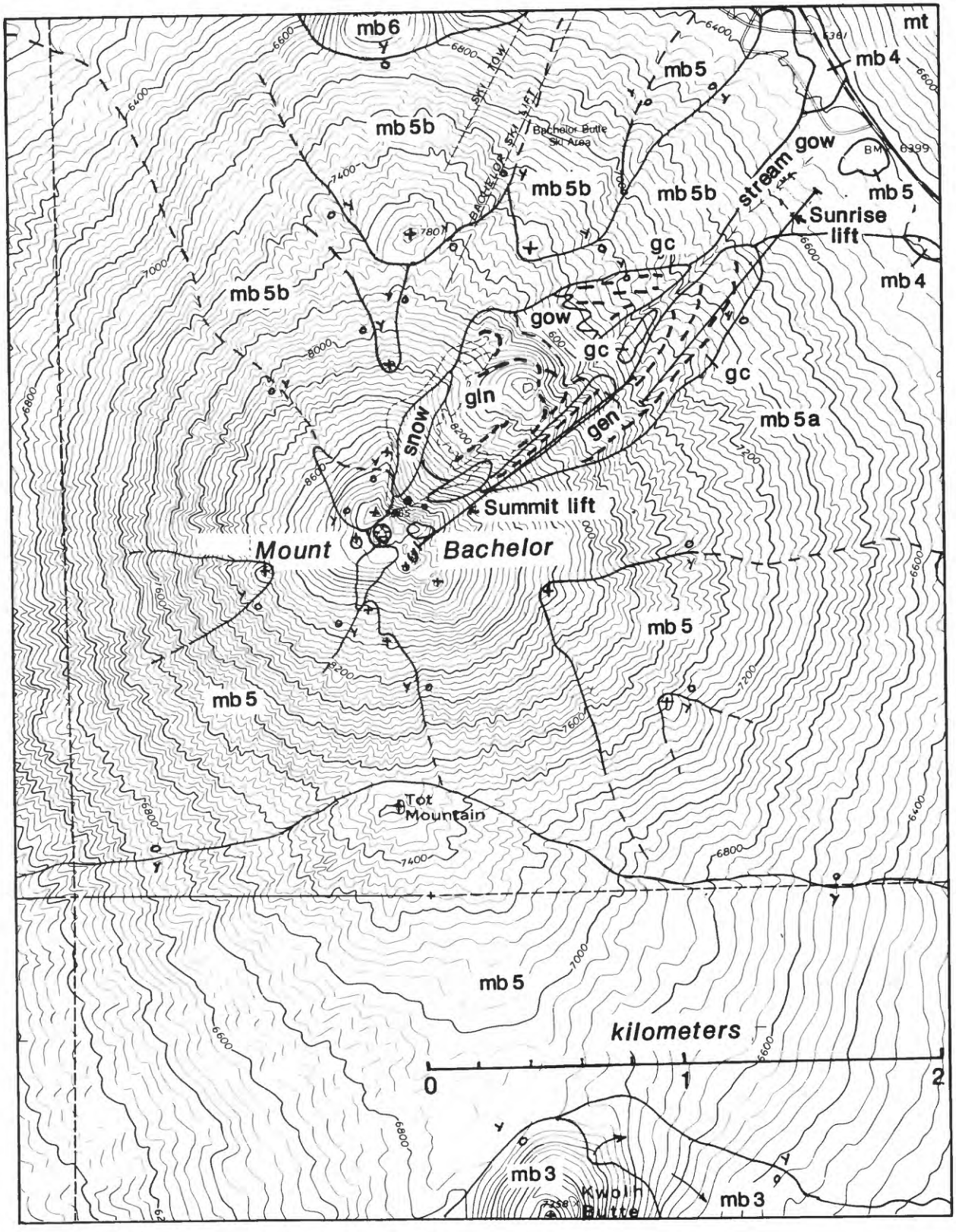
mb6
mb5
mt
mb4
mb5b
Bachelor Butte Ski Area
BACHELOR SKI LIFT
stream
gow
BM 6399
mb5
Sunrise lift
mb4
gc
mb5b
gow
gc
gc
gln
snow
gen
mb5a
Summit lift
Mount Bachelor
mb5
mb5
Tot Mountain
mb5
kilometers
0
1
2
mb3
Kwolh Butte
mb3

PALEOMAGNETIC SECULAR-VARIATION STUDIES ALONG THE MOUNT BACHELOR VOLCANIC CHAIN

by
Cynthia A. Gardner

INTRODUCTION

Lava flows of the Mount Bachelor volcanic chain (MBVC) are both too young and too K-poor to determine absolute ages by means of radiometric (K-Ar, Ar-Ar, or U-Th disequilibrium) dating techniques. This, coupled with the lack of flow-related organic material for ^{14}C analysis, prompted a paleomagnetic secular-variation study to correlate lava flows that are too widely separated to determine relative stratigraphic positions. Paleomagnetic directions can be used to correlate lava flows in the same area because the Earth's magnetic field undergoes secular variation and because volcanic rocks record the direction of the ambient geomagnetic field as they cool (see Champion, 1980; Hoblitt and others, 1985; Kuntz and others, 1986)

THEORY

Approximately 80 percent of the earth's geomagnetic field can be modeled as a simple dipole magnet, having a north and south pole inclined about 12 degrees from the Earth's axis of rotation. The dipole field can be subtracted from the observed field, leaving the non-dipole field, which has a surface pattern comprising about 12 regions approximately continental in scale (Tarling, 1983).

The dipole field undergoes long-term changes manifested by episodic reversals in the geomagnetic field -- each episode spanning about 10^4 to 10^6 years. Changes in the non-dipole field occur over shorter time intervals of 10^0 to 10^3 years . These short-term changes in the Earth's geomagnetic field at any given location are termed secular variations. In the western United States, present drift of the non-dipole or secular field is about 0.25 degrees westward per year (Tarling, 1983).

Volcanic rocks cool quickly, thereby essentially instantaneously locking in the direction of the ambient geomagnetic field. The temperature for igneous rocks at which the magnetic carriers begin to acquire their signature (the Curie temperature, about 580°C for pure magnetite) depends primarily upon composition. In volcanic rocks, the princpal carriers of magnetic signature are the iron-oxides, notably magnetite, maghemite and hematite. Magnetic stability, or ability to preserve a signature, depends upon grain size, composition, and post-cooling alteration of the minerals.

Paleomagnetic directions obtained from lava flows in a given area can be compared to assess the probability of two lava flows having been erupted at the same time. Provided that no post-cooling rotation or other tectonic disturbance has occurred, lava flows with similar paleomagnetic directions may be of the same age, whereas lava flows with dissimilar paleomagnetic directions are of different ages. Lava flows that have similar paleomagnetic directions may be of different ages because the orientation of the secular field is known to have been in the same direction at different times in the past. Thus, basic stratigraphic relationships of a given area need to be known in order to interpret paleomagnetic data.

Resolution of the data

Resolution of paleomagnetic data is a thorny problem in that neither the rate of change nor the direction of change of the secular field is constant. Estimates are made, however, to determine the minimum amount of time two different directions might represent. If the average rate of change in direction of the Earth's magnetic field is 4° per century (the rate Mankinen and others (1986) determined for the last 2000 years in central California), then sites with a cone of 95 percent confidence (alpha 95) of 2° around the mean would allow recognition of 50-year differences in time. Kuntz and others (1986) suggest that subtle tilting of lava flow surfaces probably prohibits recognition of time differences, in most cases, of less than a century. The lava flows of the MBVC do not represent a continuous record of deposition, so no attempt is made in this paper to estimate the amount of time that separates different groups of directions because of the uncertainity in knowing the path of the secular field through time.

FIELD AND LABORATORY STUDIES

Conventional, well-established methods were used to collect paleomagnetic samples and to process them in the laboratory; excellent summaries of these techniques can be found, for example, in Champion (1980) and Tarling (1983). Lava flows at approximately fifty sites were drilled in the Mount Bachelor area. All samples were drilled in the field by means of a portable drill and oriented with both magnetic- and sun-compasses. At each outcrop, several blocks separated by small joints were sampled; between 6 and 16 cores were collected. Samples from roadcuts gave

the best results; samples were also collected from lava levees, archways and walls of collapsed lava tubes, pit craters, flow tops, and lava flows exposed in the west wall of the Mount Bachelor cirque, and yielded variable results.

Remanent magnetization for each specimen was measured by means of a spinner magnetometer, and the results were corrected for the attitude of the sample in the field to determine the declination (D), inclination (I), and intensity (J) of the magnetic field at the time the lava flows cooled. (As a refresher, declination is the direction of magnetization in the horizontal plane measured in degrees clockwise from the north; inclination is the angle of dip of the magnetization measure in degrees from the horizontal; and intensity of magnetization of the rock's magnetic signal). After initial measurement of the remanent magnetization, all samples were progressively demagnetized in an alternating field-demagnetizer to test the magnetic stability and to remove any viscous or isothermal remanent overprinting or both, and remeasured.

RESULTS AND INTERPRETATIONS

A compilation of the paleomagnetic data is given in table 2. Mean site directions and corresponding cones of 95 percent confidence shown in figure 10 indicate two major groupings of directions: a shallow, slightly eastward trending group (D = 350° to 15°; I = 45° to 55°), and a steep, slightly westward trending group (D = 330° to 5°; I = 62° to 72°). Within each major group, two subgroups are identified by the similarity of paleomagntic directions for lava flows from vents from the same area (fig. 11). Paleomagnetic directions of the major shallow group cluster about D = 0° and I=50° and about D= 8° and I= 45°; directions of the major steep group cluster about D = 0° and I= 70° and about D= 340° and I= 65° (fig. 11). I have assigned each of the above four groups to an eruptive episode on the basis that eruptive activity appears not to have been continuous, but occurred as descrete pulses from localized segments of the chain. The two shallow groups constitute eruptive episode I (a and b); the tight steep cluster about D = 0° and I= 70° is assigned to episode II, and the more diffuse steep group clustered farther to the west to eruptive episode III. Episode IV is delineated by the direction of the youngest lava flows from Egan cone. (fig. 11).

Lava flows with paleomagnetic directions clustered around D=0°, I=54°, episode Ia, include porphyritic, basaltic andesite lava flows from vents along the Sheridan Mountain shield, and the basaltic flows of Red Crater and Katsuk Butte (fig. 12a). The great similarity in paleomagnetic directions from lava flows of these centers (fig. 11) suggests that their eruptions were generally coeval, which is consistent with stratigraphic interpretations. Lava flows from Sheridan Mountain are stratigraphically the oldest lava flows exposed along the MBVC (fig. 5).

Changes in eruptive products, vent locations and paleomagnetic directions suggest that stratigraphically younger lava flows on the west flank of the Sheridan shield belong to a later eruptive phase of episode I, designated here as episode Ib. Aphanitic basaltic andesite lava flows erupted from cinder cones on the west flank of the shield, and an olivine basalt flow from a pit crater just south of Sheridan Mountain have paleomagnetic directions that have shallower inclinations (I= 48°) and more easterly declinations (D = 8°) than lava flows from episode Ia, although many of the cones of 95 percent confidence of the two groups overlap (fig. 10). Episode Ib also includes two basalt lava flows from the eastern margin of the Siah chain of cinder cones (fig. 12b), which have paleomagnetic directions similar to these younger west flank Sheridan lava flows (fig. 11; table 2). Stratigraphically, these two Siah lava flows are among the oldest of the Siah chain, although they are chemically indistinguishable from later Siah lava flows.

Basalt lava flows from numerous vents coalesced to form the Siah chain of cones during episode II. Two temporally related Siah lithologic types are recognized -- an older olivine-phyric basalt overlain by younger olivine- and plagioclase-phyric basalt. Paleomagnetic directions for both types, however, are similar (D = 358°, I = 71°, fig. 11; table 2). Similarity in paleomagnetic directions of all lava flows sampled in the Siah area (fig. 12c), excluding those of episode Ib, indicates that eruptive activity along the Siah chain was brief, probably lasting no more than a century or two. The considerable difference in the paleomagnetic directions of episode Ib and those of episode II suggests a quiescent interval along the MBVC.

Eruptive activity shifted northward to the Mount Bachelor - Kwohl Butte area during episode III (fig. 12d). Lava flows from Mount Bachelor and Kwohl Butte stratigraphically overlie lava flows from the Sheridan and Siah areas and have paleomagnetic declinations more westerly (D=341°) and shallower (I=65°) than those of episode II (fig. 11; table 2). Relative timing of eruptions of the Bachelor-Kwohl lava flows is poorly constrained by the paleomagnetic data, however, largely due to the lack of suitable sampling sites. Few roads intersect lava flows in this area and the youthful, rubbly nature of the lava flows make finding suitable drill sites on the flows themselves difficult. Thus, relative ages between lava flows were determined by stratigraphy.

Numerous olivine-phyric basalt cinder cones and associated small lava flows are present on the north and south flanks of the Sheridan shield. The basalt cinder cones overlie lava flows of episode 1; however, their relationship to products of either the Siah or Bachelor-Kwohl eruptions is uncertain. Only one lava flow on the south flank was sampled (G85-16) and it yielded a paleomagnetic direction similar to that of episode II; thus, I have tenatively assigned the cinder cones on the south flank to episode II. One lava flow on the north flank also was

Table 2. Compilation of paleomagnetic data from the Mount Bachelor volcanic chain

Map unit	Type	Site	Expt	Dec	Inc	N/N1	A95	k	Arit av j
mb1a	rd cut	G84-16	5 mT	1	51	11/11	1.9	560.6	0.801
mb1a	pit	G84-14	20 mT	6	56	14/8	2.5	512.1	0.291
mb1b	flow	G84-12	20 mT	355	52	14/14	2.5	261.0	0.470
mb1b	rd cut	G84-17	20 mT	358	53	16/16	2.1	336.6	1.124
mb1b	rd cut	G84-1	10 mT	357	55	14/14	1.4	851.8	0.760
mb1b	rd cut	S82-sm1	5 mT	355	54	5/5	2.4	980.4	0.568
mb1b	rd cut	G84-5	20 mT	359	52	7/6	3.6	342.5	0.357
		avg		359	53	12/9	2.3	727.7	0.624
mr	rd cut	S82-b2	10 mT	0	56	9/8	2.1	692.0	0.250
mr	rd cut	G84-19	10 mT	358	55	8/8	1.6	1225.3	0.231
mr	tube	G85-24	10 mT	336	47	10/9	3.7	192.4	0.982
mk	flow mar	G85-21	10 mT	5	57	12/9	2.1	621.4	0.822
		avg		1	56	4/3	3.1	1555.5	0.434
mb1c	rd cut	G84-6	5 mT	5	46	6/5	2.2	1189.5	0.559
mb1c	flow mar	G84-11	30 mT	8	72	12/10	12.8	15.2	0.129
mb1c	flow top	G85-6	10 mT	9	51	10/7	2.7	518.2	1.628
mb1c	rd cut	G84-4	5 mT	11	49	14/12	2.5	393.5	0.506
mb1c	rd cut	S82-sm2	20 mT	6	44	5/4	2.5	1389.8	0.345
mb1c	pit	G85-7	30 mT	8	46	11/10	2.0	610.5	0.270
mb2a	flow mar	G85-13	5 mT	8	51	8/3	5.2	558.3	0.635
mb2a	tube	G84-24	20 mT	11	48	14/14	1.7	542.9	0.496
mb2a	flow mar	G85-22	NRM	10	56	12/12	5.2	70.4	1.363
		avg		8	48	9/7	2.3	717.5	0.634
mb2b	levee	G85-5	10 mT	358	71	7/6	3.0	497.5	0.379
mb2b	aggle	G85-4	10 mT	330	73	9/9	3.1	279.2	0.773
mb2b	rd cut	G85-1	10 mT	355	73	11/11	1.4	1016.0	0.294
mb2b	tumuli	G84-10	10 mT	7	71	15/15	2.4	271.8	0.884
mb2b	flow top	G84-7	10 mT	10	69	16/14	1.3	934.8	0.527
mb2b	flow mar	G84-3	5 mT	357	67	9/6	3.9	300.4	0.578
mb2b	rd cut	G84-9	5 mT	1	70	15/13	1.8	528.3	0.463
mb2b	rd cut	G85-16	10 mT	348	70	14/13	1.8	526.4	0.883
mb2c	rd cut	G84-2	20 mT	357	70	12/12	1.3	1116.1	0.267
mb2c	rd cut	G84-8b	10 mT	351	73	10/9	2.3	513.4	0.481
mb2c	rd cut	G84-13	10 mT	359	72	14/14	1.7	554.3	0.644
mb2c	rd cut	G84-8a	5 mT	353	70	4/4	1.7	2919.4	0.903
		avg		358	71	12/11	1.6	845.7	0.573
mb3a	tumuli	S82-b3	20 mT	6	63	5/5	0.9	1594.4	0.595
mb4a	flow mar	G85-10	NRM	13	59	12/12	2.6	273.6	0.778
mb3b	flow mar	G84-18	10 mT	338	63	10/8	3.8	210.2	1.027
mb3c	flow mar	G86-2	NRM	338	63	7/7	4.1	220.5	0.603
mb3c	flow mar	G86-1	NRM	351	57	7/5	10.8	51.3	1.522
mb3c	flow mar	G85-18	NRM	341	65	9/6	4.9	190.2	2.018
mb3d	flow mar	G85-17	30 mT	345	66	12/12	4.3	102.6	1.018
mb3d	rd cut	S82-sm3	50 mT	342	68	7/7	2.6	527.4	0.481
mb4a	flow mar	G84-23	NRM	355	63	11/7	4.2	205.7	1.504
mb4a	rd cut	G84-15	20 mT	336	67	15/14	1.3	967.8	0.386
mb4b	levee	G85-20	20 mT	352	69	8/8	2.2	634.1	0.381
mb4b	tumuli	G85-19	20 mT	326	57	7/7	2.8	455.9	0.295
mb4b	rd cut	G84-21	20 mT	346	66	15/15	1.5	624.2	0.475
mb4b	rd cut	G85-8	20 mT	347	65	9/9	2.2	529.0	0.766
mb4b	flow mar	G85-12	40 mT	339	65	13/13	2.0	410.1	0.733
mb4b	rd cut	G84-20	5 mT	342	60	13/13	1.7	566.8	0.611
mb5	rd cut	S82-b1	20 mT	293	30	6/6	31.2	5.5	0.991
mb5	levee	G86-4	40 mT	336	61	8/7	2.5	568.6	1.345
mb6?	rd cut	G86-5	5 mT	357	65	8/6	3.6	356.7	1.460
mb6?	rd cut	G86-3	NRM	331	67	6/5	4.4	300.7	0.195
mb5	flow top	G85-15	30 mT	334	65	13/10	4.6	110.3	0.484
mb5	flow mar	G85-14	10 mT	329	70	9/9	2.0	662.9	1.469
mb5	tumuli	G85-23	NRM	335	69	10/8	4.0	188.6	2.124
		avg		341	65	20/18	1.8	388.6	0.949
mb6	rd cut	G84-22	5 mT	2	65	13/11	1.9	575.1	1.071
mb6	gutter	G85-9	20 mT	356	71	11/11	2.4	360.7	0.810
lc	rd cut	s82-11	5 mT	338	69	5/4	5.3	304.1	0.626

Explanation: Map unit, map designations (fig. 5) based on vent locations, mb-lavas flows of the MBVC (1=Sheridan Mountain area; 2=Siah area; 3,4, and 5=Mount Bachelor-Kwohl Butte area; 6=Egan cone), mr-lava flows from the Red Crater chain of cones, mk-lava flows from Katsuk Butte, lc-lava flows from LeConte Crater; Type, nature of outcrop sampled; Site, field sample number; Expt, demagnetization level resulting in least dispersion of directions; Dec, declination in degrees from true north; Inc, inclination in degrees; N/N1, N-total number of samples collected per site, N1-number of samples used for calculating directions and statistics; A95, semiangle of the cone of 95 percent confidence in degrees; k, precision parameter (Fisher, 1953); Arith av j, arithmetic average intensity in amperes per meter (Am^{-1}).

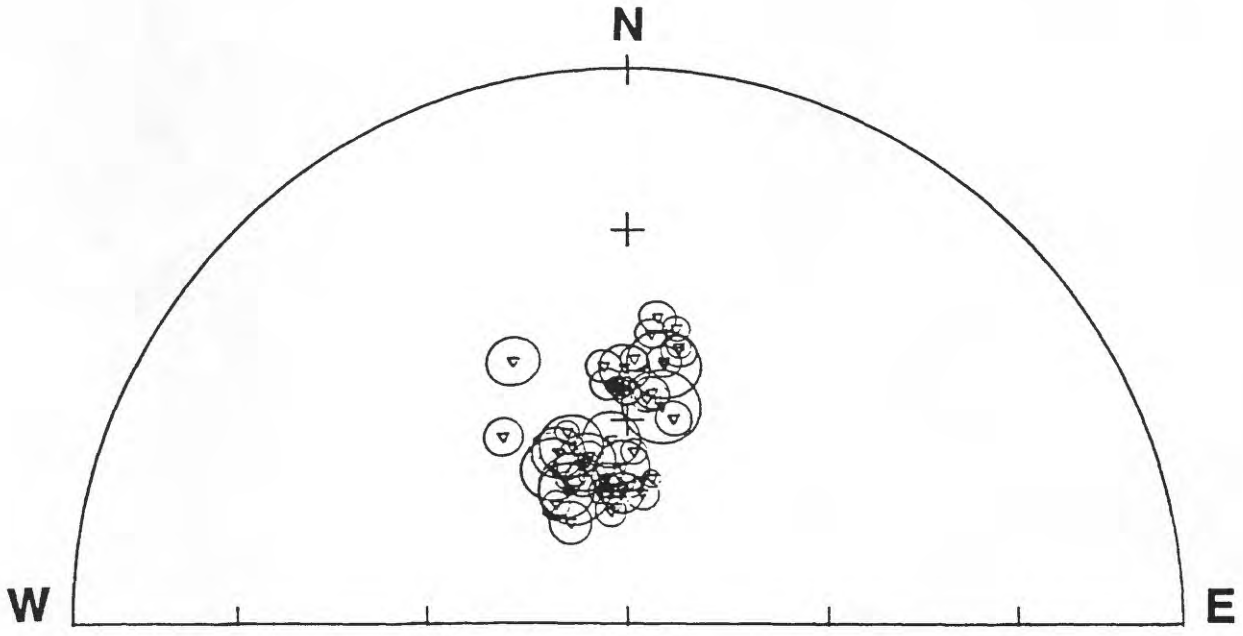

Figure 10. Lower hemisphere equal-area stereonet of mean site paleomagnetic directions with corresponding cones of 95 percent confidence. Tick marks in 30 degree intervals.

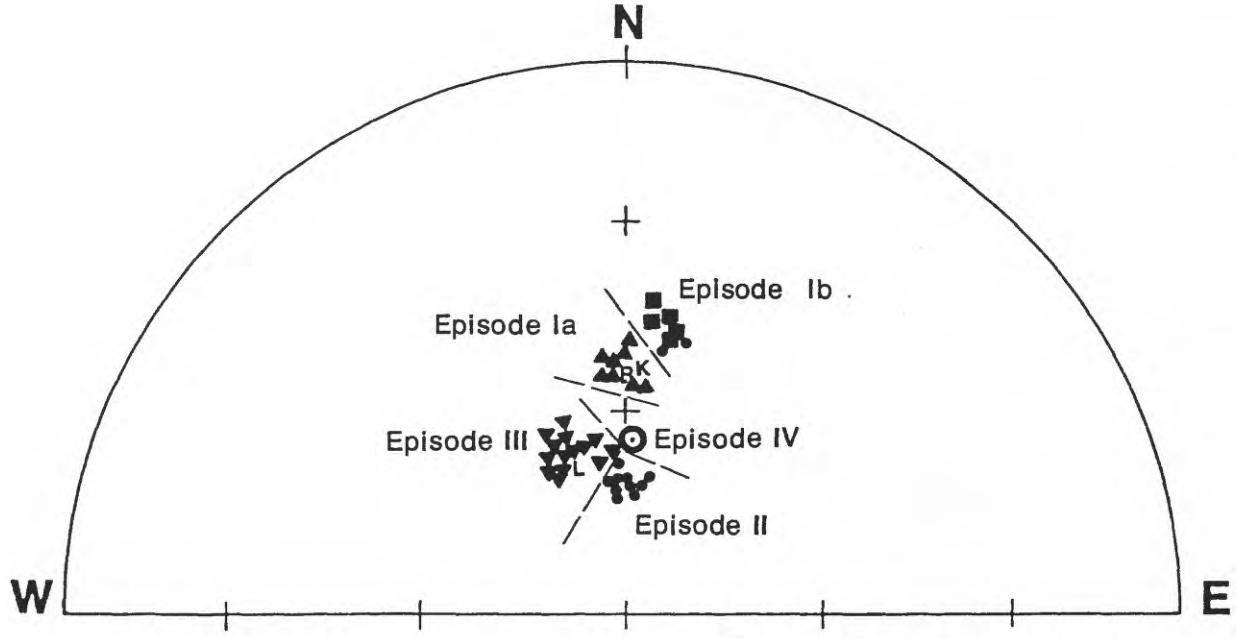

Figure 11. Lower hemisphere equal-area stereonet of mean site directions. Symbols and letters correspond to vent locations: triangles up and squares=Sheridan Mountain area; circles = Siah Butte area; triangles down = Mount Bachelor-Kwohl Butte area; circle with dot = Egan Cone; L = Le Conte Crater; R = Red Crater area; K = Katsuk Butte area. Dashed lines separate eruptive episodes.

sampled (G86-1) and it yielded a spurious direction; therefore it cannot be assigned to an eruptive episode on the basis of directional similarity. However, I have grouped the north flank cinder cones with eruptive episode III of the Bachelor-Kwohl areas on the basis of geographic position and intensity of remanent magnetization. The placement of these cinder cones within eruptive episodes is admittedly tenuous; however, difficulties in finding suitable drilling sites, coupled with the similarity of basalt chemistry throughout the MBVC, makes resolving the relative ages of these deposits problematic.

The last eruptive episode, episode IV, corresponds to the emplacement of Egan cone and associated basaltic lava flows on the north side of Mount Bachelor (fig. 12e). Basaltic andesite lava flows were also erupted from the Egan vent area, but are older than Egan cone and associated basaltic lava flows on the basis of paleomagnetic directions (table 2). Basaltic lava flows from Egan cone overlie basaltic andesite lava flows from the Mount Bachelor summit. Activity along the MBVC apparently ceased after emplacement of these youngest lava flows from Egan cone (Scott and Gardner, 1985). Differences in the paleomagnetic directions of the Egan lava flows (D= 2°; I=65°) and those of the Mount Bachelor-Kwohl Butte lava flows (D= 341°; I= 65°) suggest that a hiatus in volcanic activity occurred between episodes III and IV (fig. 11).

CONCLUSIONS

In summary, the paleomagnetic data suggest the following relations:

1) Eruptive activity along the MBVC was not continuous on the basis of clustered paleomagnetic directions. Four eruptive episodes are delineated on the basis of paleomagnetic directions and vent locations.

2) A hiatus in volcanic activity separates eruptive episodes Ib and episode II, and eruptive episodes III and IV.

3) Early eruptive activity (episode Ia and Ib) was widespread, encompassing the entire length of the chain, whereas subsequent eruptive activity (episodes II, III, and IV) was confined to locally discrete areas (fig. 12a-e).

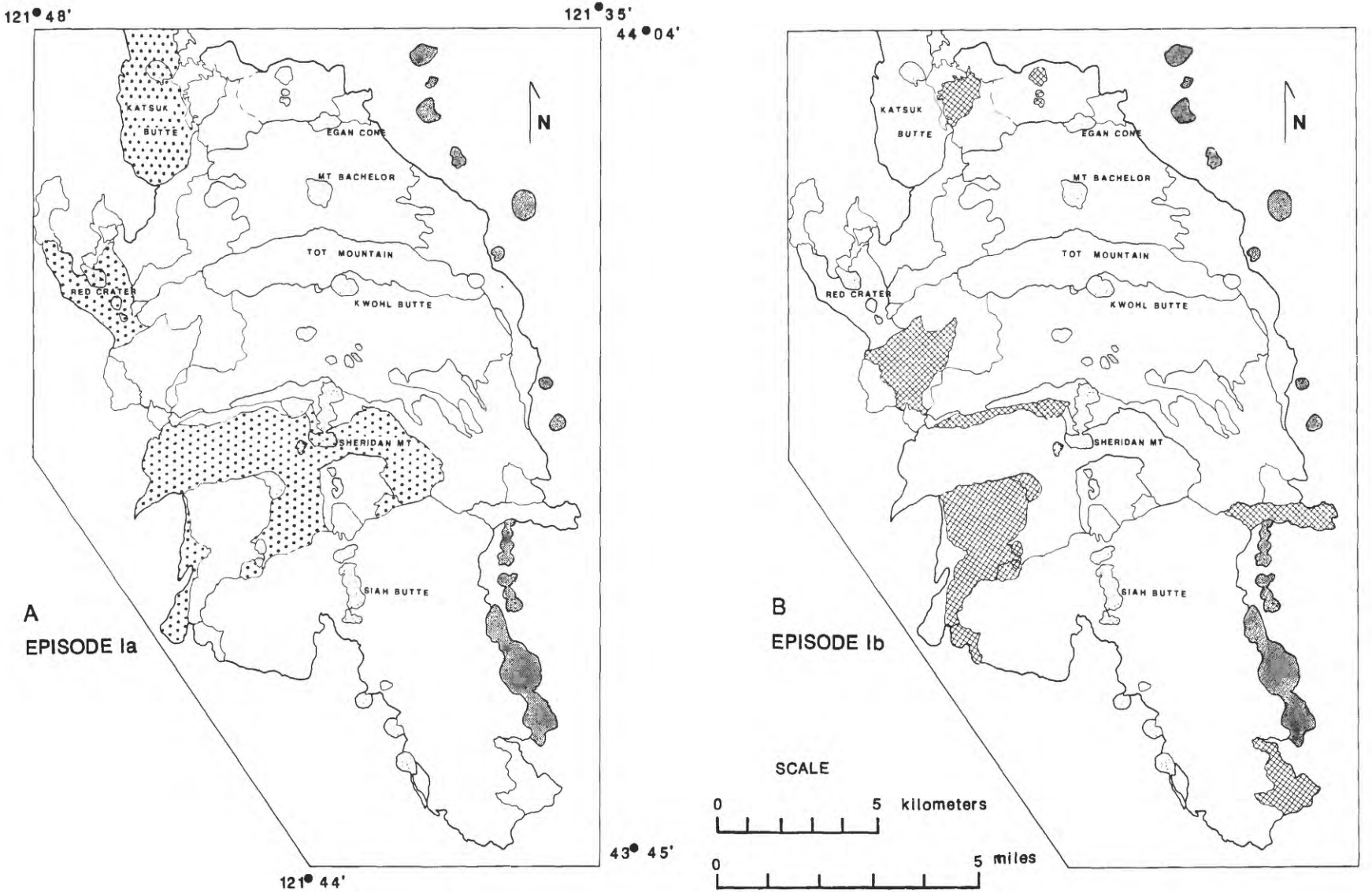

Figure 12. Maps showing the development of the Mount Bachelor volcanic chain based on paleomagnetic directions. Chain of vents shown in dark screen along east edge of maps pre-date the MBVC; pyroclastic cones of MBVC have light stipple. Episodes are discussed in text.

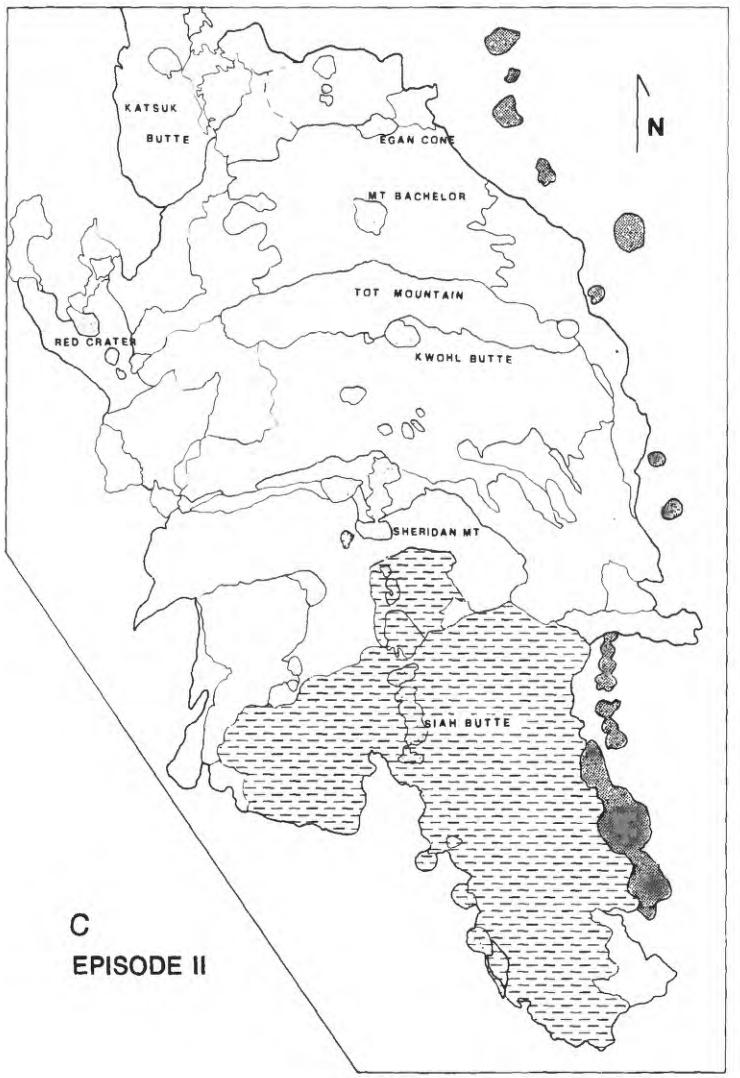

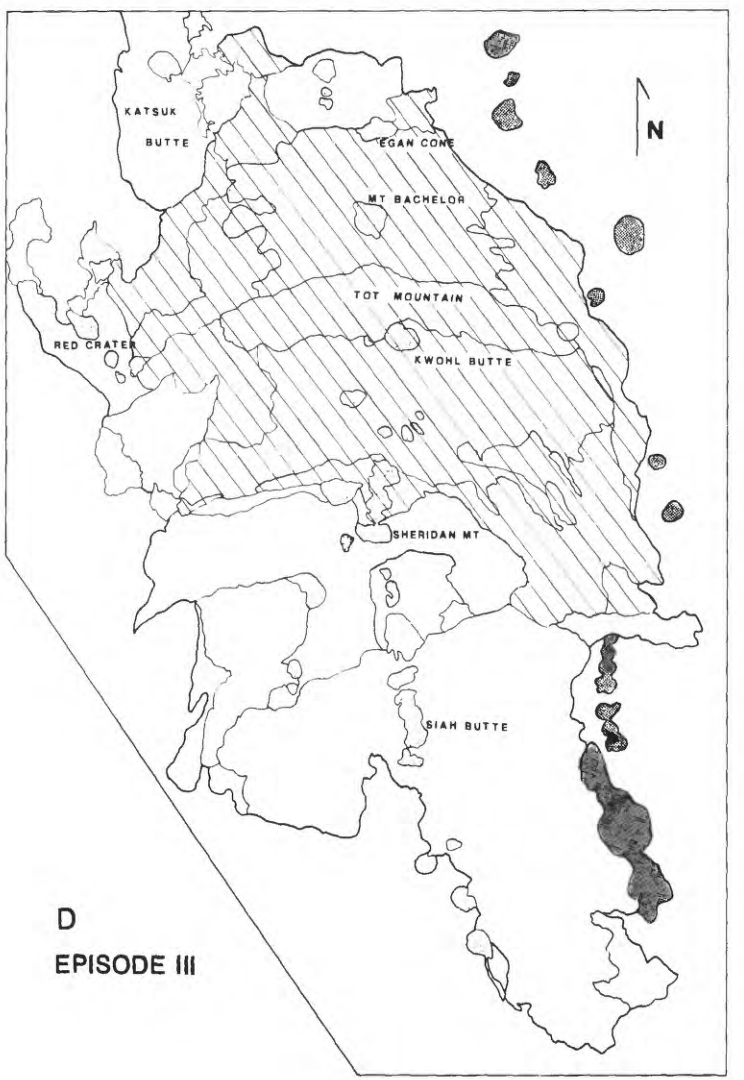

Figure 12. continued

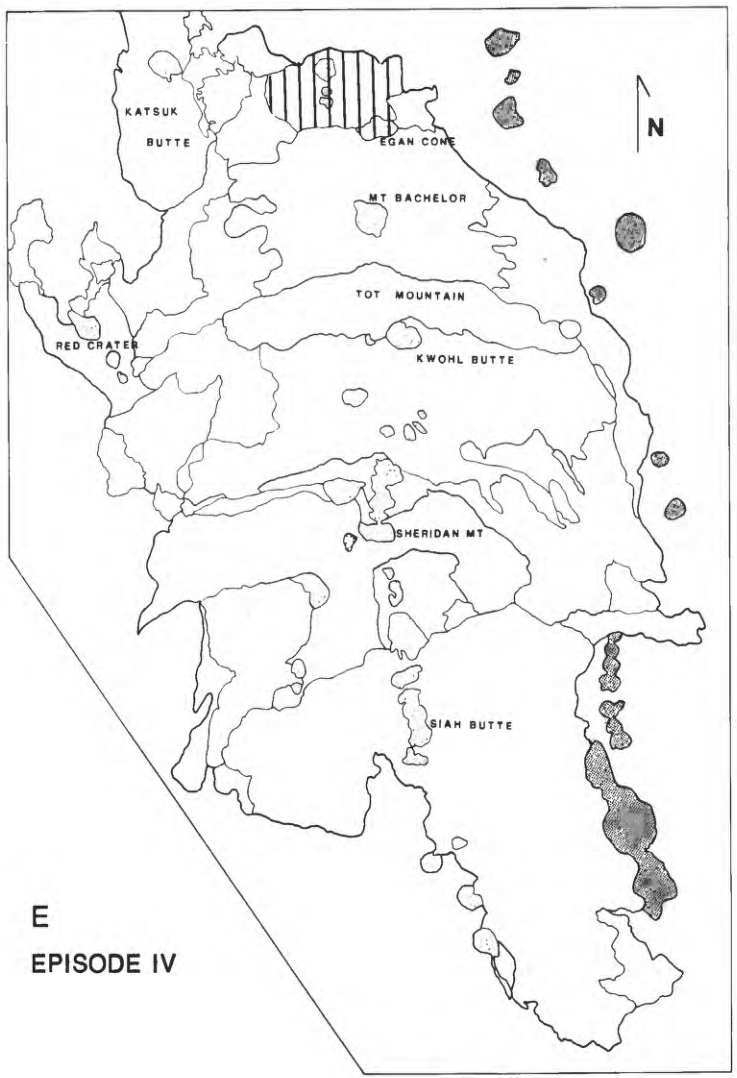

Figure 12. continued

NEOGLACIAL AND LATE-GLACIAL EROSION RATES OF MOUNT BACHELOR

by
Scott C. Lundstrom
Department of Geological Sciences and INSTAAR
University of Colorado
Boulder, CO 80309
and
William E. Scott

The volcanic and glacial stratigraphy and chronology developed for Mount Bachelor (Scott and Gardner, in press; Scott, this volume) provide an unusually good opportunity to estimate rates of glacial erosion of a Cascade volcano because preglacial and morainal landforms and their ages are relatively well constrained. Map units discussed in this paper are shown in Figures 5 and 9.

The following assumptions were used in estimating cirque and deposit volumes.

1. Moraines were assumed to lie on a planar bed and to lack ice cores. The volume of material was obtained by multiplying subdivided areas of deposit by one-half the amount of relief expressed by contour lines (contour interval = 40 ft).
2. On the basis of observations of the limited available exposures, younger neoglacial moraines (unit gln) were assumed to be cored by older neoglacial till (unit gen), which comprises 50 percent of moraine volume.
3. The moraines of Canyon Creek age (unit gc) were assumed to have twice the volume of the right-lateral moraines, because the left-lateral moraines are partly obscured by overlying lava flows of unit mb5b (fig. 9).
4. Cirque volume was derived by subtracting modern topography from a reconstructed Mount Bachelor summit cone having smooth contours and adding the volume of younger neoglacial deposits (unit gln) that lie in the cirque.

The estimated cirque volume of 10^7 m^3 divided by cirque area of 2.6×10^5 m^3 yields an estimated average erosion depth of 38.5 m, and an average erosion rate of 3.0 mm/yr when divided by 13,000 yr. As there is little, if any, glacial erosion occurring at present because of the small mass of ice and snow in the cirque, and as conditions similar to present probably existed at other times during the past 13,000 yr, rates of erosion during times of greater glacial cover were probably greater than this long-term average.

By assuming that the relative proportions of moraine volumes of late-glacial age (unit gc) and early- (unit gen) and late- (unit gln) neoglacial age are representative of the amount of cirque erosion over a constant area for the assumed duration of a glacial event, erosion rates can be calculated (table 3).

The volume estimates of the cirque and of total glacial deposits, including moraines and outwash converted to rock volume by a 0.8 multiplier, are nearly equal, and the difference (14%) may be within the error of the estimates. Therefore, little debris was transported long distances beyond the cone, which is consistent with the lack of distal alluvial deposits. (Outwash included in these measurements extends as far downstream as the fan at the base of the cone that is fed by the stream heading in the cirque (fig. 9)).

The Canyon Creek drift is by far the most voluminous and extensive of the glacial units and probably represents the time interval during which the majority of glacial erosion occurred on Mount Bachelor. The duration of the Canyon Creek advance is not well constrained, but 1,000 to 3,000 yr is permitted within the uncertainty of dating in the central Oregon Cascades and of correlative drifts elsewhere in the Pacific Northwest (Porter and others, 1983). (For purposes of this study the age of the maximum advance of Canyon Creek age is of less significance than the time during which the belt of Canyon Creek moraines was deposited). Such durations yield erosion rates of 8-24 mm/yr. Cirque glaciers of early and late neoglacial age were respectively 2-3 times less areally extensive than glaciers of Canyon Creek age, and apparently eroded at rates of about 3-6 mm/yr. The erosion-rate difference is as much as 8 times greater during the Canyon Creek advance if a duration of 1,000 yr is assumed for the Canyon Creek; however, the difference is reduced to a factor of 3 or less, if a longer duration is assumed. Likewise, the durations of neoglacial events may be significantly less than those estimated here, and the rates greater. Better evaluation of erosion-rate differences must await better dating of glacial events.

Table 3. Glacial erosion-rate data for Mount Bachelor

Deposit or landform	Volume (x 10^6 m^3)	% of total volume of moraines	Age control (kyr)	Duration of glacial event (yr)	Erosion rate (mm/yr)
Cirque	10		<13	13,000	3
Canyon Creek drift (gc)	4.0	68	<13,>9.5	1000-3000	24 8
Early neoglacial drift (gen)	1.0	17	<6.8,>2	1000-2000	6 3
Late neoglacial drift (gln)	0.9	15	<2	1000-2000	5 2
Total moraines	5.9	100			
Total outwash	5.6				
Total deposits x 0.8 (to rock equivalent)	9.2				

For example, erosion rate for Canyon Creek interval is:

$$\frac{\text{total deposits x unit gc's percent of total moraine volume}}{\text{area of cirque x assumed time interval}} = \text{erosion rate}$$

$$\frac{9.2 \times 0.68}{0.26 \times 3000} = 0.008 \text{ m/yr or } 8.0 \text{ mm/yr}$$

Despite these uncertainties, the rates of glacial erosion calculated here are clearly high relative to those reported for various settings in other parts of the world (table 4). High rates of glacial erosion on Cascade volcanoes (Mills, 1976; this study) are probably related to both (1) the highly erodible nature and high relief of steep volcanoes and (2) the high activity indices (a higher activity index, or altitudinal gradient of net balance, means that more ice is transported from accumulation area to ablation area) of temperate maritime glaciers of the Cascade Range (Meier, 1961) with resulting high rates of ice flow and glacial power (Andrews, 1972).

Table 4. Glacial erosion rates from various settings.

Location; time interval	Rate (mm/yr)	Source
Mount Bachelor, Oregon Cascades; past 13,000 yr	3-24	This study
Mount Rainier, Washington Cascades; modern	2.8-8.2	Mills, 1976
Swiss Alps; modern	1.5-2.3	Small, 1987
Colorado Front Range; neoglacial and modern	0.95-4.9	Reheis, 1975
West Norway; Younger Dryas	0.5-0.6	Larsen and Mangerud, 1981
Antarctic volcanoes, Marie Byrd Land; Quaternary	0.36-0.46	Andrews and LeMasurier,1973
Baffin Island, N.W.T., Canada; neoglacial	0.025-0.09	Andrews, 1971
"	0.008-0.076	Anderson, 1978

GEOCHEMICAL VARIATIONS OF LAVAS FROM THE MOUNT BACHELOR VOLCANIC CHAIN

by
Cynthia A. Gardner

INTRODUCTION

The central Oregon High Cascades are unique with respect to the rest of the range because of the predominance of mafic over silicic volcanism (White and McBirney 1978; Taylor, 1981; Hughes and Taylor, 1986; Sherrod, 1986). The 25-km-long, N-S-trending Mount Bachelor volcanic chain (MBVC) typifies one eruptive style of mafic volcanism found throughout the region: effusive eruptions from numerous aligned vents over a short time period (fig. 3). Between 30-50 km^3 of basalt (49-52 wt % SiO_2) and basaltic andesite (52 to 57 wt % SiO_2; LeBas and others, 1986) was erupted over the 8 to 10-k.y. history of the chain (Scott and Gardner, 1985; in press).

Detailed field (Scott and Gardner, in press) and paleomagnetic (Gardner, this volume; 1989) studies provide the stratigraphic framework within which to evaluate the geochemical variations and evolution of the MBVC. In this paper, I will briefly discuss general field characteristics, summarize the geochemistry, and show the temporal and spatial relations of the various rock types.

FIELD CHARACTERISTICS

Basaltic lava flows (49-52 wt % SiO_2) are olivine-phyric or olivine- and plagioclase-phryric, typically thin (<5 m), and fresh lava-flow interiors are medium-dark gray to medium gray. The lava flows range from dense to highly vesicular, with vesicularity varying among flows. The base of the Mount Bachelor and Kwohl Butte shields are basaltic in composition as are most of the cinder cones and associated lava flows throughout the MBVC. Areas of lava-tube formation are restricted to lava flows of basaltic chemistry.

The low-silica basaltic andesite lava flows (52-55 wt % SiO_2) are olivine- and plagioclase-phyric and in general contain more plagioclase than basalt. Cumulocrysts (aggregates of plagioclase and olivine) and glomerocrysts (aggregates of just olivine or just plagioclase) are more common than in the basalt and are useful for distinguishing between lava flows in the field. Three distinctive lithologic types are found within the basaltic andesite flows: 1) porphyritic lava flows composed of euhedral plagioclase phenocrysts up to 8 mm in size; 2) olivine-phyric lava flows with abundant laths of plagioclase microphenocryts; and 3) aphanitic lava flows. Fresh lava-flow interiors are typically medium gray to medium-dark gray, and like the basalts, range from dense to vesicular. The Sheridan shield, the cinder cone of Sheridan Mountain, and the upper sections of the Kwohl and Mount Bachelor shields are composed of low-silica basaltic andesite. Lava flows containing tumuli are common in this silica range.

High-silica basaltic andesite lava flows (55-57 wt % SiO_2), that form Tot Mountain and the steep-sided summit cone of Mount Bachelor, are olivine- and plagioclase-phyric: the lava flows of the summit cone are unique in that they contain clinopyroxene as a phenocryst phase as well. The high-silica basaltic andesite lava flows are more porphyritic and contain more abundant cumulocrysts and glomerocrysts than either the basalt or low-silica basaltic andesite lava flows and are therefore distinctive in the field. Fresh lava-flow interiors are medium gray and finely vesicular.

GEOCHEMISTRY

About 130 samples were analyzed for whole-rock major elements, 60 samples for trace elements (Cr, Ni, Rb, Sr, Y, Nb, Zr, and Zn), and 17 samples for rare earth (REE) and minor elements (Co, Sc, Ba, Cs, Rb, Sr, Hf, and Th) by the Branch of Analytical Chemistry of the U. S. Geological Survey. All geochemical analyses are in Gardner (1989), and a summary of geochemical analytical procedures is given in Baedecker (1987).

Ten geochemical groups--four basalt and six basaltic andesite groups--were distinguished along the MBVC primarily on the basis of major- and trace-element geochemistry and on the correlation of the geochemical groups with stratigraphic packages (table 5): a detailed discussion on the formation of the ten geochemical groups is in Gardner, 1989. The ten geochemical groups form three assemblages (PM1, PM2, and PM3) with distinctive compositional characteristics (fig. 13), which I interpret to represent three different magma assemblages that erupted along the MBVC.

PM1 is the most primative assemblage (most MgO- and Cr- rich and has the highest magnesium number at a given SiO_2 value); it spans most of the silica range and includes lavas of geochemical groups I, II, VII, VIII, IX, and X (table 5; fig. 13). Volumetrically, the majority of lava flows of the MBVC belong to the PM1(parental magma 1) assemblage, which includes the basalt cinder cones of the Siah chain (part of group I), Kwohl-Bachelor shield (VII), Sheridan shield (VIII), Tot Mountain (IX) and the summit cone of Mount Bachelor (X). I classify the PM1 assemblage as calc-alkaline according to the classification scheme advanced by Miyashiro (1974).

Lava flows of assemblage PM2, basalt (groups III and IV) and low-silica basaltic andesite (group V; table 5)

Table 5. Summary of geochemical analyses of rocks from the Mount Bachelor volcanic chain.

	BASALT				BASALTIC ANDESITE					
PARENTAL MAGMA	PM 1		PM 2		PM 2	PM 3	PM1			
GEOCHEM. GROUP	I	II	III	IV	V	VI	VI	VIII	IX	X
ELEMENTS										
Major (wt %)										
SiO2	51.1 ± 0.31	52.1 ± 0.72	50.0 ± 0.18	51.7 ± 0.06	52.9 ± 0.43	52.8 ± 0.44	53.7 ± 0.63	54.0 ± 0.63	55.80	56.6 ± 0.09
Al2O3	17.3 ± 0.13	17.3 ± 0.20	16.8 ± 0.11	17.4 ± 0.03	17.8 ± 0.23	18.3 ± 0.15	17.4 ± 0.25	17.4 ± 0.06	17.80	18.1 ± 0.09
Fe2O3	9.68 ± 0.20	9.59 ± 0.32	11.89 ± 0.12	11.36 ± 0.11	10.0 ± 0.42	8.89 ± 0.06	8.64 ± 0.19	8.5 ± 0.08	7.80	7.78 ± 0.13
MgO	7.68 ± 0.29	6.94 ± 0.60	7.07 ± 0.17	5.44 ± 0.10	4.86 ± 0.37	5.62 ± 0.12	5.82 ± 0.41	5.14 ± 0.13	4.47	3.36 ± 0.25
CaO	9.39 ± 0.16	8.84 ± 0.29	8.79 ± 0.03	8.48 ± 0.06	8.09 ± 0.19	8.76 ± 0.29	8.37 ± 0.09	8.75 ± 0.24	8.09	7.59 ± 0.24
Na2O	3.31 ± 0.08	3.46 ± 0.15	3.4 ± 0.08	3.64 ± 0.05	3.61 ± 0.1	3.49 ± 0.06	3.49 ± 0.06	3.45 ± 0.05	3.54	3.91 ± 0.12
K2O	0.62 ± 0.06	0.76 ± 0.11	0.61 ± 0.03	0.66 ± 0.03	0.75 ± 0.04	0.64 ± 0.04	0.94 ± 0.07	0.96 ± 0.05	1.10	123 ± 0.03
TiO2	1.35 ± 0.08	1.45 ± 0.13	1.9 ± 0.04	1.75 ± 0.02	1.49 ± 0.15	1.12 ± 0.01	1.17 ± 0.06	1.19 ± 0.04	1.04	1.07 ± 0.04
P2O5	0.3 ± 0.06	0.38 ± 0.06	0.53 ± 0.03	0.57 ± 0.02	0.36 ± 0.05	0.23 ± 0.03	0.33 ± 0.002	0.38 ± 0.02	0.28	0.27 ± 0.01
MnO	0.15 ± 0.00	0.15 ± 0.00	0.18 ± 0.00	0.17 ± 0.00	0.15 ± 0.00	0.13 ± 0.00	0.14 ± 0.0	0.14 ± 0.0	0.12	0.12 ± 0.0
Mg#	65	62	58	52	50	56	57	55	53	46
No. of samples	46	5	6	6	4	6	25	7	1	18
Trace and REE										
Cr*	270 ± 30	190 ± 8	215 ± 42	60 ± 7	44 ± 13	92 ± 19	140 ± 28	123 ± 40	85	< 20
Ni*	140 ± 16	100 ± 8	108 ± 14	56 ± 5	46 ± 10	76 ± 8	92 ± 17	58 ± 20	50	< 20
Co	38.4 ± 1.6	34.7 ± 0.14	40.1 ± 0.6	34.7	31.3	32.8 ± 1.6	32 ± 0.7	27.6 ± 1		21.1
Sc	27.2 ± 0.83	25 ± 1.9	26.8 ± 0.9	25.8	22.8	22.5 ± 0.6	22.8 ± 0.9	25.5 ± 0.9		19.5
Ba	235 ± 29	319 ± 47	301 ± 13	389	416	287 ± 49	369 ± 18	377 ± 21		461
Cs	0.27 ± 0.02	0.39 ± 0.1	0.24 ± 0.02	0.33	0.31	0.34 ± 0.0	0.44 ± 0.8	0.55 ± 0.0		0.954
Rb	11.3 ± 2.9	12.9 ± 3.9	8.7 ± 1.9	16.3	11.5	12.6 ± 1.9	13.8 ± 3.3	18.2 ± 2.8	29	28.1
Sr*	461 ± 28	531 ± 21	486 ± 18	491 ± 8	549 ± 27	630 ± 19	548 ± 20	539 ± 23	592	532 ± 20
La	11.3 ± 0.8	15.9 ± 0.8	14.9 ± 0.07	15.4	16.2	9.78 ± 1.0	15.2 ± 0.9	17.4 ± 0.64		18.3
Ce	27.4 ± 1.2	42.9 ± 1.0	38.9 ± 1.77	38.6	41.2	23.3 ± 3	35.3 ± 2.8	41.1 ± 2.2		40.4
Nd	15.6 ± 0.8	21.1 ± 0.8	22.9 ± 0.49	22.7	23.8	13.5 ± 0.8	17.4 ± 1.9	20.3 ± 0.07		18.5
Sm	4.14 ± 0.17	5.51 ± 0.47	5.82 ± 0.06	6.2	5.95	3.5 ± 0.24	4.12 ± 0.29	4.68 ± 0.25		4.62
Eu	1.44 ± 0.08	1.78 ± 0.08	1.98 ± 0.0	2.13	1.95	1.22 ± 0.06	1.41 ± 0.08	1.51 ± 0.05		1.42
Gd	4.66 ± 0.09	5.78 ± 0.25	6.56 ± 0.25	6.89	6.11	3.58 ± 0.18	4.55 ± 0.22	4.95 ± 0.41		4.91
Tb	0.72 ± 0.01	0.86 ± 0.03	1.01 ± 0.08	1.05	0.933	0.52 ± 0.02	0.70 ± 0.07	0.78 ± 0.03		0.757
Tm	0.37 ± 0.04	0.44 ± 0.02	0.51 ± 0.01	0.55	0.458	0.28 ± 0.01	0.37 ± 0.03	0.41 ± 0.02		0.411
Yb	2.37 ± 0.09	2.72 ± 0.08	3.11 ± 0.46	3.4	2.83	1.71 ± 0.06	2.25 ± 0.23	2.53 ± 0.18		2.55
Lu	0.35 ± 0.01	0.40 ± 0.01	0.46 ± 0.0	0.501	0.418	0.25 ± 0.01	0.32 ± 0.04	0.38 ± 0.03		0.373
Y*	24 ± 3	23 ± 3	34 ± 3	31 ± 3	24 ± 4	18 ± 1	25 ± 3	28 ± 3		24 ± 3
Zr*	135 ± 10	165 ± 17.5	149 ± 4	149 ± 4	138 ± 19	104 ± 8	152 ± 10	161 ± 8	161	152 ± 7
Hf	2.93 ± 0.07	4.05 ± 0.04	4.06 ± 0.16	3.58	3.94	2.36 ± 0.12	3.15 ± 0.16	3.52 ± .13		3.63
Th	0.86 ± 0.19	1.12 ± .01	0.62 ± 0.01	0.895	0.992	0.75 ± 0.06	1.39 ± 0.28	1.68 ± 0.08		2.68
Zn*	77 ± 5	83 ± 5	94 ± 7	100 ± 3	93 ± 4	80 ± 0.0	81 ± 3	81 ± 2	80	78 ± 6
Cu*	62 ± 6	60 ± 0	65 ± 4	47 ± 4	59 ± 2	62 ± 3	66 ± 5	67 ± 6	60	55 ± 8

*Explanation. Major element analyses determined by WDXRF (wave-length dispersive x-ray florescence spectroscopy); analyses of trace-elements denoted by * were determined by EDXRF (energy dispersive x-ray florescence spectroscopy); REE and trace-element analyses determined by INAA (instrumental neutron activation analysis). Mg# = (moles MgO)/(moles MgO + moles FeO). No of samples = number of samples averaged to determine geochemical group and standard deviation of the major elements. The standard deviation for the REE and other trace elements are based on a much smaller and varying number of samples, where no statistics are recorded the sample size is one. The number of samples for a given geochemical group merely reflects the sampling distribution and does not imply either a greater volume or significance of that group.*

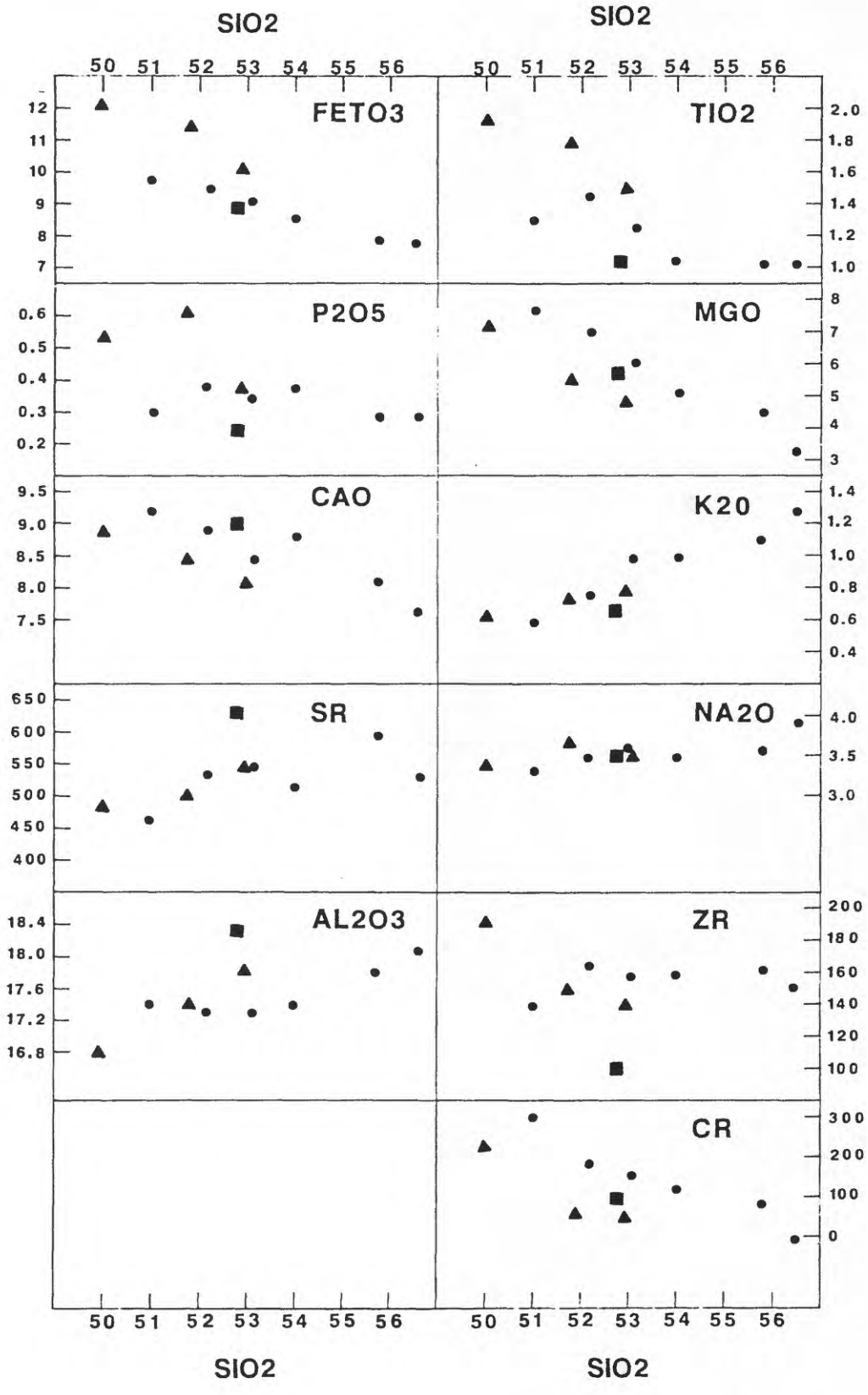

Figure 13. Geochemical variation diagrams of select oxides and trace elements plotted against SiO2 for the ten geochemical groups given in table 5. Symbols correspond to PM assemblabes; circles = PM1; triangles = PM2; and squares PM3.

of more evolved compostion, are enriched in total iron (reported as Fe_2O_3) and TiO_2 and depleted in CaO and MgO with respect to assemblage PM1 (fig. 13). This volumetrically smaller group includes basaltic lava flows from the Red Crater chain of cones (III) from Egan cone (IV) and low-silica basaltic andesite erupted from now buried vents (V). Some of the low-silica basaltic andesite lava flows of group V are plagioclase-phyric with the distinctive large, euhedral plagioclase phenocrysts described in the field characteristics section. I classify the PM2 assemblage as tholeiite (Miyashiro, 1974).

Lava flows of the PM3 assemblage are all low-silica basaltic andesite lava flows (group VI; table 5) that erupted from vents located near Sheridan Mountain. Assemblage PM3 is characterized by distinctly high concentrations of Al_2O_3 and Sr and low concentrations of Zr and REE (fig. 13; table 5). PM3 lava flows are of two distinctive lithologic types; aphanitic and plagioclase-phyric rocks with large, euhedral plagioclase phenocrysts (the latter looks similar to the PM2, group V flows) discussed in the field characteristics section. PM3 rocks are classified as calc-alkaline (Miyashiro, 1974).

SPATIAL AND TEMPORAL RELATIONS OF THE GEOCHEMICAL GROUPS

Spatial and temporal evolution of the MBVC determined by field mapping (Scott and Gardner, in press) and paleomagnetic secular-variation studies (Gardner, 1989; this volume) are shown in relation to the ten geochemical groups in figure 14. Of particular note with regard to the geochemical evolution of the MBVC are the following relationships: (1) PM1 vents are found dominantly along the central axis of the chain, whereas PM2 and PM3 vents are found dominantly along the margin or off axis of the chain; (2) during eruptive episodes I and III (figs. 14 a,b, and d; see Gardner, this volume, for an explanation of eruptive episodes) several different geochemical groups, as well as different PM assemblages, were erupted; whereas, during episodes II and IV (fig.14c and 14e), which were low-volume eruptive episodes, the chemistry of eruptive products was essentially uniform; (3) PM1, group 1 basalt was erupted during every eruptive episode except episode IV; and (4) the most silicic products were erupted at the north end of the MBVC, which is geographically closest to the silicic highlands area of the Three Sisters-Broken Top region (Hill and Taylor, this volume).

Petrologic models for the MBVC must account for differences between geochemical groups as well as for their spatial and temporal relations. Preliminary petrologic modeling (Gardner, 1989) suggests that PM1 basalt and basaltic andesite are related primarily by crystal fractionation with minor amounts of recharge and magma-mixing (O'Hara, 1977). PM2 basalt and basaltic andesite also appear related to each other by crystal fractionation, recharge and magma-mixing processes. No basaltic parent has been found in the Mount Bachelor area for the PM3 basaltic andesite, group VI lavas. This geochemical group may represent a differentiate whose basaltic parent has not been found, or may represent a 'near-primary' basaltic andesite (see Hughes, 1982; Hughes and Taylor, 1986). Geochemical indicators, REE signatures, incompatible trace element ratios, and mineral subtraction calculations (Gardner, 1989), suggest that the PM1 and PM2 magmas may have been derived from the same source region, but appear to have taken different evolutionary paths. However, these same geochemical indicators suggest that PM3 magmas were derived from a source region separate from that of the PM1 and PM2 magmas.

The high-silica basaltic andesite of the Mount Bachelor summit cone can be derived from the low-silica basaltic andesite of the Mount Bachelor shield by crystal fractionation and recharge processes without invoking assimilation of more silicic material. This is consistent with the petrography of these rocks in which there are no obvious indications of assimilation. Thus, the geographic relationship of the most siliceous products of the MBVC being situated nearest the Three Sisters-Broken Top silicic highlands area may reflect some common underlying structure in these areas that allows magmas to pond and differentiate prior to emplacement

CONCLUSIONS

Studies of both the High Cascade mafic platform north of the MBVC (Taylor, 1978; 1981; Hughes, 1982; Hughes and Taylor, 1986) and the Mount Bachelor volcanic chain (Gardner and Scott, 1987; Gardner, 1989) have shown that the mafic products of the central Oregon High Cascades are surprisingly diverse in chemical composition. The MBVC was fed by three different parental magmas, probably from two different source areas. Simultaneous eruptions of lava flows from more than one magma assemblage and geochemical group suggests that the MBVC was underlain by several small magma chambers.

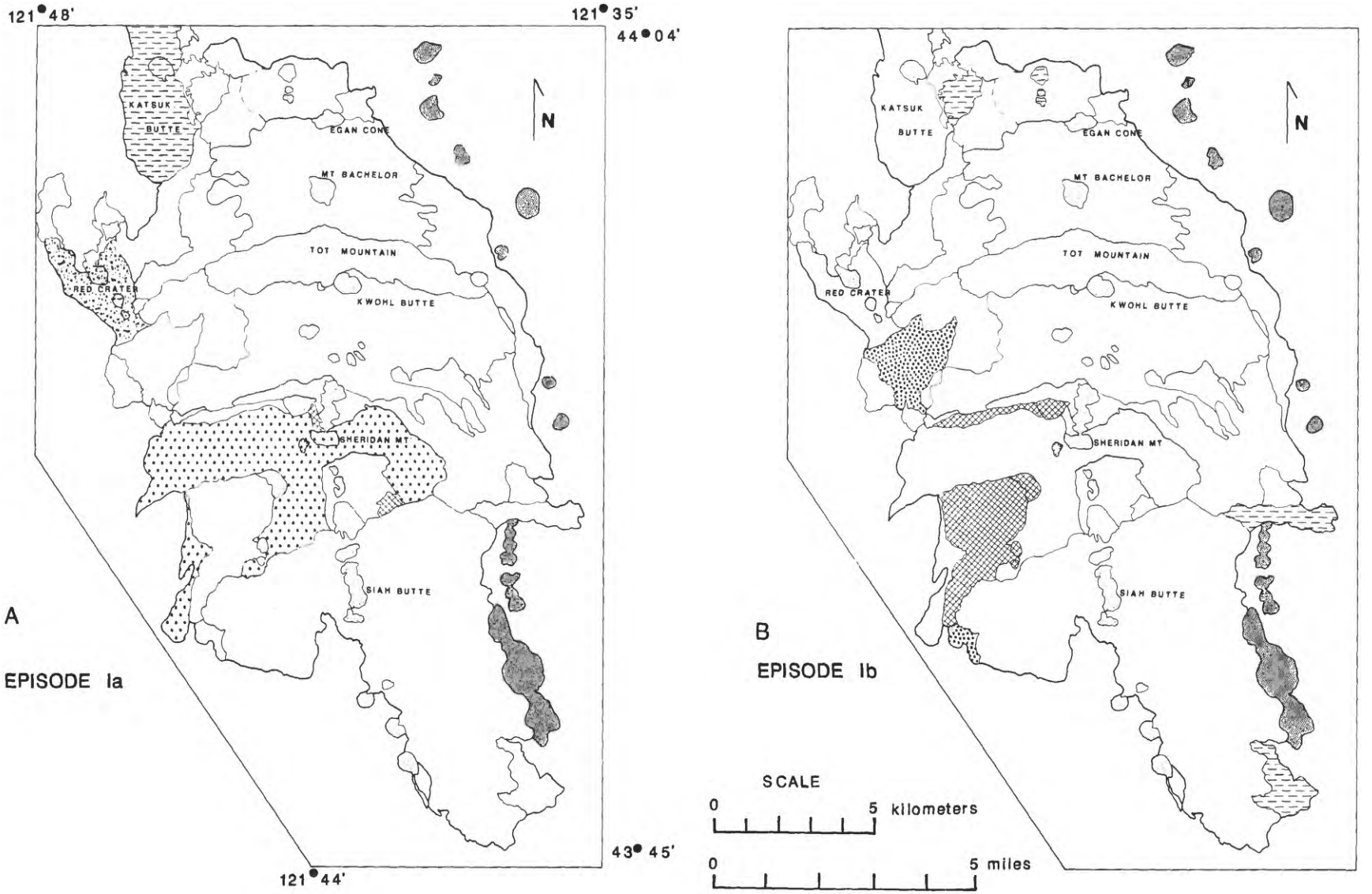

Figure 14. Maps showing the chemistry of eruptive products for each eruptive episode of the Mount Bachelor volcanic chain. Explanation of patterns shown after figure 14e.

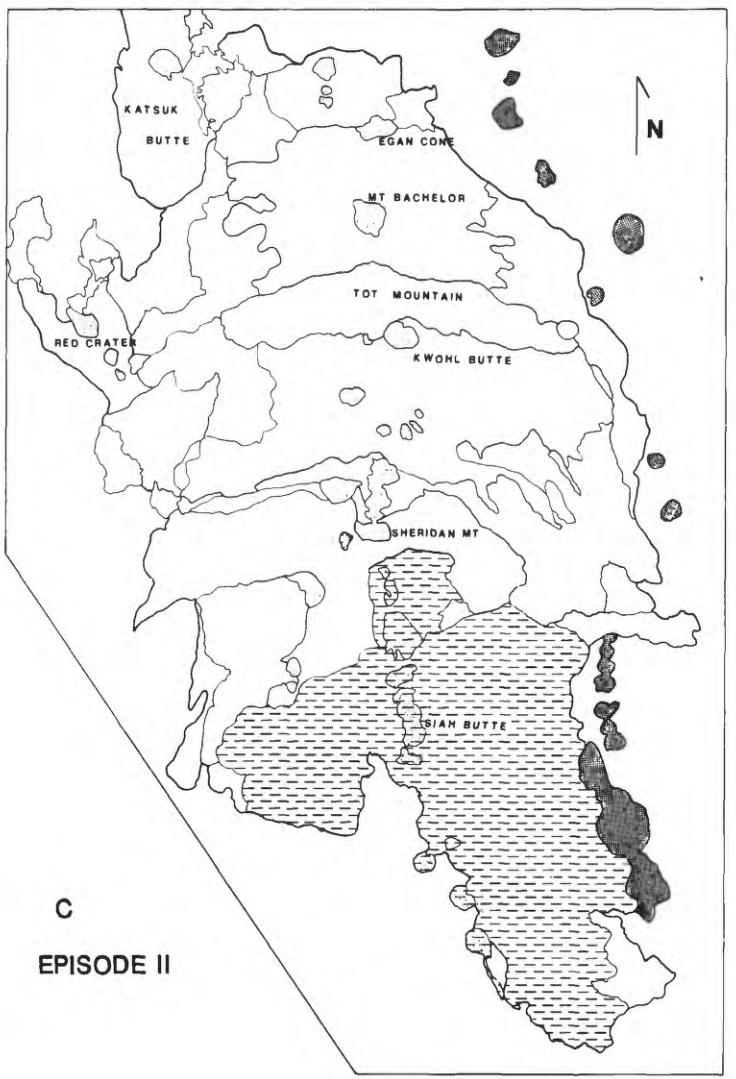

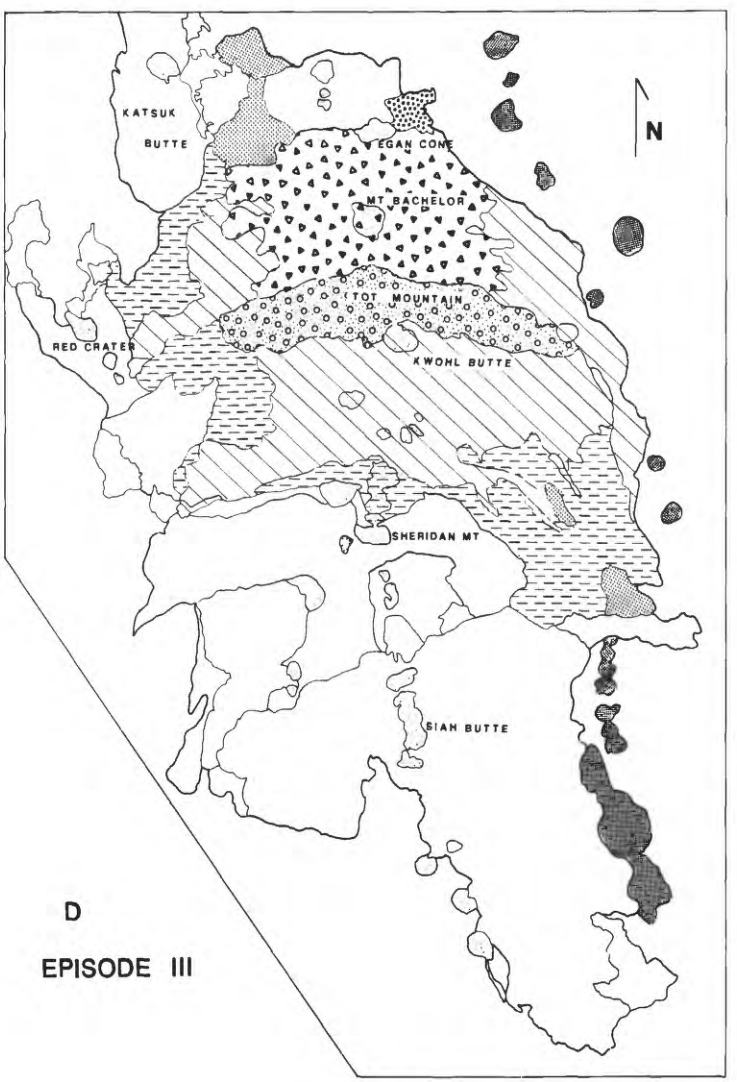

Figure 14. continued

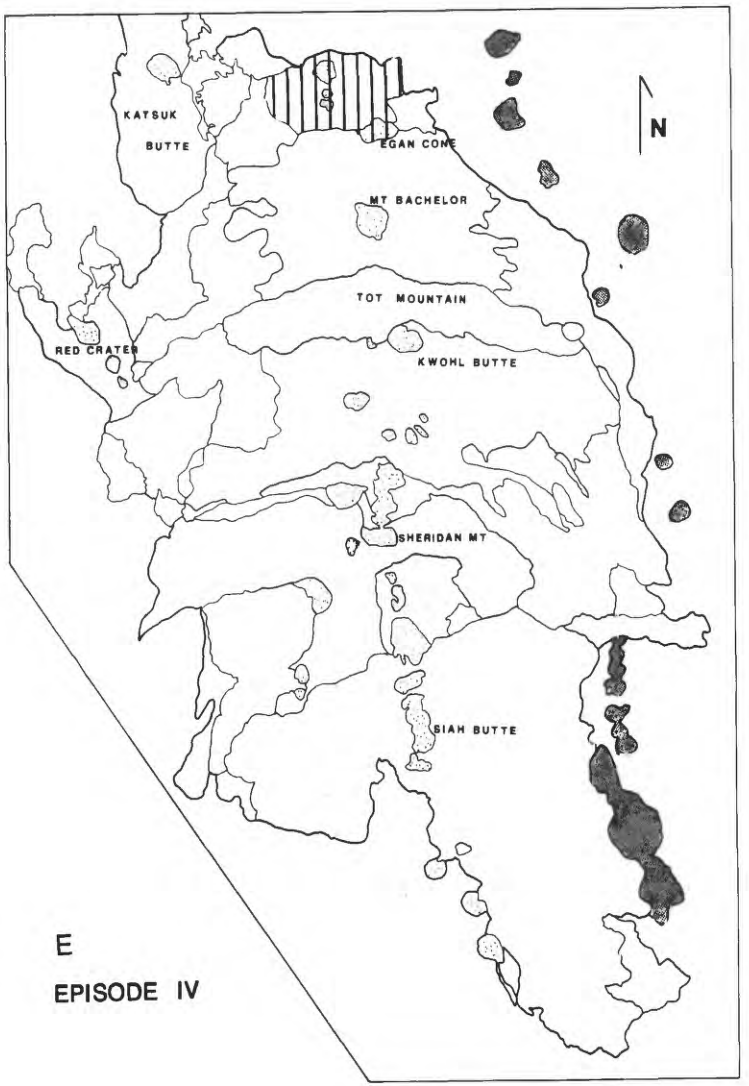

EXPLANATION

Vents of the MBVC

Vents of older cones in the MBVC region

	GEOCHEMICAL GROUP	PM TYPE
BASALTS	I	1
BASALTS	II	1
BASALTS	III	2
BASALTS	IV	2
BASALTIC ANDESITES	V	2
BASALTIC ANDESITES	VI	3
BASALTIC ANDESITES	VII	1
BASALTIC ANDESITES	VIII	1
BASALTIC ANDESITES	IX	1
BASALTIC ANDESITES	X	1

Figure 14. continued

ROAD LOG FOR DAY 2--SOUTHERN PART OF MOUNT BACHELOR VOLCANIC CHAIN AND LATE HOLOCENE RHYOLITE ERUPTIONS OF SOUTH SISTER

by
William E. Scott and Cynthia A. Gardner

The stops for Day 2 (fig. 1) focus on (1) the stratigraphic relations among some of the oldest recognized lava flows of the Mount Bachelor volcanic chain (MBVC) and end moraines and outwash fans of the Suttle Lake advance of late Wisconsin age, (2) the southernmost vents of the MBVC and the fault that extends south from them, (3) hydrovolcanic deposits and landforms in the Wuksi Butte-Twin Lakes chain that lies west of the south end of the MBVC, and (4) rhyolite tephra and lava flows from vents on the south flank of South Sister volcano.

Several maps and other figures from the road log and papers for Day 1 (especially figs. 1, 5, 7, 11-14) provide orientation and information for today's stops.

Mileage	Description of features along route
0.0	At junction of entrance road to Little Fawn Campground and USFS Road 4600-470; turn right; at 0.4 mi. bear right onto paved road.
1.1	On left, Red Crater, northernmost and largest of 2.5-km-long chain of postglacial scoria cones; road ahead is on the lava flow of Red Crater that dams Elk Lake.
1.7	Intersect Cascade Lakes Highway (Road 46) near margin of Red Crater lava flow; turn left (south).
2.5	Glacial striae and grooves on lava flows indicate direction of ice flow was to southeast, essentially parallel to road.
4.2	View on left of shield volcano of Sheridan Mountain (or Sheridan shield volcano; unit mb1) of the MBVC.
4.6	Junction with road to Lava Lake; continue south on Cascade Lakes Highway; ahead, roadcuts expose till overlying lava flows. For the next several miles, the highway traverses a belt of lateral and terminal moraines that record the apparently gradual retreat of the upper Deschutes glacier from its maximum advance of Suttle Lake age.
4.9	Meadow on left occupies a valley between two moraines that has been partly filled with sediment as a result of a locally raised base level caused by lava flows of the Sheridan shield volcano. Basal organic material in a 3.5-m-long core from the center of the meadow has an age of 12,200 ± 150 yr B.P. (W-5210); the base of a 40-cm-thick layer of Mazama ash is at 2.4 m; tephra of the Rock Mesa and Devils Hill(?) episodes is at a depth of about 25 cm. The core bottomed in gravel and sand that contains reworked scoriaceous ash that probably originated as tephra from the MBVC. The radiocarbon age provides only a minimum limiting age for deglaciation and eruptions of the MBVC because (1) deposition of organic matter did not begin until after emplacement of the lava flows, (2) the thickness of material sampled to obtain enough organic matter for dating must have accumulated over a period at least as long as several centuries, and (3) younger organic matter is probably contaminating the dated material.
7.4	Junction with road 4270; turn left and cross Deschutes River, passing Deschutes Bridge Guard Station and Campground. The well-vegetated and stable river banks result from the river experiencing only small variations in discharge through the year owing to its being fed mostly by springs. Road ahead traverses flat surface of outwash fan of Suttle Lake age of Deschutes River.
8.5	Cross Snow Creek, which is fed from springs that rise at the snout of a lava flow from the Sheridan shield volcano that occupies a narrow valley between two moraines. Road ahead climbs low scarp onto till.
9.1	Low road cuts in till.
9.4	Margin of lava flow of Sheridan shield. Park on side of road.

STOP 1--LAVA FLOW OF SHERIDAN SHIELD VOLCANO

This basaltic andesite lava flow (53.3% SiO_2) was erupted from the Sheridan shield volcano based on (1) its geometric relation with overlying flows that form the main part of the shield and (2) its chemical composition and paleomagnetic direction, which are similar to those of other lava flows of the shield. North of the stop, the lava flow is divided into at least two lobes that are separated by left-lateral moraines of the upper Deschutes valley glacier. In a few localities, the base of the flow is exposed above unweathered till, suggesting that the flow closely followed deglaciation.

In some places the margin of the flow is partly buried by outwash gravel, indicating that the drainage basin was producing coarse-grained outwash and therefore was probably still significantly glacierized. The lava flow is locally overlain by silty sand that probably originated as loess and eolian sand deflated from till and outwash surfaces. This relation suggests also that glacial conditions still prevailed in the area following the eruption of the lava flow and that active, unvegetated outwash surfaces existed along the Deschutes to provide a source of the eolian sediment. A soil formed in the mantle of eolian sediment and flow rubble is buried by Mazama ash and a scattering of young South Sister tephra.

Continue southeast on road 4270.

9.9 Road descends margin of lava flow of Stop 1 onto outwash surface; junction with road 4278; turn left onto road 4278 and park near Lodgepole Quarry.

STOP 2--OUTWASH OF SUTTLE LAKE ADVANCE

Outwash gravel in this quarry was transported from the north and contains clasts of silicic lava from the Three Sisters-Broken Top area. The outwash gravel exposed in a quarry near Deschutes Bridge in the center of the end-moraine belt and till of both right- and left-lateral moraines within several kilometers of the center lack these silicic clasts. This distribution of erratics indicates that the west and the central portion of the glacier consisted of ice from the east slope of the Cascades south of Three Sisters, which is composed mostly of basalt and basaltic andesite. Silicic clasts are abundant only in the far eastern part of the moraine and outwash belt. The relation of the outwash in this quarry to left lateral moraines of the upper Deschutes glacier suggests that the streams that deposited the outwash probably occupied an ice-marginal position against a pre-MBVC upland area to the east.

The area north, west, and east of the quarry is now covered by lava flows from the Sheridan shield volcano (unit mb1) and from the Siah chain of vents (unit mb2). The steep-fronted lava flow directly north of the pit is from one of several scoria cones on the west flank of the Sheridan shield that were erupted after the shield was formed (episode 1b of fig. 12). The lava flows are lithologically distinct in both hand specimen and chemistry from lavas of the shield and also have a different paleomagnetic direction, suggesting that a significant period of time elapsed between the formation of the shield and the eruptions of the cones (fig. 11).

The low margin of the lava flow of Stop 1 west of the quarry suggests that the margin is partly buried by outwash. If so, the distribution of the lava flow and the pre-MBVC topography must have allowed meltwater streams to continue flowing east of the lava flow and to transport outwash through this reach.

A soil and surface lag of stones formed in the outwash is buried by about 50 cm of Mazama ash. The soil is formed in gravel and silty sand that is probably loess mixed with gravel. The soil is oxidized to a depth of 55 cm and consists of a Bw and oxidized C horizons. The outwash is gray and contains well rounded pebble and cobble gravel in a sandy matrix.

Return to road 4270 and turn left (southeast). The road continues on outwash; flow fronts of lavas of the Siah chain (unit mb2) lie in the forest to the left of the road.

11.1 Junction with paved road 40; turn left (east) on 40. The road climbs the north flank of Lookout Mountain, a normally magnetically polarized shield volcano of middle(?) Pleistocene age.
11.7 View to left of margin of lava flow of Siah chain.
12.5 Slow down for view to left of scoria cones of Siah chain, Sheridan shield, Mount Bachelor summit above Sheridan, and South Sister. Note scoria cones on Sheridan's summit and flanks.
14.1 Junction with road 4240; turn right on 4240.
15.0 On left are the Three Trappers. Two of the scoria cones belong to the Siah chain and one older cone is probably related to Lookout Mountain.
15.9 Dry Butte, another cone of the Siah chain, is on the left. Scoria of Dry Butte is exposed in roadcuts.
16.7 Quarry on left in informally named "South Dry Butte", the southernmost scoria cone of the MBVC. The vents to the south are small fissures that erupted mostly spatter.
17.0 Road curves to right and crosses low spatter-rimmed pits that are difficult to see through the trees.
17.3 Road crosses fault scarp that is oblique to the trend of the MBVC.
17.6 Junction with road 4040 and south end of MBVC. Park along side of road 4240.

STOP 3--TWO VENTS AT THE SOUTH END OF THE MOUNT BACHELOR VOLCANIC CHAIN

The southmost vents of the MBVC (figs. 5, 15) lie just west of the road junction and are the only vents along the chain other than vents in the Katsuk area at the north end that show evidence of magma having interacted with groundwater. The vents are marked by elongate craters about 100 m long, 50-75 m wide, and about 15-20 m deep. These vents are also the lowest in altitude of any in the MBVC and lie about 2 km north of and 30 m higher than the top of the sedimentary fill in the Lapine basin. This basin lies between the High Cascades and Newberry volcano and may contain a sedimentary fill as thick as 1 km (Couch and Foote, 1985). The groundwater table in the Lapine basin was probably higher than that along many other parts of the MBVC, and therefore the chance for rising magma to interact with groundwater was also greater. Of course, similar evidence in other parts of the MBVC may be buried by a thick cover of scoria and lava flows.

A shallow quarry and cuts along road 4040 expose loose to moderately indurated lithic tephra. The tephra is composed of gray lapilli and ash that is much less scoriaceous than the tephra found elsewhere along the MBVC. Although not as glassy as the hyaloclastite of Katsuk and Talapus Buttes that will be seen at Stop 5, the density of the tephra and its contrast with the later agglutinate spatter suggests some quenching of magma occurred at depth, probably as a result of interaction with groundwater. The deposit also contains large (>1 m) dense, angular blocks of a diktytaxitic basalt lava flow that crops out on the flanks of Lookout Mountain and also in the southern vent. The lithic tephra has a local distribution; there is none in roadcuts along road 4040 just a few tens of meters west of the vent. Presumably the deposit was once there, but has since been eroded.

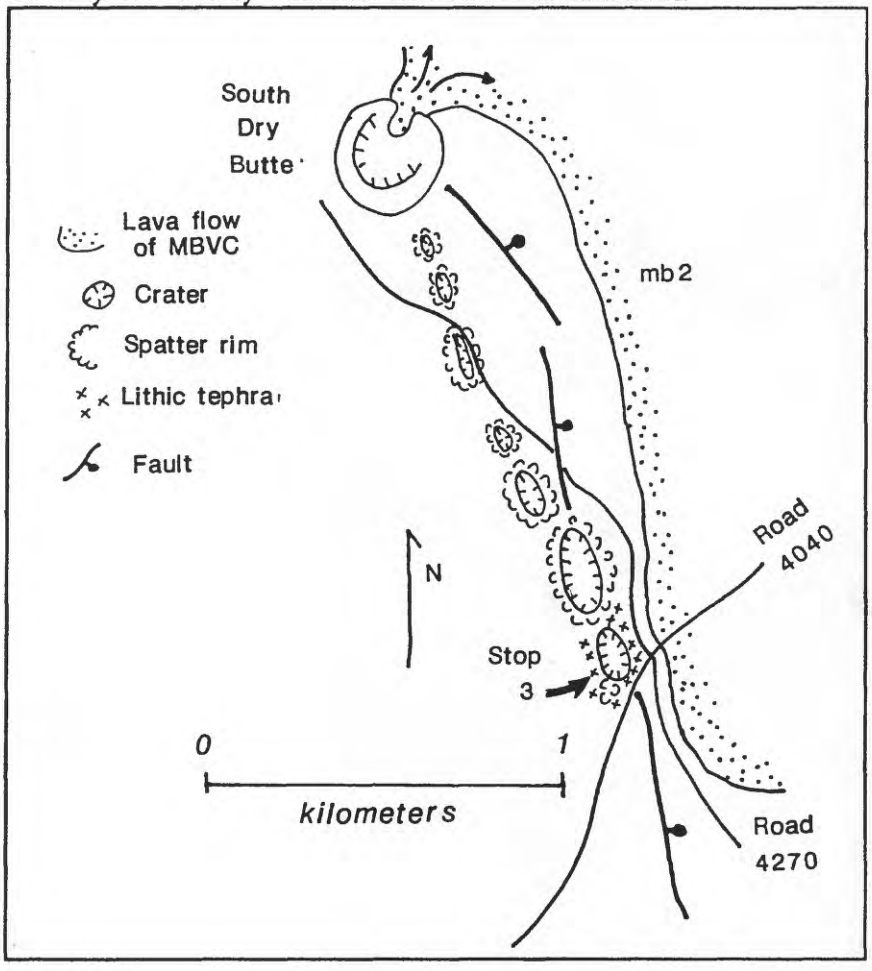

Figure 15. Sketch map of the south end of the Mount Bachelor volcanic chain near Day 2–Stop 3.

The lithic tephra is overlain by agglutinate spatter and thin basalt lava flows (49.8 % SiO_2) that erupted from the southwest corner of the southern vent and from much of the northern pit. An oxidized zone occurs along the contact of the spatter and lithic tephra in the part of the quarry adjacent to the southeast corner of the northern vent, but is thought to be related to oxidation by shallow groundwater moving along the base of the spatter rather than to soil formation. No such zone occurs in the roadcuts, where thin lava flows directly overlie the lithic tephra. However, a lag of coarse rubble on the lithic tephra and below the spatter in the quarry suggests that there may be some time break between deposition of the two units.

The paleomagnetic direction obtained from the thin lava flows in the Road 4040 cuts is identical with others

from the Siah chain, and suggests that eruptions of the southmost vent were broadly synchronous with those that formed large scoria cones and numerous lava flows along other parts of the Siah chain.

A fault trends south of the MBVC and can be seen south of road 4040 and west of road 4240. The fault forms an assymetric graben with a 2- to 4-m-high scarp on the west and a 1-m-high antithetic scarp on the east. The fault can be traced south for several kilometers as a discontinuous zone of scarps and flexures. Scarps are locally vertical, as high as 5 m, and some have up to 2-m-wide open cracks at their base. Rocks of the MBVC are apparently not offset by the fault. One possibility in light of historical Hawaiian rift eruptions (Pollard and others, 1983) is that at least some displacement on the fault occurred just before the initiation of eruptions along the southern end of the chain as a feeder dike neared the surface.

Continue south on road 4240. Margins of lava flows of the MBVC are visible on left; the fault veers west of the road. The road is on lava flows of Lookout Mountain.

19.4 Junction with paved road 42 at Fall River Guard Station; turn left (east) on road 42.
20.2 Entrance to Fall River Campground; good stop for lunch. Fall River is another spring-fed stream, rising a short distance upstream near Fall River Guard Station. The stream is incised in sediment of the Lapine basin, which are poorly exposed in the south bank. The southernmost extent of lava flows of the MBVC is on the north side of Fall River, about 1 km below the campground.
20.4 Return to road 42 and turn left, heading west.
21.1 Junction with road 4240; continue on road 42.
25.3 Views to right of Round Mountain, a 350-m-high scoria cone on the south flank of Lookout Mountain shield volcano. No other scoria cones in the area come close to the size of Round Mountain.
25.8 Junction with paved road 4260 to Twin Lakes and Wickiup Reservoir; turn left onto 4260.
27.7 Twin Lakes Resort; view of South Twin Lake.
28.3 Turn into small parking area on right side of road.

STOP 4--SOUTH TWIN LAKE TUFF RING

Hike a short distance through the forest to the rim of the tuff ring on the south side of South Twin Lake.

South Twin Lake is at the south end of a 7-km-long, north-trending chain of vents, the Wuksi Butte-Twin Lakes chain (WBTLC; fig. 16), which erupted olivine basalt during latest Pleistocene time. The north end of the WBTLC is offset about 8 km west of the south end of the MBVC in an en echelon pattern. The WBTLC eruptions may have been contemporaneous with some of the early MBVC eruptions. The northern vents of the WBTLC are marked by scoria cones surrounded by broad aprons of lava flows; hydroclastic deposits are exposed locally, but make up a small volume of the surface deposits. The southern vents produced only hydroclastic deposits and are marked by three tuff rings about 1 km in diameter and one about 0.5 km in diameter. The rings have steep inner walls and gently sloping outer flanks. The rings are composed of fall and base-surge deposits that were generated by numerous explosions as basaltic magma interacted with shallow groundwater in the western part of the Shukash-Lapine basin.

Hike back to the parking area and head to the exposures along the shore of Wickiup Reservoir, which here occupies a narrow valley of the Deschutes River.

The shoreline exposures reveal about 1.5 m of indurated tuff at a distance of about 200 m from the shore of South Twin Lake. Plane-parallel and wavy bedded and low-angle, cross-stratified tuff shows evidence of transport outward from the crater by base surges. The tuff overlies fluvial pebble gravel and sand, which, in turn, lies unconfomably on strongly deformed fine-grained sediments and diatomite of the basin-fill sequence.

The age of the tuff and other eruptive products of the WBTLC are not well constrained. Its lava flows east of Crane Prairie Reservoir are overlain by loess and ash in which a well developed soil (75 cm of oxidation; Bw and Cox horizons; 7.5 YR colors in Bw) formed prior to burial by Mazama ash. The lava flows overlie and are, in turn, partly buried by outwash of Suttle Lake age; the tuff at Stop 4 overlies unweathered gravel that is probably outwash of Suttle Lake age. These relations suggest that the WBTLC, as most of the MBVC, dates from the later part of the Suttle Lake advance, and is considerably older than Mazama ash.

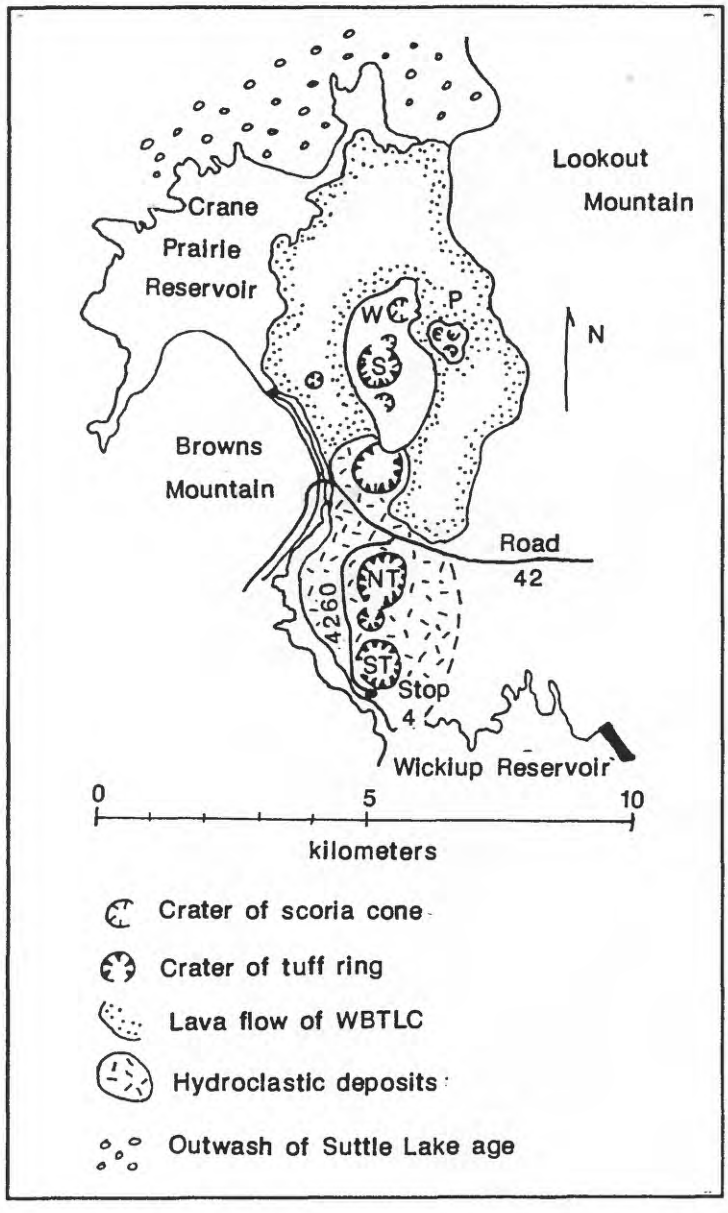

Figure 16. Sketch map of the Wuksi Butte-Twin Lakes volcanic chain and location of Day 2–Stop 4. W, Wuksi Butte; S, Shukash Butte; P, Palanush Butte; NT, North Twin Lake; ST, South Twin Lake.

Return to cars and head north on road 4260 to road 42.

28.9 Junction with road 42; turn left (west) on 42.

30.2 Browns Mountain Crossing of the Deschutes River. Above this point the Deschutes flows through a narrow valley between an old shield volcano, Browns Mountain, on the west and the latest Pleistocene lava flows and tuffs of the WBTLC on the east.

30.4 Road to Crane Prairie Dam. Roadcuts ahead are in weathered lava flows of Browns Mountain. Rounded boulders are the result of incipient spheroidal weathering.

33.1 On left, margin of a young-appearing lava flow from The Twins, a large shield volcano on the crest of the High Cascades. These lava flows are buried by moraines of Suttle Lake age 4 km west of here, so they must be older than 20,000 yr.

33.7 Junction with Cascade Lakes Highway (Road 46); turn right (north). Roadcuts ahead are in the lava flows discussed at mile 33.1; note the locally well-preserved rubbly flow top beneath a mantle of eolian sediment and tephra.

34.3 Views ahead to Cultus Mountain, Middle and South Sister, Broken Top, and Mount Bachelor.

35.1 Roadcuts expose Mazama ash over a well-developed soil formed in pebble gravel and sand. Gravel overlies well-bedded sand and silt. Significance of these sediments is not known, but they are definitely older than the Suttle Lake advance.

35.4 Lava-flow margin at north edge of meadow. Road ahead crosses late Pleistocene lava flows from vents along the Cascade crest. Numerous springs issue from the ends of these flows.

37.4 On right, turnoff to Osprey Observation Site.

38.0 Road is on outwash of Suttle Lake age, which floors much of the Crane Prairie basin. Cultus Mountain, on left, had major ice tongues of High Cascades ice cap of Suttle Lake age terminating on both its southeast and northeast flanks; their moraines dam Little Cultus and Cultus Lakes.

41.1 Cross Cultus River, another spring-fed stream, which heads at the base of Bench Mark Butte.

41.4 Junction with road 40; continue north on Cascade Lakes Highway.

42.6 Roadcuts here, and for the next 1.5 mi, expose glassy dacite (65.7% SiO_2, one analysis) of Bench Mark Butte, which marks an isolated occurrence of dacite in an area that is covered mostly by basalt and basaltic andesite. The flow contains numerous mafic inclusions. The butte is up to 120 m thick, flat-topped, and composed of numerous steep-sided lobes. Its age is not well known, but till of end

moraines and outwash of Suttle Lake age lap onto its north and west flanks. Its well-preserved morphology suggests a late Pleistocene age.

44.4 Roadcuts in till of Suttle Lake age that marks the outermost moraine of the upper Deschutes valley glacier. Numerous other moraines are passed in the next 3 mi.

45.2 Junction with road 4270 at Deschutes Bridge; continue north. See log for Day 2 from mile 7.4-1.7 and log for Day 1 from mile 1.7-8.7.

52.9 North shore of Devils Lake, which is dammed by lava flow of Le Conte Crater; park here or in turnout 0.25 mi ahead on right, just past young rhyolite lava flow.

STOP 5--DEVILS LAKE, TALAPUS AND KATSUK BUTTES, AND DEVILS HILL CHAIN OF DOMES

This stop focuses on two topics: (1) The formation of Talapus and Katsuk Buttes, and (2) the rhyolite tephra and lava flows and domes of the late Holocene Rock Mesa and Devils Hill eruptive episodes of South Sister. Figure 17 shows the relations among key geologic units in the area around Stop 5.

Talapus and Katsuk Buttes

Katsuk and Talapus Buttes are two scoria cones that sit atop a gently south-sloping plateau composed of thin (1-3 m) basalt lava flows. The flows display breccia, locally ropy surfaces, tumuli, and other well-preserved flow-top features. They have obviously not been glaciated, and the reconstruction of the upper Deschutes glacier shown in Figure 7 indicates that, had the plateau been present, it would have been overridden by ice about 200-300 m thick. The cones and flows are typical of those along the MBVC, except that they terminate in a steep slope that ranges in height from 25 to 110 m (higher slopes probably occurred near the north end, but they have been partly buried by the lava flow of Le Conte Crater on the west and sediments of Sparks Lake basin on the east. Another atypical feature is the hydrovolcanic deposits (hyaloclastite, in part palagonitized) that are exposed in the lower slopes at the north end of the plateau and in roadcuts both east and west of the young rhyolite flow. Till and erratics are locally present on the slopes underlain by hyaloclastite (Taylor, 1978).

These features imply the following origin:

(1) Initial hydrovolcanic eruptions probably occurred in a lake melted into the receding glacier of Suttle Lake age; the glassy hyaloclastite resulted from the rapid quenching of basaltic lava in the water-filled vent followed by explosions that ejected the debris into the lake and onto the surrounding ice or till. The hyaloclastite consists of light-olive-gray to gray, poorly to well-bedded lapilli-and-ash tuff that contains scattered large clasts of juvenile basalt and accidental fragments. The upper part of the tuff in most exposures has been palagonitized and is orange-brown. In all localities the tuff is pervasively faulted and deformed, probably as a result of syn- and post-depositional mass movements and subsidence caused by melting of underlying glacier ice.

(2) As the lake filled with hyaloclastite or drained by opening of channels through the ice margin, water was excluded from the vent, and normal subaerial Strombolian eruptions ensued. The scoria cones of Talapus and Katsuk Buttes were then constructed. Subsequently, lava flows issuing from vents between and at the base of the cones filled the depression that remained in the glacier. Thus the thin flows "sky-out" at the steep plateau margins against a now-vanished buttress, and form a surface that may have coincided roughly with the surface of the glacier.

A glacier having the slope and thickness of the lava plateau would have had a basal shear stress of about 0.3 bars, which is less than typical values of basal shear stress (0.5-1.5 bars). Such a low value of basal shear stress suggests that the glacier through which the eruptions occurred was thin and perhaps stagnant. Alternatively, the lava-flow surface may provide only a minimum estimate of ice thickness, and the glacier may have been somewhat thicker. The glacier was probably not greatly thicker than the plateau, in light of the lack of evidence of ice reforming over the plateau following the eruptions. Till and erratic clasts are found only along the base of the north end of the plateau and in roadcuts immediately to the east, in which till overlies faulted, bedded hyaloclastite.

Slump blocks composed of the plateau-capping basalt flows lie along the central portions of both the east and west margins of the plateau. Slumping of the steep plateau margin occurred after deglaciation and was perhaps facilitated by underlying bodies of palagonitized hyaloclastite and(or) sediments.

The paleomagnetic direction of lava flows at the plateau rim is similar to that of lava flows from the Red Crater area and of the earliest recognized lava flows of the Sheridan shield (episode 1a; fig. 12A), which suggests that they could all be coeval.

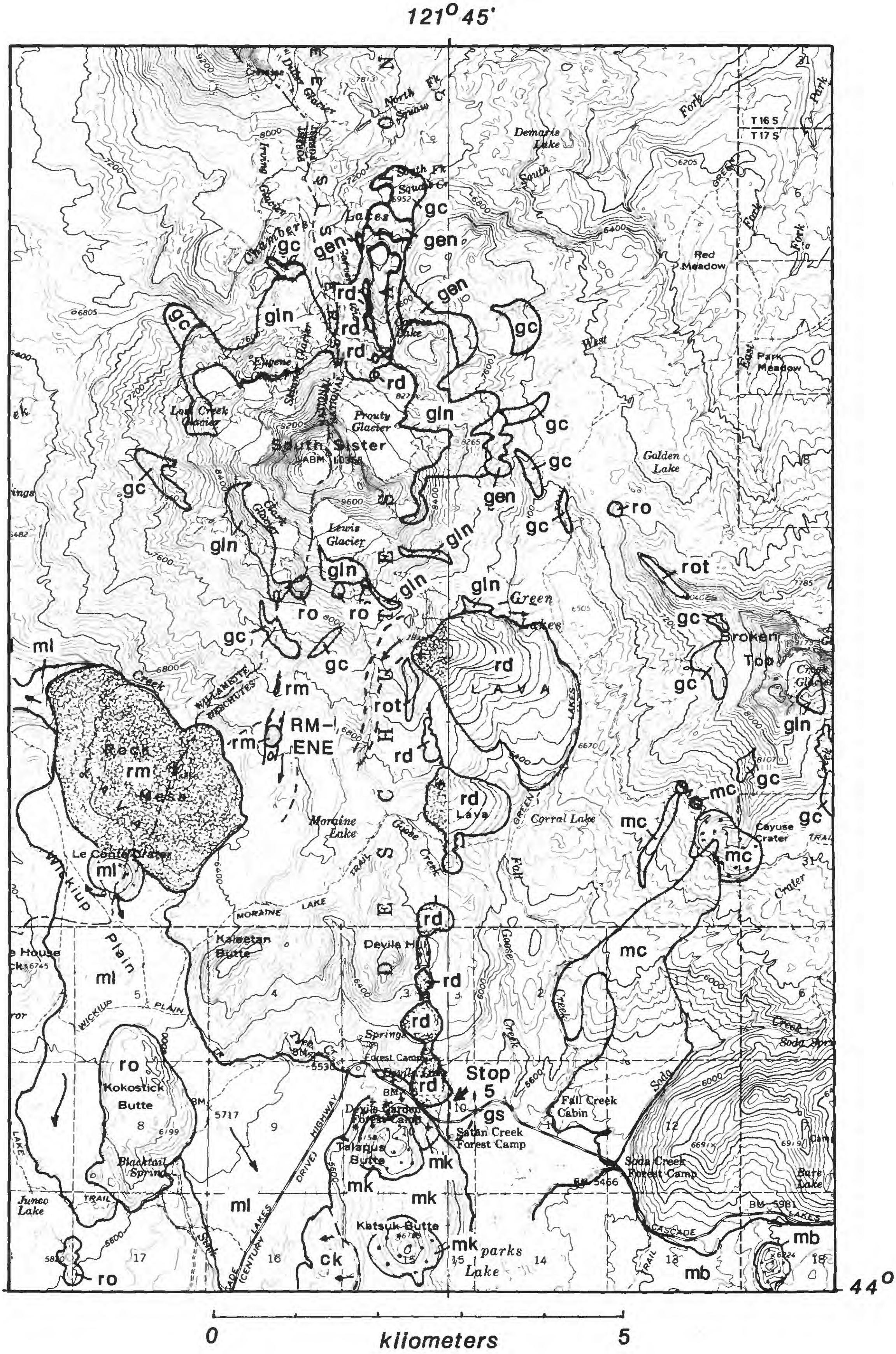
121° 45'
44°
0
kilometers
5
South Sister
Prouty Glacier
Lewis Glacier
Clark Glacier
Eugene Glacier
Lost Creek Glacier
Irving Glacier
Chambers
Lakes
Demaris Lake
Red Meadow
Park Meadow
Golden Lake
Green Lakes
Broken Top
Rock Mesa
Le Conte Crater
Wickiup Plain
Moraine Lake
Kaleetan Butte
Devils Hill
Kokostick Butte
Blacktail Spring
Junco Lake
Talapus Butte
Katsuk Butte
Devils Garden Forest Camp
Satan Creek Forest Camp
Soda Creek Forest Camp
Fall Creek Cabin
Cayuse Crater
Corral Lake
Sparks Lake
Stop 5
T16 S
T17 S
gc
gen
gln
rd
ro
rot
rm
RM–ENE
ml
mc
mk
mb
ck
gs

Figure 17. Map showing selected geologic features around South Sister and Day 2–Stop 5. Glacial deposits: gln, late neoglacial till; gen, early neoglacial till; gc, till of Canyon Creek age; gs, till of Suttle Lake age (shown only near Stop 5). Mafic lava flows, scoria deposits (stippled), and hydrovolcanic deposits (crosses): mc, Cayuse Crater; mb, Mount Bachelor volcanic chain; ml, Le Conte Crater; and mk, Talapus and Katsuk Buttes. Unit ck is large landslide that originated on west side of Talapus-Katsuk plateau. Silicic volcanic rocks: rd, Devils Hill eruptive episode; rm, Rock Mesa eruptive episode (unit at about 7200 feet altitude northeast of Rock Mesa includes only tephra vents, no lava flows or domes are present); ro, rhyolite and dacite lava flows and domes of pre-Suttle Lake age (numerous units around South and Middle Sister are omitted, but include Devils Hill and Kaleetan Butte); rot, thick rhyolite tephra deposits of pre-Suttle Lake age on ridge tops (includes a mantle of Holocene tephra). Dashed lines near units rd and rm show approximate extents of pyroclastic flows. Thick tephra deposits associated with the eruptions of units rd and rm are not shown, but surround most of the vents. Crosses on units rd and rm show locations of vents for large lava flows. Mapping taken or modified from Taylor (1978), Taylor and others (1987), Wozniak (1982), Clark (1983), Scott (1987), and Scott (unpublished mapping).

Holocene rhyolite eruptions of South Sister

Two tephra units erupted from vents on the flank of South Sister between 2300 and 2000 yr B.P. (Scott, 1987) are exposed at Stop 5 and are best viewed in roadcuts below the talus of the young rhyolite lava flow or in roadcuts east of the flow. The tephras lie on a soil formed in Mazama ash and hydrovolcanic deposits of the Katsuk-Talapus area. The lower tephra is about 10 cm thick and consists of a basal lapilli and coarse ash bed about 3-4 cm thick and an upper light-gray to brownish-gray ash deposit that contains a conspicuous brick-red marker bed of fine ash about 0.5-1.0 cm thick. The upper tephra is about 65 cm thick and is much coarser grained than the lower unit; individual pumice bombs are as large as 20-30 cm. Lithic fragments are commonly more than 20 cm in diameter in the upper tephra, and several 50-cm-diameter blocks of dacite and rhyolite occur in the layer in nearby roadcuts. A significant component of the tephra is juvenile, subpumiceous to glassy, light-gray to black rhyolite; many of the larger clasts display glassy, breadcrusted surfaces. Evidence of reworking, slight weathering, and accumulation of thin peat between the two tephra layers, which is not well-displayed in the exposures at Stop 5, suggests that they were erupted at least 100 yr apart, but no more than a few centuries (Scott, 1987).

The coarse grain-size of the upper tephra indicates that it was erupted from nearby vents at the south end of the Holocene Devils Hill chain of vents (Devils Hill itself is a Pleistocene rhyolite dome that lies just west of the south end of the chain; fig. 17). Lithic fragments of the Pleistocene rhyolite are abundant in the upper tephra layer.

The lower unit with its brick-red marker bed and underlying lapilli can be traced northwestward, thickening and coarsening, to an inferred graben containing several small domes that lies 1.2 km east of Rock Mesa (RM-ENE; figs. 17, 18). Thick rims of tephra along the graben indicate that it was a major tephra vent, even though it subsequently produced only small lava domes. This vent also erupted several small pyroclastic flows. A few small elongate craters and open cracks form a 400-m-long chain of vents beginning a few hundred meters north of the graben. These vented a small amount of tephra, largely after tephra eruptions at RM-ENE had ceased.

Tephra presumably erupted from the vent that subsequently was the source of the Rock Mesa lava flow overlies the tephra of RM-ENE and forms a south-trending lobe (fig. 19), which is the source of much of the scattered pumice on the ground surface seen at earlier Day-2 stops. The tephras from the Rock Mesa and RM-ENE vents are chemically identical (table 6), but can be distinguished in proximal areas by their assemblages of accidental lithic fragments. The lithics of the RM-ENE tephra are dominantly andesite, dacite, and rhyolite, whereas the tephra from the Rock Mesa vent contains a conspicuous proportion of basalt and basaltic andesite.

The tephra units exposed at Stop 5 can be traced over several hundred square kilometers to the north and east (fig. 19). The pumiceous character of the tephra-fall deposits of the Rock Mesa and Devils Hill episodes, their pattern of dispersal (restricted largely to within 30 km of vents), and their associated pyroclastic-flow and surge deposits indicate the sub-Plinian nature (Walker, 1973, 1981) of these eruptions.

The rhyolite lava flow that overlies the tephras marks the south end of the Devils Hill chain of lava flows and domes that extends north in several segments for 5.5 km to an altitude of almost 8000 feet on the southeast flank of South Sister (fig. 17). Following a gap of several kilometers, the chain continues as a 1.2-km-long segment of small domes on the northeast flank. Several lines of evidence developed at Medicine Lake volcano and the Mono and Inyo volcanoes (Bailey and others, 1983; Fink and Pollard, 1983; Miller, 1985; Eichelberger and others, 1985) suggest that eruptions along the chain were fed by dikes or segments of a single dike (fig. 20; Scott, 1987). These include: (1) Structural features, such as aligned vents, grabens, cracks, and linear fractures over

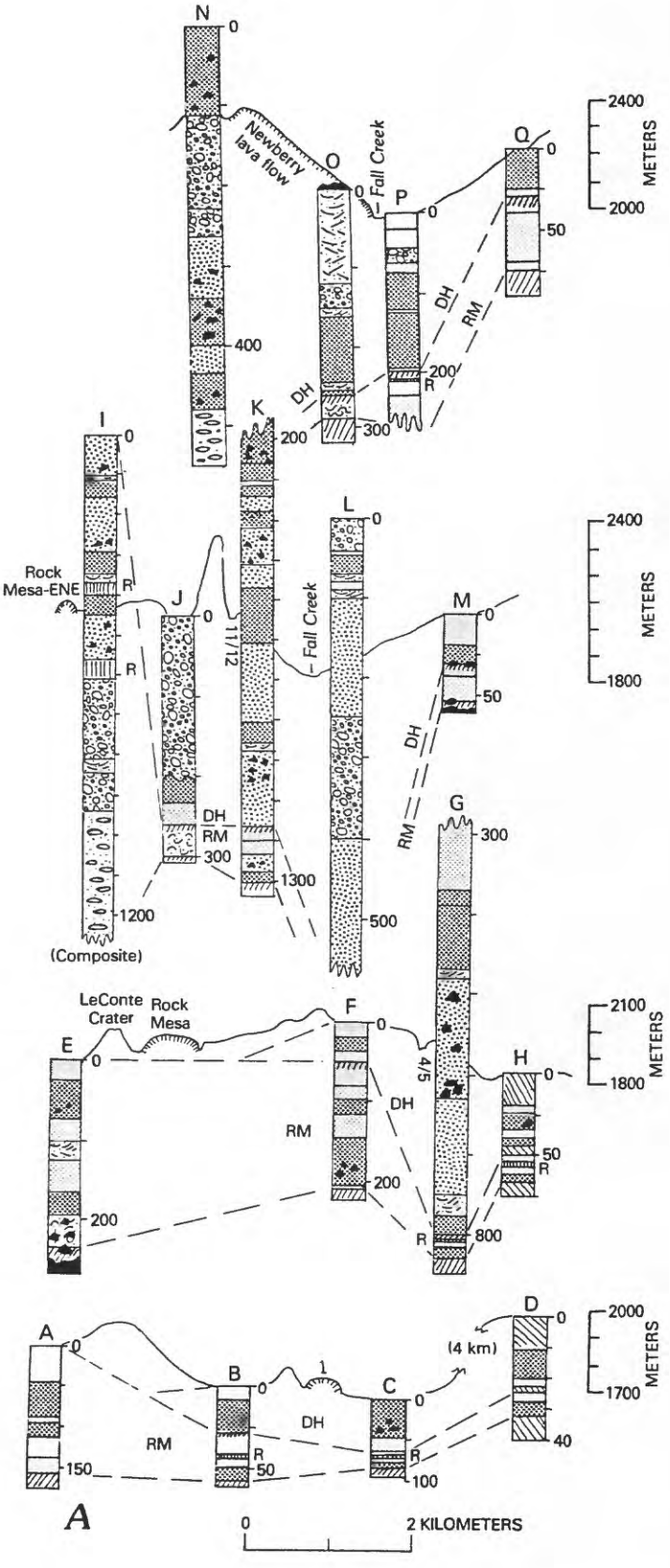
N
Newberry lava flow
O
Fall Creek
P
Q
2400
METERS
2000
DH
RM
400
200
R
300
I
K
L
M
Rock Mesa-ENE
J
11/12
Fall Creek
1800
1200
1300
500
50
G
300
(Composite)
LeConte Crater
Rock Mesa
F
E
4/5
H
2100
1800
200
800
D
2000
1700
(4 km)
A
B
C
150
100
40
A
0
2 KILOMETERS

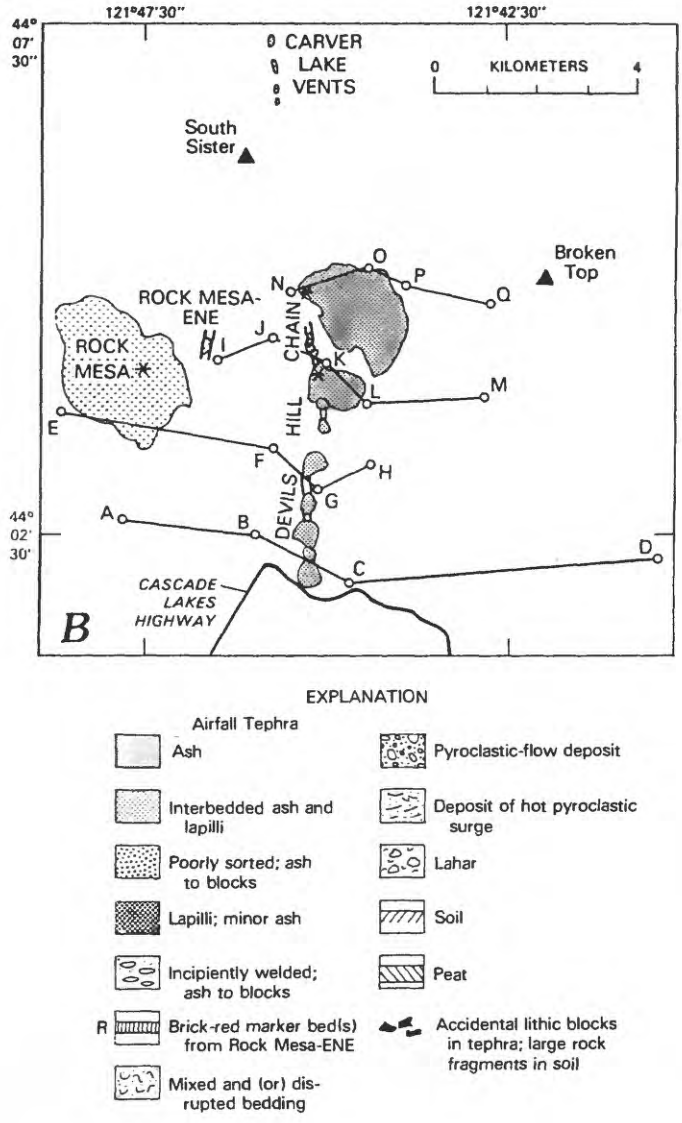

Figure 18. Stratigraphic sections of fragmental deposits of the Rock Mesa (RM) and Devils Hill (DH) eruptive episodes (A) and index map (B) to locations of sections. Units are generalized, especially on longer sections. Most tephra-fall deposits are composed of a few to many beds. The altitude scales (in meters) refer to the topographic profiles; the tops of many sections are shown above the topographic profiles in order to save space on the figure. Note that the thickness scales (in centimeters) differ among sections. On sections K and G, the tops of the upper units are not shown. Section L is shown on the east side of Fall Creek, although it lies on the west side. Surface soils are not shown. The base of the Newberry lava flow is shown on section O. Figure from Scott (1987).

vents of flows and domes parallel to vent alignments, (2) tephra and lava erupted from numerous vents along the Devils Hill chain is of remarkably similar chemical composition (all samples are indistinguishable within analytical uncertainty; table 6), which suggests that eruptions were fed from a single source, and (3) eruptions along the chain were nearly synchronous as shown by the tephra erupted from numerous vents forming a single depositional sequence without evidence of substantial interruptions.

During eruptions of the chain, the inferred feeder dikes were locally enlarged, probably by brecciation and erosion (e.g., Delaney and Pollard, 1981), and these areas emerged as principal conduits. Therefore, the dikes did not supply magma uniformly to vents, especially during the lava-extrusion stage that followed the tephra eruptions. The cumulative-volume curve of Figure 20 shows that several of the higher-altitude vents on the southeast flank of South Sister were the source of most of the erupted material.

Table 6. Means and standard deviations of analyses of eruptive products of the Rock Mesa, Devils Hill, and Carver Lake vents.

(See notes below)

	Rock Mesa pumice and lava n=6	Devils Hill pumice n=6	Devils Hill lava n=13	Carver Lake pumice and lava n=4	Analytical error*	All Devils Hill and Carver Lake samples n=23	Analytical error†
SiO_2	73.5 ± 0.1	72.5 ± 0.2	72.6 ± 0.1	72.7 ± 0.1	± 0.13	72.6 ± 0.2	± 0.19
Al_2O_3	14.2 ± 0.1	14.7 ± 0.1	14.6 ± 0.1	14.5 ± 0	± 0.07	14.6 ± 0.1	± 0.05
Fe_2O_3§	0.62 ± 0.01	0.70 ± 0.02	0.69 ± 0.01	0.68 ± 0.02	± 0.03**	0.69 ± 0.02	± 0.02**
FeO§	1.30 ± 0.02	1.47 ± 0.02	1.46 ± 0.03	1.44 ± 0.04		1.46 ± 0.04	
MgO	0.55 ± 0.03	0.62 ± 0.02	0.60 ± 0.03	0.55 ± 0.04	± 0.02	0.60 ± 0.04	± 0.06
CaO	1.76 ± 0.04	1.99 ± 0.03	1.96 ± 0.02	2.02 ± 0.02	± 0.02	1.98 ± 0.03	± 0.02
Na_2O	4.21 ± 0.06	4.40 ± 0.07	4.54 ± 0.05	4.50 ± 0.01	± 0.09	4.45 ± 0.06	± 0.07
K_2O	3.41 ± 0.03	3.14 ± 0.04	3.18 ± 0.02	3.15 ± 0.03	± 0.01	3.16 ± 0.03	± 0.03
TiO_2	0.28 ± 0.01	0.32 ± 0.01	0.32 ± 0.01	0.32 ± 0.01	± 0.01	0.32 ± 0.01	± 0.01
P_2O_5	0.08 ± 0.01	0.09 ± 0.01	0.09 ± 0.01	0.08 ± 0	± 0.01	0.09 ± 0.01	± 0.01
MnO	0.04 ± 0	0.05 ± 0	0.05 ± 0.01	0.04 ± 0.01	± 0.01	0.05 ± 0.01	± 0.01
Ba	822 ± 34	793 ± 5	804 ± 6		± 40		
Be	1 ± 0	1 ± 0	1 ± 0		± 1		
Ce	38 ± 3	37 ± 1	41 ± 2		± 6		
Co	3 ± 1	4 ± 0	4 ± 0		± 4		
Cr	4 ± 1	3 ± 1	3 ± 1		± 4		
Cu	6 ± 1	8 ± 2	7 ± 1		± 7		
Ga	16 ± 1	15 ± 1	17 ± 1		± 2		
La	21 ± 1	21 ± 1	22 ± 0		± 2		
Li	32 ± 1	33 ± 4	32 ± 1		± 3		
Sc	3 ± 0	4 ± 1	4 ± 1		± 4		
Sr	193 ± 12	228 ± 4	223 ± 5		± 11		
V	15 ± 1	18 ± 1	18 ± 1		± 2		
Y	16 ± 1	16 ± 1	17 ± 0		± 2		
Yb	2 ± 0	2 ± 1	2 ± 0		± 2		
Zn	33 ± 2	39 ± 1	36 ± 2		± 4		

* *Standard deviation of 49 samples prepared from the same standard; each sample counted once in same day.*

† *Standard deviation of one sample counted 62 times in a 6-month period.*

§ *Fe values from laboratory reported as Fe_2O_3. Fe_2O_3 and FeO values calculated assuming $Fe^{+2}/Fe_T = 0.7$, which is approximately the ratio reported by Clark (1983) for South Sister rhyodacite lavas.*

** *Analytical error for Fe oxides is that reported with all Fe as Fe_2O_3.*

Notes: The groups of samples averaged in each of the first 4 columns were counted in separate lots; their standard deviations should be compared with the analytical errors in column 5. The analytical error that takes into account long-term drift (column 7) should be compared with the combined analyses of products of the Devils Hill and Carver Lake vents in column 6. Analytical errors for XRF analyses are from J. Taggart (U.S. Geological Survey, personal commun., 1985). Minor and trace elements, in parts per million, determined by induction-coupled plasma emission spectroscopy (ICP; P.H. Briggs and D.B. Hatfield, analysts, U.S. Geological Survey). Analytical errors for ICP analyses are from F. Lichte (U.S. Geological Survey, personal commun., 1985).

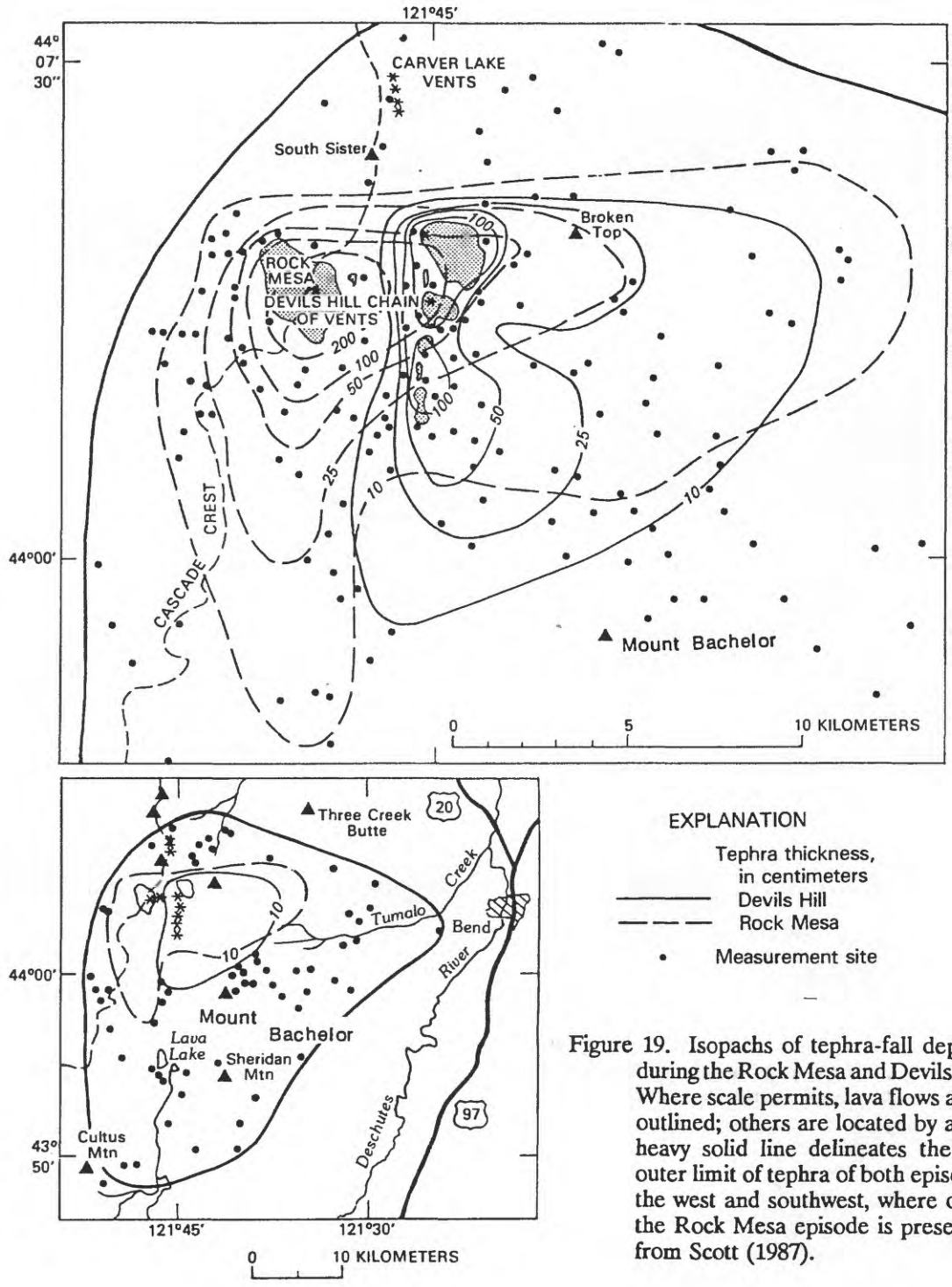

Figure 19. Isopachs of tephra-fall deposits erupted during the Rock Mesa and Devils Hill episodes. Where scale permits, lava flows and domes are outlined; others are located by asterisks. The heavy solid line delineates the approximate outer limit of tephra of both episodes except in the west and southwest, where only tephra of the Rock Mesa episode is present. Modified from Scott (1987).

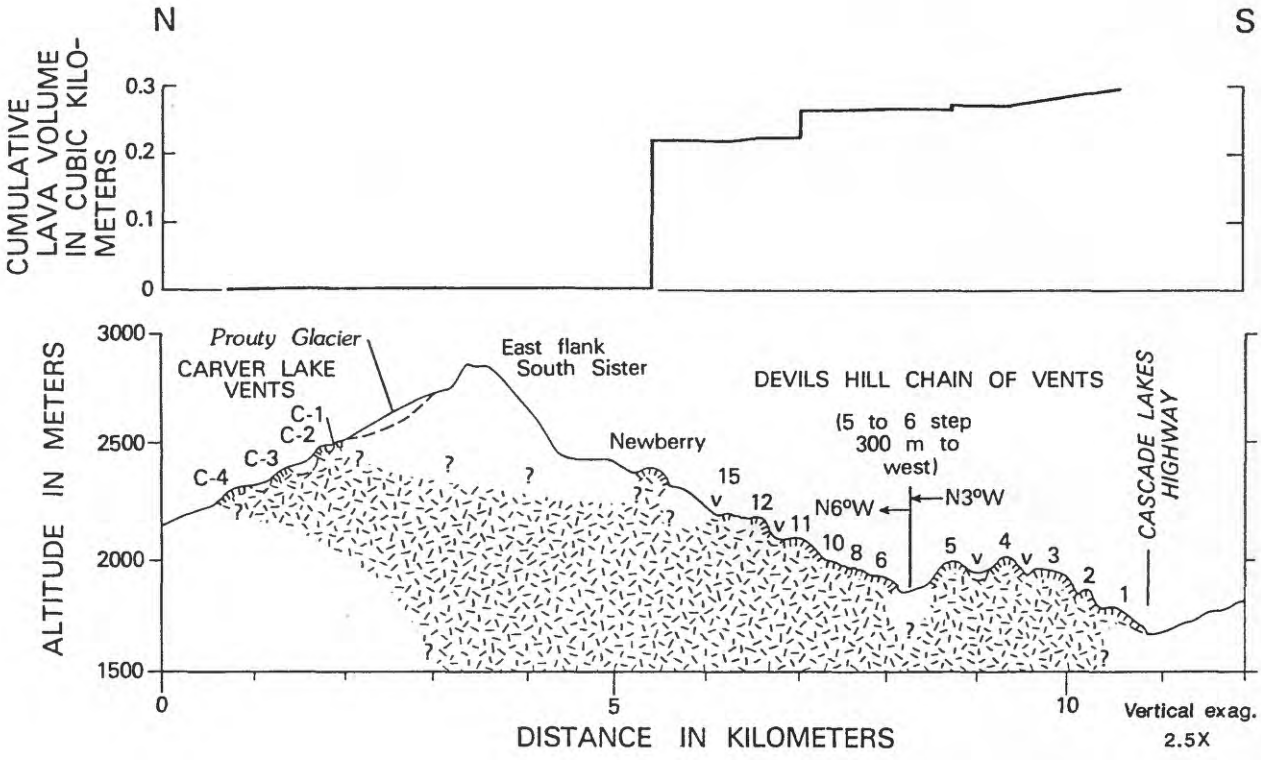

Figure 20. Vertical section along the trend of the Devils Hill chain of vents (1-Newberry) and Carver Lake vents (C-1 to C-4) showing inferred extent of feeder dike (patterned; lower sketch) and the cumulative volume of lava erupted from vents or groups of vents (upper graph). The vents from 6 to C-4 are projected onto a section oriented N6°W, even though the strike of individual segments ranges up to N13°W. V's show locations of grabens not filled by lavas. Queries indicate great uncertainty in estimating the extent of the inferred dike. The volume erupted from each vent is shown by a vertical line, except where small volumes from closely spaced vents are represented by a gently sloping line. Tephra volume is not included, as it represents only about 5 percent of the total volume of erupted magma. Based on the tephra's distribution (fig. 19), subequal amounts were erupted from the 1-5 and the 6-Newberry vent areas, and an insignificant volume erupted from the C-1 to C-4 vent areas. Figure from Scott (1987).

ROAD LOG FOR DAY 3--MIDDLE QUATERANRY PYROCLASTIC-FALL AND -FLOW UNITS NEAR BEND

by
Brittain E. Hill and William E. Scott

This one-half day trip stops at two sites (fig. 1) to view several pyroclastic-flow and tephra-fall deposits of mid-Quaternary age (fig. 21). Investigations of these deposits by Taylor (1981), Hill (1985, 1987, 1988), and Hill and Taylor (this volume) have concluded that the units were all erupted from vents in a silicic eruptive center (Tumalo volcanic center) that lay east of present Broken Top volcano. In addition, recent work by Sarna-Wojcicki and his colleagues (this volume) has provided age constraints on some of these units based on K-Ar dating and tephrostratigraphic correlations. Formerly assumed to be of late Tertiary or early Pleistocene age, the units are now thought to range in age from about 0.65 to 0.3 Ma.

Mileage	Description of features along route
0	At junction of entrance road to Little Fawn Campground and USFS Road 4600-470, follow directions for Day 1 and head toward Mount Bachelor on the Cascade Lakes Highway (Road 46).
15.8	Entrance road to Sunrise Lodge, Mount Bachelor Ski Area; continue east on Road 46. For next mile on right, lava flows of the Mount Bachelor summit cone and shield are partly buried by outwash of late-glacial and neoglacial age derived from the glacier on the north flank of Mount Bachelor. On left are lava flows of Tumalo Mountain, which predate the maximum of the last glaciation. Thick deposits of reworked Mazama ash and underlying scoria of the Mount Bachelor volcanic chain are exposed locally.
18.1	On the left, bouldery outwash of Suttle Lake age that lies just south of moraines deposited at margin of ice lobe that wrapped around the east side of Tumalo Mountain (fig. 5).
18.4	Junction with road to Sun River; stay on Road 46. Most of the hills on both sides of the road are scoria cones that are much older than Mount Bachelor and Tumalo Mountain; a few of the hills are rhyolite domes related to the Tumalo volcanic center.
21.4	Road follows narrow outwash channel from ice lobe that terminated just north and northwest of highway. Lack of streams today reflects high permeability of fractured volcanic bedrock.
25.6	Road cuts on left expose colluvium that contains a large proportion of matrix. The degree of soil formation is similar to that in till of Suttle Lake age, which suggests that during the last glaciation colluvial transport (solifluction?) was a very active process on these gentle to moderate slopes.
28.3	View to southeast of Newberry volcano, a shield-shaped volcano with a 5-km-wide summit caldera. Newberry is composed of silicic ignimbrites, silicic domes and lava flows, and hundreds of basaltic scoria cones, fissure vents, and related lava flows (MacLeod and others, 1981). Although not high in altitude, the volcano is among the largest (by volume) Quaternary volcanoes in the western conterminous U.S.
29.2	Abandoned quarries in outwash gravel that was transported in channel of mile 21.4. Outwash deposits of both Suttle Lake and pre-Suttle Lake age (on basis of weathering-rind thickness) are present.
34.9	Turn left toward the Bend city baseball fields and Cascade Junior High School. Park in the lot at the baseball fields and walk north across the fields, head northeast on unpaved roads to abandoned pumice quarry on north side of old Brooks-Scanlon Road, which is closed to traffic by line of large boulders. Quarry is on private land.

STOP 1--LAVA ISLAND ASH-FLOW TUFF, TUMALO ASH-FLOW TUFF, AND BEND AIR-FALL PUMICE

This abandoned quarry exposes a 7-m-thick section of Bend Pumice of Taylor (1981) overlain directly by Tumalo Tuff of Taylor (1981). The tuff shows lateral and vertical changes in welding, and also has a well developed basal layer that contains coarse pumice clasts. Lava Island Tuff of Taylor (1981) lies disconformably on Tumalo Tuff and is thoroughly devitrified. See paper by Hill and Taylor (this volume) for information about these units.

Mileage	Description of features along route
35.4	Return to intersection with Century Drive (Cascade Lakes Highway); turn left.
35.7	Intersection with Colorado Avenue. Continue on Century Drive.
36.5	Intersection with 3-way stop. Stop and continue straight ahead (north) on 14th NW St.

36.9 Intersection with NW Newport Ave.; turn left on Newport. Much of the following road log is taken from Taylor (1981).

37.2 Road to Central Oregon Community College on right. Newport Ave. becomes Shevlin Park-Market Rd. at milepost 0. The road lies in a valley between two early(?) Pleistocene basaltic shield volcanoes (Awbrey and Overturf Buttes) and through which four pyroclastic flows passed from west to east.

38.4 Curve to right. Pumice quarries on left reveal Tumalo Tuff overlying Bend Pumice.

38.7 Curve to left. The last 0.5 mi. of road has followed the northwest-striking Tumalo fault. Rocks on the southwest side (rangeward) of the fault have been displaced downward. In this vicinity, Desert Springs Tuff of Taylor (1981), Bend Pumice, and Tumalo Tuff have all been faulted; Shevlin Park Tuff of Taylor (1981) has not, but has been faulted farther to the southeast.

39.9 Cross Tumalo Creek; entrance to Shevlin Park, which contains many good exposures of Shevlin Park Tuff. Road becomes Johnson Road.

Recommended side trip. Turn left into Shevlin Park. Follow park road 0.6 mi. southwest to Red Tuff Gulch on the north side of Tumalo Creek. A 3-m-thick section of Desert Springs Tuff, which contains two flow lobes, crops out here. Moderately welded Tumalo Tuff and Shevlin Park Tuff are exposed about 150 m up the gulch. Reworked pumice lapilli, ash, and obsidian of basal Bend Pumice are well exposed along the park road just to the southwest. Large blocks of welded Tumalo Tuff and Desert Springs Tuff occur in alluvium overlying Bend Pumice.

40.2 Top of grade; turn left on gravel road to Bull Springs Tree Farm. Bear right at first two roads that head off to left.

40.7 First of two roads to right; bear left at both.

41.4 Intersection with old Brooks-Scanlon Road (Road 4606) at abandoned quarry; turn right. Skirt and cross margins of several High Cascade basalt lava flows.

43.0 Road turns sharply to right, crossing shallow canyon; pull off either side of road and park in flat area around Columbia Southern Canal.

STOP 2--TUMALO TUFF, BASALTIC ANDESITE LAVA FLOW, AND SHEVLIN PARK TUFF

At this stop, one can examine outcrops of 0.3-Ma Shevlin Park Tuff near the canal and in the roadcuts and also have a good view of the Tumalo volcanic center, from which the mid-Quaternary pyroclastic-flow deposits and tephras were erupted.

The roadcut exposes Tumalo Tuff, which is overlain disconformably by a High Cascade basaltic andesite lava flow from an unknown vent. The tuff has been locally reddened by the heat of the lava flow. The lava flow is overlain by Shevlin Park Tuff, the youngest unit erupted from the Tumalo volcanic center. The Shevlin Park Tuff, which is gray and andesitic in composition, fills a channel cut through the lava flow and Tumalo Tuff.

CAUTION: THE ROADCUTS ARE TREACHEROUS. THE LAVA FLOW OVERLYING TUMALO TUFF IS LOCALLY UNDERCUT AND CONTAINS LARGE OPEN FRACTURES. DO NOT FURTHER UNDERMINE THE LAVA FLOW. BE CAUTIOUS WHILE EXAMINING THE CONTACT AND BE AWARE OF THE IMPACT OF YOUR ACTIVITIES ON OTHERS AND THEIRS ON YOU. LESS DANGEROUS OUTCROPS OF SHEVLIN PARK OCCUR ON THE NORTH SIDE OF THE CANYON.

End of field trip. Turn around and head back to Johnson Road.

If you are heading south of Bend, return along trip route to mileage 35.7 and turn east on Colorado Avenue and continue to Division Street and U.S. 97.

If you are heading north on U.S. 97 or west on U.S. 20, turn left at Johnson Road and continue 4.2 mi. to junction with Tumalo Market Road. (At junction, good exposures of Desert Springs Tuff, below road, and Bend Pumice and Tumalo Tuff, in quarries above road, occur 0.4 mi. to north along Tumalo Market Road). Turn right on Tumalo Market Road and then immediately turn left (north) and continue about 1 mi. to U.S. 20. Late Pleistocene outwash gravels underlie the valley bottom. Those heading north on U.S. 97 turn right on U.S. 20 and continue to junction with U.S. 97.

OREGON CENTRAL HIGH CASCADE PYROCLASTIC UNITS IN THE VICINITY OF BEND, OREGON

by
Brittain E. Hill and Edward M. Taylor, Department of Geology
Oregon State University, Corvallis, OR 97331-5506

Unlike most areas in the Oregon High Cascade range, the area west of Bend, Oregon, contains at least five ash-flow tuffs and two major air-fall pumice deposits (fig. 21; table 7). These pyroclastic units were not erupted from the present stratovolcanoes (Three Sisters, Broken Top) of the Oregon central High Cascades (OCHC) area. Instead, they were erupted from a large silicic vent complex, the Tumalo volcanic center (TVC; Hill, 1988), which is located east of Broken Top and west of Bend. The TVC encompasses the "silicic highland" of Taylor (1978), and forms a 25-km-long, south-trending belt of silicic domes and andesitic cinder cones from Three Creek Butte to Edison Butte. The most significant results of ongoing investigations are that the TVC produced the largest silicic eruptions in the OCHC less than 0.4 Ma, and that these eruptions preceded the construction of the Three Sisters and Broken Top stratovolcanoes. The purpose of this part of the field trip is to examine some of the features of the pyroclastic units around Bend, and to show that these units represent major eruptions from the TVC.

DESERT SPRINGS TUFF

The Desert Springs Tuff of Taylor (1981) is the oldest of the Pleistocene High Cascade pyroclastic deposits. Where the basal contact is exposed, the Desert Springs overlies the Miocene to upper Pliocene(?) Deschutes Formation (Smith et al., 1987). The Desert Springs contains at least two distinct flow lobes that form one cooling unit. Although complete sections are not exposed, the Desert Springs has an average thickness of about 12 m, with one preserved section 30 meters thick. An idealized vertical section contains a poorly welded 2-m-thick basal zone, a 5-to-10-m-thick, pink-to-tan firmly welded zone of vapor-phase alteration, and an upper poorly welded zone of fresh black glass about 5 m thick. Where preserved, the contact between the flow lobes occurs in the pink welded zone. The Desert Springs Tuff is characterized by black dacitic pumice lapilli and bombs up to 0.5 m in diameter, which contain up to 15 percent phenocrysts: plagioclase (An_{45}), orthopyroxene (Fs_{50}) and augite (both with abundant inclusions of apatite), and titanomaghemite. Outcrops of the Desert Springs Tuff are scattered, but their distribution and westward increase in extent of welding indicate that the tuff was erupted from the TVC area. The mineralogy and chemistry of the Desert Springs Tuff are also similar to several TVC domes near Bearwallow Butte.

BEND PUMICE

The Bend Pumice of Taylor (1981) is a rhyodacitic, vitric air-fall lapilli tuff that is best exposed along the roads leading to Tumalo State Park. The 2-m-thick basal zone of the Bend Pumice consists of pumice lapilli, ash, and perlitic obsidian, and has been locally reworked and mixed with gravel and sand. The basal zone is thought to represent the preliminary stage of a climactic eruption (Hill, 1985). The basal zone is overlain by 3-13 m of air-fall lapilli and ash, which progressively increases in average grain size upsection. Westward increases in average grain size, unit thickness, and size of volcanic rock fragments (Hill, 1987) all indicate that the Bend Pumice was erupted from the TVC. In addition, the major and trace element composition of the Bend Pumice is nearly identical to several of the silicic domes that are preserved in the area of Three Creek Butte and Triangle Hill (Hill, 1987).

The Bend Pumice has been correlated with the Loleta ash bed (Sarna-Wojcicki and others, 1987; this volume), which has an estimated age of 0.35 to 0.39 Ma. K-Ar determinations for plagioclase separates from the overlying Tumalo Tuff yielded an average age of 0.29 ± 0.12 Ma, while obsidian fragments from the basal zone of the Bend Pumice have an average age of 0.42 ± 0.01 (Sarna-Wojcicki and others, this volume). As the obsidian is interpreted to mark a preliminary stage of the eruption that climaxed with the emplacement of the Bend Pumice and Tumalo Tuff, a best age for the eruption is thought to be about 0.4 Ma, which is at least 0.5 million years younger than previous estimates for this eruption (Armstrong and others, 1975).

TUMALO TUFF

The Tumalo Tuff of Taylor (1981) is a pink-to-tan, rhyodacitic, vitric ash-flow tuff that overlies Bend Pumice. The absence of a normally graded top to the Bend Pumice and the nonerosive basal contact of the Tumalo Tuff indicates that the Tumalo Tuff was produced through collapse of the Bend Pumice eruption column. The Bend Pumice and overlying Tumalo Tuff represent the eruption of at least 10 km^3 of nearly

homogeneous rhyodacitic magma (Hill, 1985).

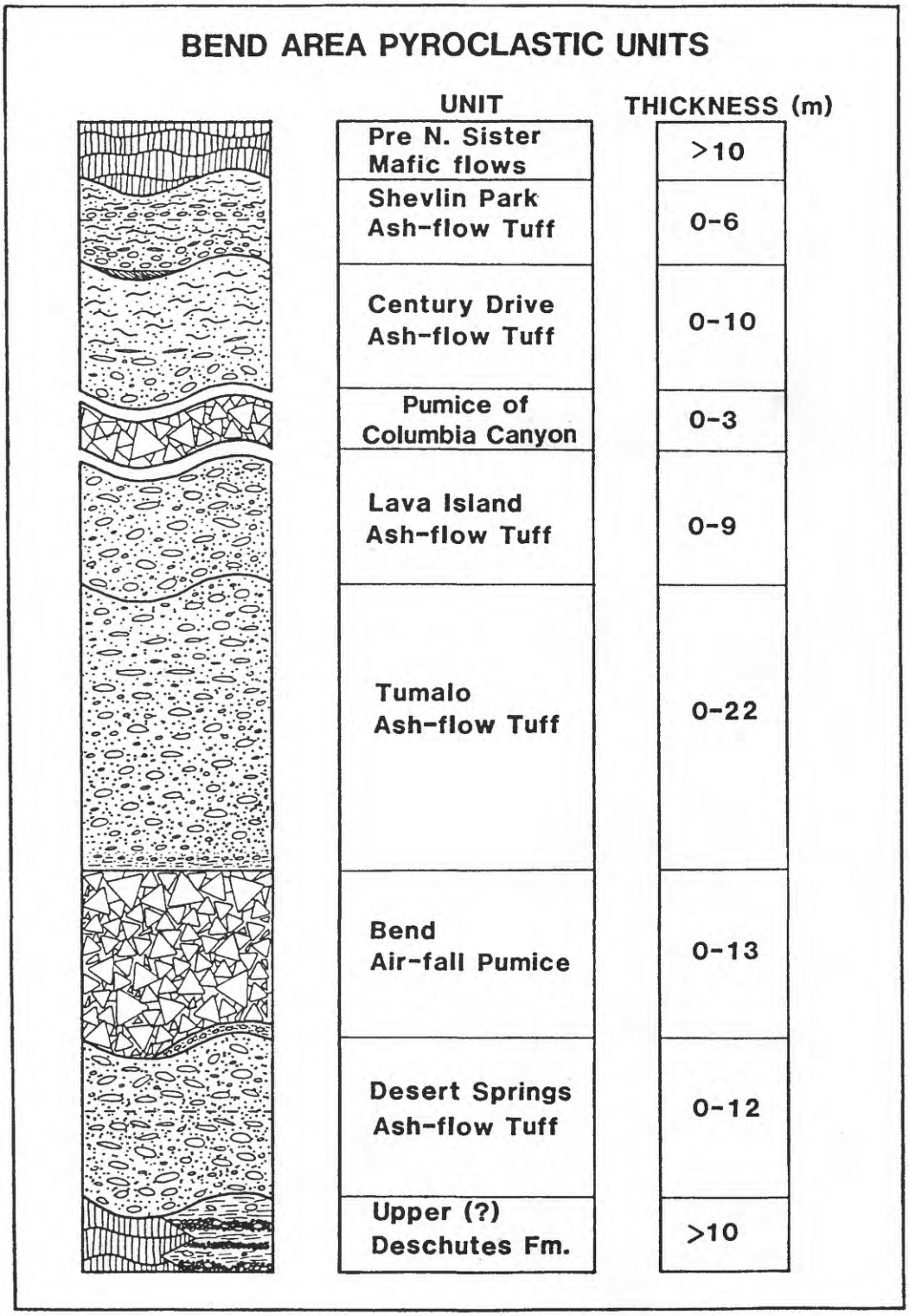

Figure 21. Schematic stratigraphic section of pyroclastic units erupted from the Tumalo volcanic center.

Table 7. Major and trace element compositions of High Cascade pyroclastic units in the vicinity of Bend. TT, Tumalo Tuff. All analyses water-free, with total iron as FeO. X, determined by X-ray fluorescence (Na_2O & MgO for average analyses by atomic absorption spectroscopy). I, determined by instrumental neutron activation analysis, Oregon State University.*

	Desert Springs Tuff	Average Bend Pumice	Average Tumalo Tuff	Average TT Banded Dacite	Pumice of Columbia Canyon	Shevlin Park Tuff	Century Drive Tuff	
Number of analyses	1	7 (1)	19	7	1	1	1	Method
SiO_2	68.0	74	74	66	67.0	61.5	58.5	X
TiO_2	0.72	0.14	0.15	0.91	0.81	1.28	1.51	X
Al_2O_3	15.6	14	15	17	17.1	17.6	17.4	X
FeO*	4.24	1.9	2.0	5.6	4.12	6.53	7.88	X
MnO	0.09	(0.07)	-	-	0.13	0.22	0.16	X
MgO	0.45	0.1	0.1	1.4	0.83	1.50	2.26	X
CaO	2.12	0.9	0.9	3.6	2.39	3.83	5.36	X
Na_2O	4.64	4.9	4.7	5.2	4.33	5.16	4.78	X
K_2O	3.25	3.4	3.5	1.9	2.16	1.65	1.02	X
P_2O_5	0.19	(0.03)	-	-	0.16	0.47	0.37	X
Sc	9.52	4.5	4.6	12.4	11.05	18.33	21.82	I
V	25	(<1)	-	-	36	105	159	X
Cr	3	1	1	13	3	4	10	I
Co	5.87	0.6	0.5	6.0	2.12	11.60	15.38	I
Ni	12	3	2	8	7	7	3	I
Zn	66	(105)	-	-	87	108	66	X
Rb	77	67	75	46	44	26	16	X
Sr	209	56	58	305	278	396	498	X
Cs	1.40	2.8	2.8	1.8	1.60	1.20	0.80	I
Ba	755	780	850	729	616	519	503	X
La	25.2	29.7	30.1	27.9	19.8	20.8	19.3	I
Ce	57.2	60	63	61	39.9	49.8	39.9	I
Nd	27.1	26	27	32	22.1	23.9	24.1	I
Sm	6.27	6.1	6.2	7.8	6.06	6.13	6.24	I
Eu	1.49	0.77	0.77	1.99	1.37	1.71	1.92	I
Tb	0.97	0.96	1.00	1.03	0.87	0.88	0.96	I
Yb	3.7	4.3	4.4	4.3	3.4	2.9	3.2	I
Lu	0.51	0.69	0.69	0.67	0.50	0.43	0.49	I
Zr	293	170	170	159	231	203	176	X
Hf	7.9	6.8	7.2	6.5	5.5	5.2	4.6	I
Nb	18.6	(17)	-	-	14.3	12.9	9.5	X
Ta	1.01	1.24	1.28	1.13	0.66	0.72	0.61	I
Ga	24	(24)	-	-	21	20	24	X
Y	34	(34)	-	-	36	30	32	X
Th	7.5	8.0	8.2	5.2	3.8	3.3	3.0	I
U	2.6	2.5	2.6	1.9	1.4	1.2	0.9	I
Source	a	b	b	b	a	a	a	

a = B.E. Hill, unpublished analyses
b = Hill, 1985

The basal 0.25 to 1.5 m of the Tumalo Tuff consists of a coarse pumice-depleted zone (layer 2a; terminology of layers after Sparks and others, 1973, and Wilson and Walker, 1982) and local surge (layer 1p) deposits. The main nonsorted part of the Tumalo Tuff (layer 2b) ranges in thickness to 22 m, and is the product of a single flow. Welding ranges from nonwelded to slightly welded (small amounts of pumice collapse). With the exception of the basal 1 m and the interior of large pumice bombs, the Tumalo Tuff has undergone low-grade vapor-phase alteration.

Both the Bend Pumice and Tumalo Tuff have a distinct mineral assemblage: plagioclase (An_{32}), ferrohypersthene (Fs_{58}), fresh black hornblende, titanomagnetite (Usp_{42}), apatite and zircon. They also contain the most iron-rich orthopyroxenes that have been observed in the OCHC. Banded pumice, which represents the mingling of rhyodacitic and unrelated dacitic magmas (Hill, 1985), is found in proximal (western) exposures. Although imbrication of pumice clasts in the Tumalo Tuff indicates a northeast direction of flow (Mimura, 1984), the direct association with the Bend Pumice indicates the Tumalo Tuff was erupted from the TVC and channeled by northeast-trending drainages (Hill, 1985, 1987).

LAVA ISLAND TUFF

The Lava Island Tuff of Taylor (1981) is a purple to grey, intensely devitrified ash-flow tuff that directly overlies the Tumalo Tuff. It is best exposed along the Deschutes River at Meadow Campground (T18S, R11E, S23). The basal contact with the Tumalo Tuff is sharp and erosive, with no intervening deposits. The Lava Island Tuff closely resembles welded sections of the Tumalo Tuff and has a similar composition and mineralogy except the ferrohypersthene is rimmed with augite, and both pyroxenes contain abundant apatite inclusions. The Lava Island Tuff may thus represent a flow lobe of the Tumalo Tuff that was derived from a deeper, gas-rich part of the magma chamber.

PUMICE OF COLUMBIA CANYON

This informally named vitric air-fall lapilli tuff occurs underneath the Shevlin Park Tuff in a steep canyon along the Columbia Canal (T17S, R11E, S17), and overlies several mafic lava flows north of the TVC. It has an average grain size (about 1 cm) that is similar to the Bend Pumice at the Columbia Canyon outcrop and contains abundant angular fragments of black obsidian up to 4 cm in diameter, both of which suggest this unit was erupted from a TVC vent. While the composition of the pumice of Columbia Canyon is distinctive (table 7), it has not been correlated with any other unit in the OCHC. Owing to its limited distribution and obsidian content, the pumice of Columbia Canyon is probably related to a small dome-forming eruption in the TVC .

CENTURY DRIVE TUFF

The Century Drive Tuff of Taylor (1981) is a variably welded vitric ash-flow tuff containing both rhyodacitic(?) and andesitic pumice. It is best exposed along Tumalo Creek west of Shevlin Park, where it forms large, densely welded outcrops. The Century Drive Tuff is restricted to scattered outcrops in the area south and west of Bend, and it appears to be more densely welded in exposures closer to the TVC, suggesting eruption from a TVC vent.

SHEVLIN PARK TUFF

The Shevlin Park Tuff of Taylor (1981) is an andesitic vitric ash-flow tuff that is distributed around a 180° sector east of and centered on Triangle Hill in the TVC (Hill, 1988). The Shevlin Park Tuff forms one cooling unit, and may contain two flow lobes and base-surge deposits in more proximal exposures. The Shevlin Park Tuff contains plagioclase (An_{46-38}), hypersthene (En_{64}), olivine (Fo_{78}), and titanomagnetite. The distribution of the Shevlin Park Tuff, along with increases in degree of welding and average pumice size, indicates that this unit was erupted from the TVC. It is probably associated with the Triangle Hill vent complex, which consists of silicic domes and andesitic cinder cones arranged in a roughly circular pattern around Triangle Hill. This complex has a diameter of about 3 km, and is centered on a -10 mgal gravity anomaly (Couch and others, 1982).

A noteworthy Shevlin Park Tuff outcrop occurs in the upper reaches of the North Fork of Squaw Creek (T16S, R9E, S29-30). At this location the Shevlin Park Tuff is overlain by a basaltic andesite flow of normal magnetic polarity , which is in turn overlain by the oldest basaltic andesites clearly associated with North Sister (Taylor, 1987). Because North Sister is the oldest stratovolcano of the Three Sisters, this exposure clearly demonstrates that pyroclastic volcanism associated with the TVC predated construction of the Three Sisters. Basaltic andesite flows from the Tam MacArthur Rim area partly cover the Triangle Hill vent complex, indicating that Tam MacArthur Rim and contemporaneous Broken Top volcanism (Taylor, 1978) postdate TVC volcanism as well.

AGE AND CORRELATION OF MID-QUATERNARY ASH BEDS AND TUFFS IN THE VICINITY OF BEND, OREGON

by

A. M. Sarna-Wojcicki[1], C. E. Meyer[1], J. K. Nakata[1], W. E. Scott[2], B. E. Hill[3], J. L. Slate[4], and P. C. Russell[5]

[1] U.S. Geological Survey, 345 Middlefield Rd., Menlo Park, CA 94025
[2] U.S. Geological Survey, Cascades Volcano Observatory, 5400 MacArthur Blvd, Vancouver, WA 98661
[3] Department of Geology, Oregon State University, Corvallis, OR 97331
[4] Department of Geological Sciences, University of Colorado, Boulder, CO 80302

INTRODUCTION

In this section, we discuss the sequence of mid-Quaternary pyroclastic rocks and sediments in the vicinity of Bend, Oregon, that are the subject of the Day 3 trip and place this sequence in a wider temporal and regional perspective. We discuss previously published age data and results of our recent work, which suggest that this sequence is much younger than previously thought. We will also discuss correlations of the pyroclastic units to distal localities in Oregon, Nevada, California, and the northeastern Pacific Ocean.

Of more local interest, dating the sequence of young tuffs and pumice beds exposed in the vicinity of Bend provides information on the timing and frequency of volcanic eruptions in the central Oregon Cascade Range and makes it possible to quantify the rates of deposition and erosion in the area. This information, in turn, provides important information to the studies of volcanic hazards, geothermal-resources assessment, and geomorphic processes in this area, and in the High Cascades a few tens of kilometers to the west. Such a chronology can be developed by direct isotopic dating of the local units, as well as by obtaining age data by correlation of local tephra layers to distal equivalents.

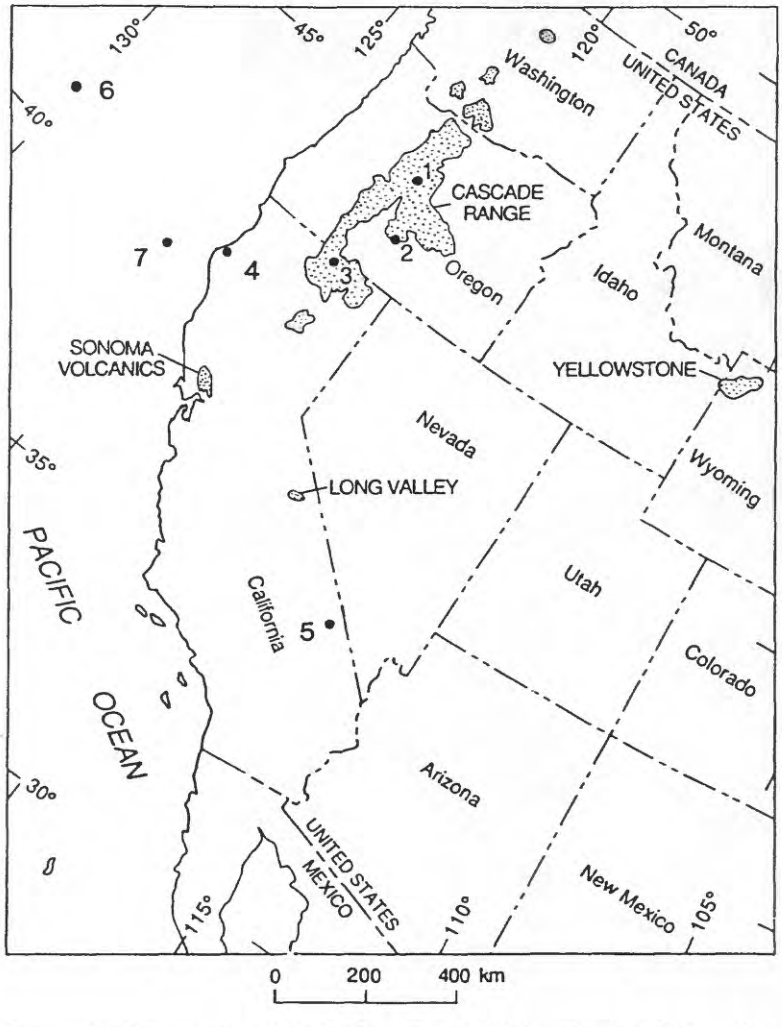

Figure 22. Localities discussed in this report and shown in the correlation chart (fig. 24). 1 - Bend; 2 - Summer Lake; 3 - Tulelake; 4 - Humboldt basin; 5 - Lake Tecopa; 6 - DSDP Site 36; 7 - DSDP Site 173. Patterned areas - major source areas of explosive, silicic, late Cenozoic volcanism.

BACKGROUND TO THIS STUDY

Sarna-Wojcicki and others (1987) became interested in the pyroclastic units in the vicinity of Bend while attempting to find the sources and proximal deposits of several widespread ash beds that they had identified and dated in the Humboldt basin of northwestern California, in deep-ocean sediments at DSDP sites in the Pacific Ocean to the west, and at several other sites in the conterminous western U.S. (fig. 22). Among these ash beds are the

Rio Dell and Loleta ash beds, dated about 1.5 Ma and 0.35-0.39 Ma, respectively, by tephrochronology, correlation of isotopic ages, magnetostratigraphy, and biostratigraphy. The chemical composition of these ash beds suggested that they were erupted from the High Cascades; moreover, because their composition is intermediate between those erupted from the northern Cascade Range (e.g., Mount St. Helens) and the southern Cascade Range (e.g., Lassen Peak area), we suspected that they were erupted in the central High Cascades. E.M. Taylor of Oregon State University and N.S. MacLeod of the USGS, among others, suggested that the Bend Pumice of Taylor (1981), a thick and locally extensive silicic airfall unit, might be a good candidate for the proximal equivalent of one of these ash beds.

Previously determined ages of the volcanic units near Bend were scattered and rather imprecise. K-Ar ages on the Bend Pumice and Tumalo Tuff of Taylor (1981) (0.5±0.9 Ma, Armstrong and others, 1975; 2.5±2.0, 2.6±2.2, and 3.98±1.9 Ma, Fiebelkorn and others, 1983) suggested that some of these units may be as old as late Pliocene.

Because of these results, we expected that Bend Pumice might correlate with the older Rio Dell ash bed. To our surprise, the composition of its volcanic glass as determined by electron microprobe matched the younger Loleta ash bed (table 8; fig. 23).

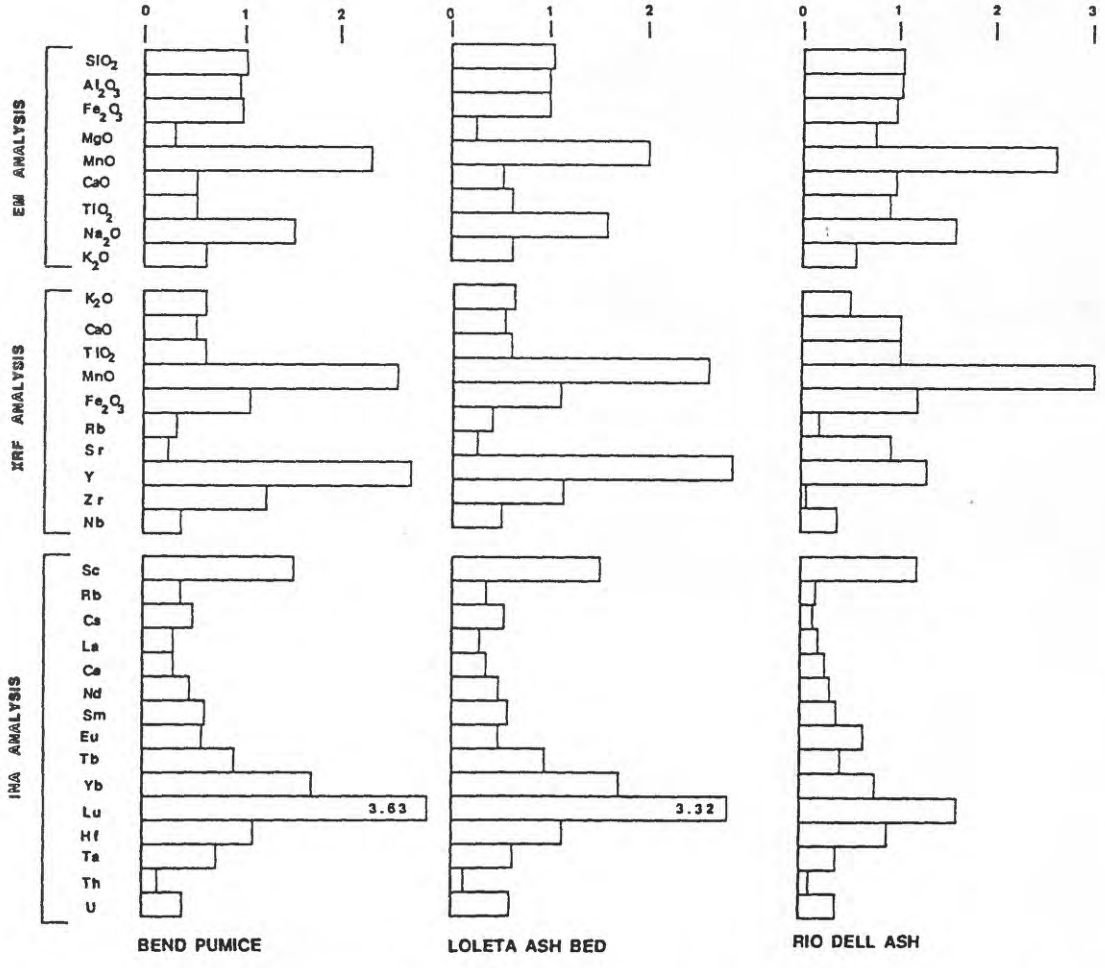

Figure 23. Histograms comparing the chemical composition of volcanic glass of the Bend Pumice and the Loleta and Rio Dell ash beds. Values represented are oxide and element concentrations shown in table 8, divided by the concentrations of the same oxides and elements in USGS rock standard G-1.

Table 8. Chemical analyses of the Bend Pumice, and the Loleta and Rio Dell ash beds. Electron-microprobe analysis by C. E. Meyer, USGS, Menlo Park; energy-dispersive X-ray fluorescence analysis by J. L. Slate, USGS, Menlo Park; instrumental neutron-activation analysis for the Bend Pumice from Hill (1985; average of whole-rock samples 8201A, 9111B, and 9111C), and by H. R. Bowman, Lawrence Berkeley Laboratory, Univ. of Calif., Berkeley (glass of the Loleta and Rio Dell ash beds). Oxides are in weight percent; elements in parts per million. Electron-microprobe oxide concentrations are recalculated to 100 percent; totals given are before recalculation. The Bend Pumice is from an abandoned pumice quarry NW of Bend, OR; the Loleta ash bed is from the marine Hookton Fm., stratigraphically overlying the Rockland ash bed, in the Humboldt Basin, CA; the Rio Dell ash bed is from the upper part of the marine Rio Dell Fm., in the Centerville Beach section, Humboldt Basin, CA. nd, not determined.

Oxide or element	Bend Pumice (BPT-1)	Loleta ash bed (SM-ASH-5)	Rio Dell ash bed (RD-2)	Analytical method
SiO_2	74.85	74.74	74.05	
Al_2O_3	13.71	13.86	14.46	
Fe_2O_3	1.94	1.92	1.92	
MgO	0.11	0.10	0.28	
MnO	0.07	0.06	0.08	Electron
CaO	0.74	0.74	1.35	microprobe
TiO_2	0.14	0.17	0.24	
Na_2O	5.09	5.28	5.26	
K_2O	3.34	3.14	2.36	
Total (Orig.)	95.38	94.30	94.05	
K_2O	3.38	3.64	2.76	
CaO	0.77	0.75	1.44	
TiO_2	0.160	0.153	0.268	
MnO	0.078	0.078	0.091	
Fe_2O_3	2.09	2.09	2.33	Energy
Rb	80	80	42	dispersive
Sr	57	58	238	XRF
Y	35	37	17	
Zr	262	259	211	
Nb	9	12	8	
Sc	4.63	4.59	3.67	
Mn	nd	503	571	
Rb	72	80	36	
Cs	2.9	3.3	0.8	
La	30	29	20	
Ce	60	61	41	
Nd	26	28	18	
Sm	6.1	5.3	3.3	
Eu	0.77	0.66	0.90	Neutron
Tb	0.96	0.96	0.43	activation
Dy	nd	5.9	2.3	
Yb	4.3	4.3	2.0	
Lu	0.69	0.63	0.30	
Hf	6.8	7.1	5.4	
Ta	1.2	1.0	0.6	
Th	8.0	7.9	4.2	
U	2.5	2.5	1.4	

We followed up the probe analyses with energy-dispersive X-ray fluorescence of glass separates, and compared instrumental neutron activation analysis of the Bend Pumice (Hill, 1985) with our analysis of the Loleta ash bed (Sarna-Wojcicki and others, 1987). These analyses also indicated that the Loleta ash bed and Bend Pumice were the same unit (table 8; fig. 23).

K-AR ANALYSES AND THE AGE OF THE BEND PUMICE

Some geologists familiar with the local geology around Bend doubted that the Bend Pumice and associated units could be as young as our correlations indicated, based in part on their perception of the rates at which deposition and erosion operated within this area--a perception possibly conditioned by the early isotopic ages on these units. We therefore attempted to date the Bend Pumice directly. To avoid or minimize detrital or xenocrystic contamination, we sampled the Tumalo Tuff, a coarse ash-flow unit that immediately overlies the Bend Pumice and was produced by the same eruptive episode (Hill, 1985). We collected large (to 0.5 m) pumice blocks from the Tumalo Tuff, near the town of Tumalo. Several centimeters of the outer parts of these were removed and the cores were crushed to separate crystals for age analysis. These blocks were largely aphyric, and only plagioclase feldspar was present in sufficient quantity for K-Ar dating. The four ages on feldspars are scattered and imprecise, due to the low potassium content of the feldspar grains, the young age of the tuff, and the resulting high content of atmospheric relative to radiogenic argon (table 9). However, a weighted average of the four ages, 0.3±0.1 Ma, is in agreement with our stratigraphic, magnetostratigraphic, and isotopic age data on correlated units (fig. 24).

Table 9. Ages and analytical data for K-Ar analysis of the Tumalo tuff (ashflow), near Tumalo (1, 2), the pumice lapilli airfall tuff with obsidian clasts underlying the Bend pumice (3-5), just west of the town of Bend, OR, and dacitic pumice clasts from the Tumalo tuff 10 km west of Bend (6, 7). Analysts: samples 1-5, J. K. Nakata; samples 6, 7, P. C. Russell. K2O analyses: T. Fries, M. Dyslin, U.S.G.S., Menlo Park, CA.

Sample number	Material dated	K_2O, wt %	weight, g	Radiogenic ^{40}Ar, 10^{-12} mol/g	Atmospheric ^{40}Ar, %	Calc. age, Ma
1a	plag.	0.676 ± 0.01	7.0982	0.18134	98.25	0.19 ± 0.08
1b	"	"	6.8884	0.26515	98.31	0.27 ± 0.11
2a	"	0.671 ± 0.005	6.2084	0.37452	98.29	0.39 ± 0.14
2b	"	"	6.4030	0.29085	98.35	0.30 ± 0.12
					Weighted average (1, 2):	0.29 ± 0.12
3	obsid.	3.485 ± 0.007	6.3622	2.19205	54.13	0.44 ± 0.01
4	"	"	14.5722	2.03216	77.46	0.40 ± 0.01
5	"	"	8.5685	2.0679	70.10	0.41 ± 0.02
					Weighted average (3-5):	0.42 ± 0.01
6	hornb.	0.369 ± 0.008	8.8034	0.68890	97.46	1.30 ± 0.23
7	"	"	8.8125	0.55282	97.52	1.04 ± 0.20

Constants (Steiger and Jager, 1977):

$^{40}K/K = 1.167 \times 10^{-4}$ mol/mol

$\lambda = 4.962 \times 10^{-10}$ yr^{-1}

$\lambda_\epsilon + \lambda'_\epsilon = 0.581 \times 10^{-10}$ yr^{-1}

In an attempt to improve the precision of the K-Ar ages by analyzing a phase richer in potassium, we subsequently collected obsidian fragments from an airfall lapilli tuff that directly underlies the thick, coarse-

grained, airfall layer of the Bend Pumice (within the basal Bend Pumice as defined by Hill and Taylor, this volume) just west of the town of Bend. This tuff has a sharp depositional contact with the Bend Pumice, shows no evidence of weathering at the top, and has not been reworked at this locality. Furthermore, there is very little difference in chemistry of the obsidian clasts and glass shards of the overlying Bend Pumice (table 10), suggesting that they were probably deposited close in time, and were probably part of the same eruptive episode that culminated with the Tumalo Tuff (Hill, 1985). The weighted average age of the obsidian clasts (table 9) is 0.42±0.01 Ma; this age provides only a maximum age for the Bend Pumice because the obsidian clasts may have been derived from a unit (for example, a dome) that is older than the ash which contains them, and because the airfall ash containing the clasts underlies the Bend Pumice. The two sets of K-Ar ages, however, bracket the age of the Bend Pumice between about 0.3 and 0.4 Ma. A subsequent analysis of a hornblende separate obtained from the dacitic part of the Tumalo Tuff banded pumices gives significantly older ages of about 1.1 and 1.3 Ma (table 9). Hill (1985) showed that the dacitic pumice was a minor part of the Bend-Tumalo eruption, and was not genetically related to the bulk of the rhyodacitic eruption. We suspect that the hornblende separates contain inherited radiogenic argon or xenocrysts.

TEPHROSTRATIGRAPHY

We have analyzed several other tuffs in addition to the Bend Pumice in order to determine their age and correlation. Electron-microprobe analysis of the Desert Springs Tuff of Taylor (1981), which underlies the Bend Pumice as well as the underlying pumice lapilli tuff with obsidian clasts, indicates that the Desert Springs matches closely with the Rye Patch Dam ash bed of Davis (1978), found in the Humboldt River area of northwestern Nevada.

The Loleta ash bed, the distal equivalent of the Bend Pumice, overlies the Rockland ash bed within the marine Hookton Formation of the Humboldt basin, in northwestern California (fig. 24). The Rockland ash bed has been dated at 0.40±0.02 Ma by fission-track analysis on zircons and at 0.45±0.30 Ma by K-Ar analyses on hornblende and plagioclase (Meyer and others, 1980; Gilbert, 1969; Sarna-Wojcicki and others, 1985; C. E. Meyer and others, unpublished data). These data provide another maximum age constraint for the Bend Pumice that is consistent with other stratigraphic and age data, except for the ages of hornblendes from the dacitic pumices in the Tumalo Tuff.

The pumice of Columbia Canyon is chemically similar to ash bed SL-NN at Summer Lake, in south-central Oregon; and the Shevlin Park Tuff matches ash bed SL-JJ, at Summer Lake (figs. 22, 24; table 10; Davis, 1985). The last unit contains a bimodal population of silicic and mafic shards, and both types are found within the Shevlin Park Tuff, near Bend, and ash bed SL-JJ, at Summer Lake (table 10). The correlated units define a characteristic sequence that is repeated at other sites without violating superposition, thus strengthening the correlations.

MAGNETOSTRATIGRAPHY

All the tuffs within the sequence described here are normally magnetized. Although Armstrong and others (1975) reported the presence of a reversely magnetized lava flow above the Bend Pumice, subsequent measurements have failed to confirm this polarity. No units with reversed magnetization have been found above or within the Quaternary tuffs overlying the Deschutes Formation, an observation that is compatible with the sequence being deposited during the Brunhes Normal Polarity Chron, and with a mid-Quaternary or younger age, but at odds with an age of 1.1 to 1.3 Ma.

CORRELATION OF THE DESERT SPRINGS TUFF AND OTHER UNITS IN THE VICINITY OF BEND TO THE DEEP-SEA OXYGEN-ISOTOPE RECORD

Because the distal equivalent of the Desert Springs Tuff, the Rye Patch Dam ash bed, underlies the Lava Creek B ash bed with small stratigraphic separation at Tulelake, it is close to it in age (Sarna-Wojcicki and others, in press). The Lava Creek B ash bed is also found at Lake Tecopa, California, where it lies near the top of a pluvial lake-bed sequence. The age of the Lava Creek B ash bed, 0.62 Ma (Izett and Wilcox, 1982), places it close in time to the end of oxygen isotope stage 16 (Shackleton and Opdyke, 1973; Imbrie and others, 1984). These data suggest that the end of this oxygen isotope stage and that of the pluvial stage were synchronous. The slightly older Desert Springs Tuff and its distal correlative were probably erupted during the maximum of stage 16 (Sarna-Wojcicki and others, in press).

Table 10. Electron-microprobe analysis of volcanic glass from pumice beds, and airfall and ashflow tuffs in the vicinity of Bend, OR, and correlative distal ash beds. Oxide concentrations are in weight percent, recalculated to 100 percent (fluid-free). Analysts: C. E. Meyer, U.S. Geological Survey, Menlo Park, CA, and J. O. Davis, Desert Research Institute, Reno, NV (samples DR-30B, DR-30W, DR-70, and LD-61).

Sample	SiO_2	Al_2O_3	Fe_2O_3	MgO	MnO	CaO	TiO_2	Na_2O	K_2O
Shevlin Park Tuff (SPAT-1, -2) and Summer Lake ash bed JJ (DR-30B): (mafic glass shards); ca. 0.15 Ma									
SPAT-1	58.95	14.87	9.22	3.15	0.18	6.31	1.60	4.17	1.55
SPAT-2	56.83	16.32	9.76	3.29	0.16	6.61	1.63	4.22	1.18
DR-30B	57.52	16.29	9.22	3.04	0.15	6.15	1.59	4.53	1.51
Shevlin Park Tuff (SPAT-3) and Summer Lake ash bed JJ (DR-30W): (silicic glass shards)									
SPAT-3	74.91	14.05	1.81	0.14	0.06	0.88	0.16	5.14	2.84
DR-30W	73.27	14.45	2.27	0.16	0.05	0.96	0.20	5.26	3.01
Pumice of Columbia Canyon (BPT-CC) and Summer Lake ash bed NN (DR-70)									
BPT-CC	69.34	15.31	3.70	0.72	0.13	2.12	0.67	5.70	2.30
DR-70	69.70	15.07	3.79	0.67	0.09	2.16	0.68	5.12	2.71
Bend Pumice (BPT-1) and Loleta ash bed (SM-ASH-4, -5); ca. 0.4-0.3 Ma									
BPT-1	74.85	13.72	1.94	0.11	0.07	0.74	0.14	5.09	3.34
SM-ASH-4	74.69	13.92	1.93	0.11	0.06	0.73	0.17	5.18	3.21
SM-ASH-5	74.74	13.86	1.92	0.10	0.06	0.74	0.17	5.28	3.14
Obsidian from pumice lapilli tuff containing obsidian clasts: clear (1) and with microlites (2); 0.41 Ma									
BPT-OB(1)	75.30	13.73	1.69	0.09	0.06	0.71	0.12	4.93	3.38
BPT-OB(2)	75.42	13.54	1.79	0.10	0.07	0.69	0.13	4.80	3.46
Desert Springs Tuff: black, glassy fiamae from welded tuff (DST-1), and dark brown pumice clasts (DST-3); Rye Patch Dam ash bed (LD-61); ca. 0.63 Ma									
DST-1	72.69	13.39	3.21	0.38	0.07	1.47	0.43	4.75	3.61
DST-3	71.31	14.58	3.19	0.39	0.09	1.48	0.44	4.40	4.12
LD-61	71.07	14.70	3.32	0.37	0.09	1.45	0.45	4.99	3.56
Ash bed at 130.4 m in Tulelake core (T-558) and Rio Dell ash bed (RD-2); ca. 1.5 Ma									
T-558	73.61	14.73	1.87	0.34	0.08	1.31	0.31	4.88	2.86
RD-2	74.84	14.13	1.85	0.28	0.08	1.31	0.26	4.92	2.39

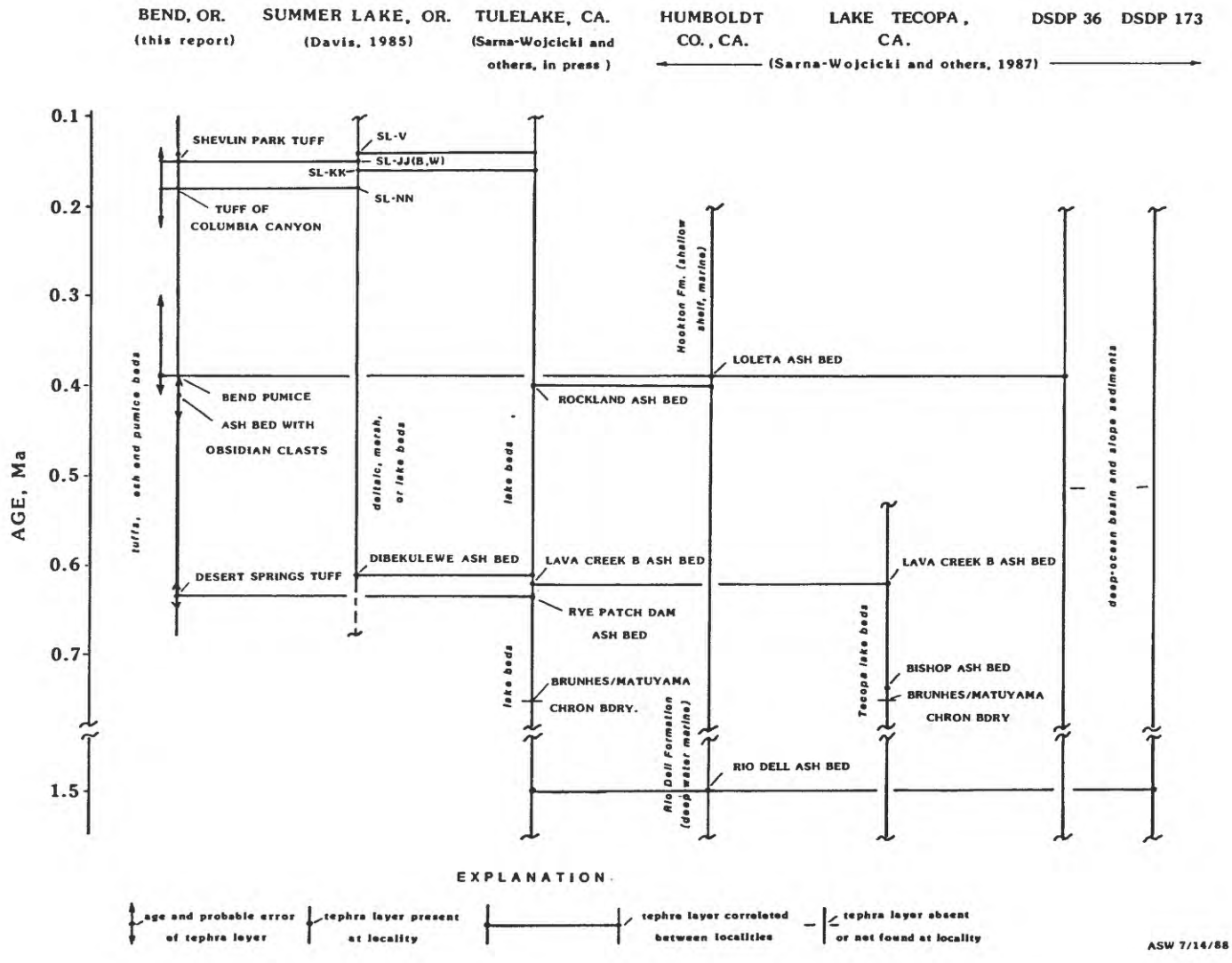

Figure 24. Correlation chart of Quaternary tephra layers at several localities in California, Oregon, and the northeastern Pacific Ocean.

CONCLUSIONS

The sequence of mid-Quaternary volcanic deposits in the vicinity of Bend is much younger than previously supposed; consequently the frequency of volcanic eruptions and the rates at which processes of deposition, erosion, and tectonism have operated in this area were also more rapid than previously supposed--actually about three to ten times more rapid. These conclusions have important implications for the study of process geomorphology, volcanic hazards, and assessment of geothermal potential in this region. Specifically, the presence of a young, thick, and extensive silicic tuff such as the Bend Pumice, representing the equivalent of at least 10 km^3 of rhyodacitic magma (Hill, 1985), has stimulated a search for the vent complex from which this tuff was erupted (Hill, 1987), and for possible associated geothermal resources.

We conclude that the Desert Springs Tuff, the lowest unit in the sequence of pyroclastic units exposed in the Bend area (fig. 24) correlates with the Rye Patch Dam ash bed (Davis, 1985). Correlation of this unit to a cored section at Tulelake in northern California provides an age of about 0.63 Ma for this layer by interpolation

between the Lava Creek B ash bed (0.62 Ma) close above, and the Brunhes/Matuyama Chron boundary (0.73 Ma) below (fig. 24; Sarna-Wojcicki and others, in press). We further conclude that the Bend Pumice is a proximal equivalent of the Loleta ash bed found in sediments of the Humboldt basin in northwestern California and in sediments of the eastern Pacific Ocean (DSDP Site 36; Sarna-Wojcicki and others, 1987), and that this tephra layer has a mid-Pleistocene age of between about 0.4 and 0.3 Ma. Lastly, the age of the Shevlin Park Tuff is estimated to be about 0.15 Ma on the basis of correlation with the Summer Lake section of south-central Oregon (Davis, 1985), and correlation of tephra layers from that locality to Tulelake, where approximate age control is obtained from a sedimentation-rate curve derived from tephrochronology and magnetostratigraphy in the core (fig. 24; Sarna-Wojcicki and others, in press).

COMBINED REFERENCES

Anderson, L.W., 1978, Cirque glacier erosion rates and characteristics of neoglacial tills, Pangnirtung Fiord area, Baffin Island, N.W.T., Canada: Arctic and Alpine Research, v. 10, p. 749-760.

Andrews, J.T., 1971, Estimates of variations in glacial erosion from the volume of corries and moraines: Geological Society of America Abstracts with Programs, v. 3, p. 493.

Andrews, J.T., 1972, Glacial power, mass balances, velocities, and erosion potential: Zeitschrift fur Geomorphologie Supplement, v. 13, p. 1-17.

Andrews, J.T., and LeMasurier, W.E., 1973, Rates of Quaternary glacial erosion and corrie formation, Marie Byrd Land, Antarctica: Geology, v. 1, p. 76-80.

Armstrong, R.L., Taylor, E.M., Hales, P.O., Parker, D.J., 1975, K-Ar dates for volcanic rocks, central Cascade Range of Oregon: Isochron/West,.v. 13, p. 5-7.

Bacon, C.R., 1983, Eruptive history of Mount Mazama and Crater Lake caldera, Cascade Range, U.S.A.: Journal of Volcanology and Geothermal Research, v. 18, p. 57-115.

Bacon, C.R., 1985, Implications of silicic vent patterns for the presence of large crustal magma chambers: Journal of Geophysical Research, v. 90, no. B13, p.11,243-11,252.

Baedecker, P.A., ed., 1987, Methods for geochemical analysis: U.S. Geological Survey Bulletin 1770.

Bailey, R., MacDonald, R.A., and Thomas, J.E., 1983, The Inyo-Mono Craters: Products of an actively differentiating rhyolite magma chamber, eastern California [abs]: Eos, (American Geophysical Union Transactions), v. 64, p. 336.

Beget, J.E., 1984, Tephrochronology of late Wisconisn deglaciation and Holocene glacier fluctuations near Glacier Peak, North Cascade Range, Washington: Quaternary Research, v. 21, p. 304-316.

Burke, R.M., and Birkeland, P.W., 1983, Holocene glaciation in the mountain ranges of the western United States, in Wright, H.E., Jr., ed., The Holocene, v. 2 of Late Quaternary environments of the United States: Minneapolis, University of Minnesota Press, p. 3-11.

Champion, D.E., 1980, Holocene geomagnetic secular variation in the western United States: Implications for the global geomagnetic field: U.S. Geological Survey Open-File Report 80-824, 277 p.

Clark, J.G., 1983, Geology and petrology of South Sister volcano, High Cascade Range, Oregon: Eugene, University of Oregon, Ph.D. dissertation, 235 p.

Couch, R., and Foote, R., 1985, The Shukash and Lapine basins: Pleistocene depressions in the Cascade Range of central Oregon [abs]: Eos, (American Geophysical Union Transactions), v. 66, no. 3, p. 24.

Couch, R.W., Pitts, G.S., Gemperle, M., Braman, D.E., Veen, C.A., 1982, Gravity anomalies in the Cascade Range in Oregon: Structural and thermal implications. Oregon Department of Geology and Mineral Industries Open-File Report O-82-9, 43 p.

Crandell, D.R., 1965, The glacial history of Washington and Oregon, in, Wright, H.E., Jr., and Frey, D.G., eds., The Quaternary of the United States: Princeton, N.J., Princeton University Press, p 341-353.

Crandell, D.R., and Miller, R.D., 1974, Quaternary stratigraphy and extent of glaciation in the Mount Rainier region, Washington: U.S. Geological Survey Professional Paper 847, 59 p.

Crowe, Bruce, and Nolf, Bruce, 1977, Composite cone growth modeled after Broken Top, a dissected High Cascade volcano [abs]: Geological Society of America Abstracts with Programs, v. 9, p. 940-941.

Davis, J. O., 1978, Quaternary tephrochronology of the Lake Lahontan area, Nevada and California. Nevada Archeological Research Paper 7, 137 p.

Davis, J. O., 1985, Correlation of Quaternary tephra layers in a long pluvial sequence near Summer Lake, Oregon. Quaternary Research, v. 23, p. 38-53.

Delaney, P.T., and Pollard, D.D., 1981, Deformation of host rocks and flow of magma during growth of minette dikes and breccia-bearing intrusions near Ship Rock, New Mexico: U.S. Geological Survey Professional Paper 1202, 61 p.

Dethier, D.P., 1980, Reconnaissance study of Holocene glacier fluctuations in the Broken Top area, Oregon [abs.]: Geological Society of America Abstracts with Program, v. 12, no. 3, p. 104.

Driedger, C.L., and Kennard, P.M., 1986, Ice volumes on Cascade volcanoes--Mount Rainier, Mount Hood, Three Sisters, and Mount Shasta: U.S. Geological Professional Paper 1365, 28 p.

Eichelberger, J.C., Lysne, P.C., Miller, C.D., and Younker, L.W., 1985, Research drilling at Inyo domes, California: 1984 results: Eos, (American Geophysical Union Transactions), v. 66, no. 17, p. 186-187.

Fiebelkorn, R.B., Walker, G.W., MacLeod, N.S., McKee, E.H., and Smith, J.G., 1983, Index to K-Ar determinations for the state of Oregon: Isochron/West, v. 37, p. 3-60.

Fink, J.H., and Pollard, D.D., 1983, Structural evidence for dikes beneath silicic domes, Medicine Lake volcano, California: Geology, v. 11, p. 458-461.
Fisher, R.A., 1953, Dispersion on a sphere: Proceedings of the Royal Society of London, v. A217, p. 295-305.
Gardner, C.A., 1989, Temporal, spatial, and petrologic variations of lava flows from the Mount Bachelor volcanic chain, central Oregon High Cascades: Boulder, University of Colorado, M.S. thesis, 188 p.
Gardner, C.A., and Scott, W.E., 1987, Temporal, spatial, and petrologic variations of lavas from the Mount Bachelor volcanic chain, Oregon High Cascades [abs]: Eos, (American Geophysical Union Transactions), v. 68, no. 44, p. 1526.
Gilbert, N.J., 1969, Chronology of post-Tuscan volcanism in the Manton area, California: Berkeley, University of California, M.S. thesis.
Hammond, P.E., 1979, A tectonic model for evolution of the Cascade Range, in, Armentrout, J.M., Cole, M.R., and Terbest, H., Jr., eds., Cenozoic paleogeography of the western United States: Pacific Coast Paleogeography Symposium 3: Los Angeles, Society of Economic Paleontologists and Mineralogists, Pacific Section, p. 219-237.
Hill, B.E., 1985, Petrology of the Bend Pumice and Tumalo Tuff, a Pleistocene Cascade eruption involving magma mixing: Corvallis, Oregon State University, M.S. thesis, 101 p.
Hill, B.E., 1987, The widespread Loleta ash and its proximal equivalents had an Oregon central High Cascade source: Geological Society of America Abstracts with Program, v. 19, no. 7, p 703.
Hill, B.E., 1988, The Tumalo Volcanic Center: A large Pleistocene vent complex on the east flank of the Oregon central High Cascades: Geological Society of America Abstracts with Program, v. 20, no. 7, p. A398.
Hoblitt, R.P., Reynolds, R.L., and Larson, E.E., 1985, Suitability of non-welded pyroclastic-flow deposits for studies of magnetic secular variation: A test based on deposits emplaced at Mount St. Helens, Washington, in 1980: Geology, v. 13, p. 242-245.
Hughes, S.S., 1982, Petrochemical evolution of the High Cascade volcanic rocks in the Three Sisters region, Oregon: Corvallis, Oregon State University, Ph.D. dissertation, 199 p.
Hughes, S.S., and Taylor, E.M., 1986, Geochemistry, petrogenesis, and tectonic implications of central High Cascade mafic platform lavas: Geological Society of America Bulletin, v. 97, no. 8, p. 1024-1036.
Imbrie, J., Hays, J.D., Martinson, D.G., McIntyre, A., Mix, A.C., Morley, J.J., Pisias, N.G., Prell, W.L., and Shackleton, N.J., 1984, The orbital theory of Pleistocene climate: Support from a revised chronology of the marine $\partial^{18}O$ record, in Berger, A. L., and others, eds., Milankovitch and Climate, Part I: The Netherlands, Reidel, p. 269-305.
Izett, G.A., and Wilcox, R.E., 1982, Map showing localities and inferred distributions of the Huckleberry Ridge, Mesa Falls, and Lava Creek ash beds (Pearlette family ash beds) of Pliocene and Pleistocene age in the western United States and Canada. U.S. Geological Survey Miscellaneous Investigations Series Map I-1325, scale 1:4,000,000.
Kienle, C.F., Nelson, C.A., and Lawrence, R.D., 1981, Faults and lineaments of the southern Cascades, Oregon: Oregon Department of Geology and Mineral Industries Special Paper 13, 23 p.
Kuntz, M.A., Champion, D.E., Spiker, E.C., and Lefebvre, R.H., 1986, Contrasting magma types and steady-state, volume-predictable, basaltic volcanism along the Great Rift, Idaho: Geological Society of America Bulletin, v. 97, p. 579-594.
Larsen, E., and Mangerud, J., 1981, Erosion rate of a Younger Dryas cirque glacier at Krakenes, western Norway: Annals of Glaciology, v. 2, p. 153-160.
LeBas, M.J., Le Maitre, R.W., Strecheisen, A., and Zanettin, B., 1986, A chemical classification of volcanic rocks based on the total alkali-silica diagram: Journal of Petrology, v. 27, p. 745-750.
MacLeod, N.S., Sherrod, D.R., Chitwood, L.A., and McKee, E.H., 1981, Newberry volcano, Oregon, in Johnston, D.A., and Donnelly-Nolan, Julie, eds., Guides to some volcanic terranes in Washington, Idaho, Oregon, and northern California: U.S. Geological Survey Circular 838, p. 85-103.
Mankinen, E.A., Gromme, C.S., Dalrymple, G.B., Lanphere, M.A., and Bailey, R.A., 1986, Paleomagnetism and K-Ar ages of volcanic rocks from Long Valley caldera, California: Journal of Geophysical Research, v. 91, p. 633-652.
Meier, M.F., 1961, Mass balance of South Cascade Glacier, 1957-1960: U.S. Geological Survey Professional Paper 424-B, p. 206-211.
Meyer, C.E., Woodward, M.J., Sarna-Wojcicki, A.M., and Naeser, C.W., 1980, Zircon fission-track age of 0.45 million years on ash in the type section of the Merced Formation, west-central California: U.S. Geological Survey Open-File Report 80-1071.

Miller, C.D., 1985, Holocene eruptions of the Inyo volcanic chain, California–Implications for possible eruptions in Long Valley caldera: Geology, v. 13, p. 14-17.
Mills, H.H., 1976, Estimated erosion rates on Mount Rainier, Washington: Geology, v. 4, p. 401-406.
Mimura, Koji, 1984, Imbrication, flow direction and possible source areas of the pumice-flow tuffs near Bend, Oregon: Journal of Volcanology and Geothermal Research, v. 21, p. 45-60.
Miyashiro, A., 1974, Volcanic rock series in island arcs and active continental margins: American Journal of Science, v. 274, p. 321-355.
Nolf, Bruce, 1969, Broken Top breaks: Flood released by erosion of glacial moraine: The Ore Bin, v. 31, no. 11, p. 182-188.
O'Hara, M.J., 1977, Geochemical evolution during fractional crystallization of a periodically refilled magma chamber: Nature, v. 266, p. 503-507.
Patterson, W.S.B., 1981, The physics of glaciers: Oxford, U.K., Pergamon Press, 380 p.
Pierce, K.L., 1979, History and dynamics of the glaciation in the northern Yellowstone National Park area: U.S. Geological Survey Professional Paper 729-F, 90 p.
Pollard, D.D., Delaney, P.T., Duffield, W.A., Endo, E.T., and Okamura, A.T., 1983, Surface deformation in volcanic rift zones: Tectonophysics, v. 94, no. 1-4, p. 541-584.
Porter, S.C., 1976, Pleistocene glaciation in the southern part of the North Cascade Range, Washington: Geological Society of America Bulletin, v. 87, p. 61-75.
Porter, S.C., Pierce, K.L., and Hamilton, T.D., 1983, Late Wisconsin mountain glaciation in the western United States, in Porter, S. C., ed., The late Pleistocene, v. 1 of Late-Quaternary environments of the United States: Minneapolis, University of Minnesota Press, p. 71-111.
Priest, G.R., Woller, N.M., Black, G.L., and Evans, S.H., 1983, Overview of the geology of the central Oregon Cascade Range, in Priest, G.R., and Vogt, B.F., eds., Geology and geothermal resources of the central Oregon Cascade Range: Oregon Department of Geology and Mineral Industries Special Paper 15, p. 3-28.
Reheis, M.J., 1975, Origin, transport, and deposition of debris on Arapaho Glacier, Front Range, Colorado, U.S.A.: Journal of Glaciology, v. 19, p. 407-420.
Rieck, H.J., Sarna-Wojcicki, A.M., and Adam, D.P., in press, Magnetostratigraphy and tephrochronology of upper Pliocene and Quaternary lake sediments, Tulelake, northern California: U.S. Geological Survey Open-File Report, 51 p.
Russell, I.C., 1905, Preliminary report on the geology and water resources of central Oregon: U.S. Geological Survey Bulletin 252, 138 p.
Sarna-Wojcicki, A.M., Meyer, C.E., Bowman, H.R., Hall, N.T., Russell, P.C., Woodward, M.J., and Slate, J.L., 1985, Correlation of the Rockland ash bed, a 400,000-year-old stratigraphic marker in northern California and western Nevada, and implications for middle Pleistocene paleogeography of central California: Quaternary Research, v. 23, p. 236-257.
Sarna-Wojcicki, A.M., Morrison, S.D., Meyer, C.E., and Hillhouse, J.W., 1987, Correlation of upper Cenozoic tephra layers between sediments of the western United States and eastern Pacific Ocean and comparison with biostratigraphic and magnetostratigraphic age data: Geological Society of America Bulletin, v. 98, p. 207-223.
Sarna-Wojcicki, A.M., Lajoie, K.R., Meyer, C.E., Adam, D.P., and Rieck, H.J., in press, Tephrochronologic correlation of upper Neogene sediments along the Pacific margin, conterminous United States, in Morrison, R.B., ed., the Quaternary of the Unglaciated Unites States: Geological Society of America, Decade of North American Geology Volume, Boulder, CO.
Scott, W.E., 1977, Quaternary glaciation and volcanism, Metolius River area, Oregon: Geological Society of America Bulletin, v. 88, no. 1, p. 113-124.
Scott, W.E., 1987, Holocene rhyodacite eruptions on the flanks of South Sister volcano, Oregon, in Fink, J.H., ed., The emplacement of silicic domes and lava flows: Geological Society of America Special Paper 212, p. 35-53.
Scott, W.E., and Gardner, C.A., 1985, Late Pleistocene-early Holocene development of the Bachelor Butte volcanic zone, Cascade Range, Oregon [abs]: Eos, (American Geophysical Union Transactions), v. 64, p. 1141.
Scott, W.E., and Gardner, C.A., in press, Geologic map of the Mount Bachelor volcanic chain and surrounding area, Cascade Range, Oregon: U.S. Geological Survey Miscellaneous Investigations Map I-1967, scale 1:50,000.

Shackleton, N.J., and Opdyke, N.D., 1973, Oxygen isotope and paleomagnetic stratigraphy of Equatorial Pacific core V28-238: Oxygen isotope temperature and ice volumes on a 10,000 and 100,000 year time scale: Quaternary Research, v. 3, p. 39-55.

Sherrod, D.R., 1986, Geology, petrology, and volcanic history of a portion of the Cascade Range between latitudes 43°-44° N, central Oregon, U.S.A.: Santa Barbara, University of California, Ph. D. dissertation, 320 p.

Small, R.J., 1987, Moraine sediment budgets, in Gurnell, A.M., and Clark, M.J., eds., Glaciofluvial sediment transfer: An alpine perspective: New York, John Wiley and Sons, p. 165-197.

Smith, G.A., Snee, L.W., and Taylor, E.M., 1987, Stratigraphic, sedimentologic, and petrologic record of late Miocene subsidence of the central Oregon High Cascades: Geology, v. 15, p. 389-392.

Sparks, R.S.J., Self, S., and Walker, G.P.L., 1973, Products of ignimbrite eruptions: Geology, v. 1, p. 115-118.

Steiger, R. H., and Jager, E., 1977, Subcommision on geochronology: Convention on the use of decay constants in geo- and cosmochronology. Earth and Planetary Science Letters, v. 36, p. 359-362.

Tarling, D.H., 1983, Paleomagnetism--principles and application in geology, geophysics, and archeology: New York, Chapman and Hall, 379 p.

Taylor, E.M., 1978, Field geology of the S.W. Broken Top quadrangle, Oregon: Oregon Department of Geology and Mineral Industries Special Paper 2, 50 p.

Taylor, E.M., 1981, Central High Cascade roadside geology, Bend, Sisters, McKenzie Pass, and Santiam Pass, Oregon, in Johnston, D.A., and Donnelly-Nolan, Julie, eds., Guides to some volcanic terranes in Washington, Idaho, Oregon, and northern California: U.S. Geological Survey Circular 838, p. 55-58.

Taylor, E.M., 1987, Field geology of the northwest quarter of the Broken Top 15' quadrangle, Deschutes County, Oregon: Oregon Department of Geology and Mineral Industries Special Paper 21, 20 p.

Taylor, E.M., MacLeod, N.S., Sherrod, D.R., and Walker, G.W., 1987, Geologic map of the Three Sisters Wilderness, Deschutes, Lane, and Linn Counties, Oregon: U.S. Geological Survey Miscellaneous Field Studies Map MF-1952, scale 1:63,360.

Venkatakrishnan, Ramesh, Bond, J.G., and Kauffman, J.D., 1980, Geological linears of the northern part of the Cascade Range, Oregon: Oregon Department of Geology and Mineral Industries Special Paper 12, 25 p.

Waitt, R.B., Jr., Yount, J.C., and Davis, P.T., 1982, Regional significance of an early Holocene moraine in Enchantment Lakes basin, North Cascade Range, Washington: Quaternary Research, v. 17, p. 191-210.

Walker, G.P.L., 1973, Explosive volcanic eruptions--A new classification scheme: Geologische Rundschau, v. 62, p. 431-446.

Walker, G.P.L., 1981, Plinian eruptions and their products: Bulletin Volcanologique, v. 44, no. 3, p. 223-240.

White, C.M., and McBirney, A.R., 1978, Some quantitative aspects of orogenic volcanism in the Oregon Cascades, in Smith, R.B., and Eaton, G.P., eds., Cenozoic tectonics and regional geophysics of the western Cordillera: Geological Society of America Memoir 152, p. 369-388.

Wilson, C.J.N., and Walker, G.P.L., 1982, Ignimbrite depositional facies: the anatomy of a pyroclastic flow: Journal of the Geological Society of London, v. 139, p. 581-592.

Wozniak, K.C., 1982, Geology of the northern part of the southeast Three Sisters quadrangle, Oregon: Corvallis, Oregon State University, M.S. thesis, 98 p.

Wozniak, K.C., and Taylor, E.M., 1981, Late Pleistocene summit construction and Holocene flank eruptions of South Sister volcano, Oregon [abs]: Eos (American Geophysical Union Transactions), v. 62, no. 6, p. 61.

Zoback, M.L., and Zoback, Mark, 1980, State of stress in the conterminous United States: Journal of Geophysical Research, v. 85, no. B11, p. 6,113-6,156.